Partial migration in Hudson River white perch: influence of climate change on a dominant resident species

Final Report to the Hudson River Foundation Grant #009/13A

For the period: June 1 2013 – 30 December 2016

PI Information: Dr. David H. Secor, PO Box 38, Solomons, MD 20688

Report Author(s): David H. Secor and Brian K. Gallagher

Department: Chesapeake Biological Laboratory, University of MD Center for Environmental Science

E-mail: secor@cbl.umces.edu

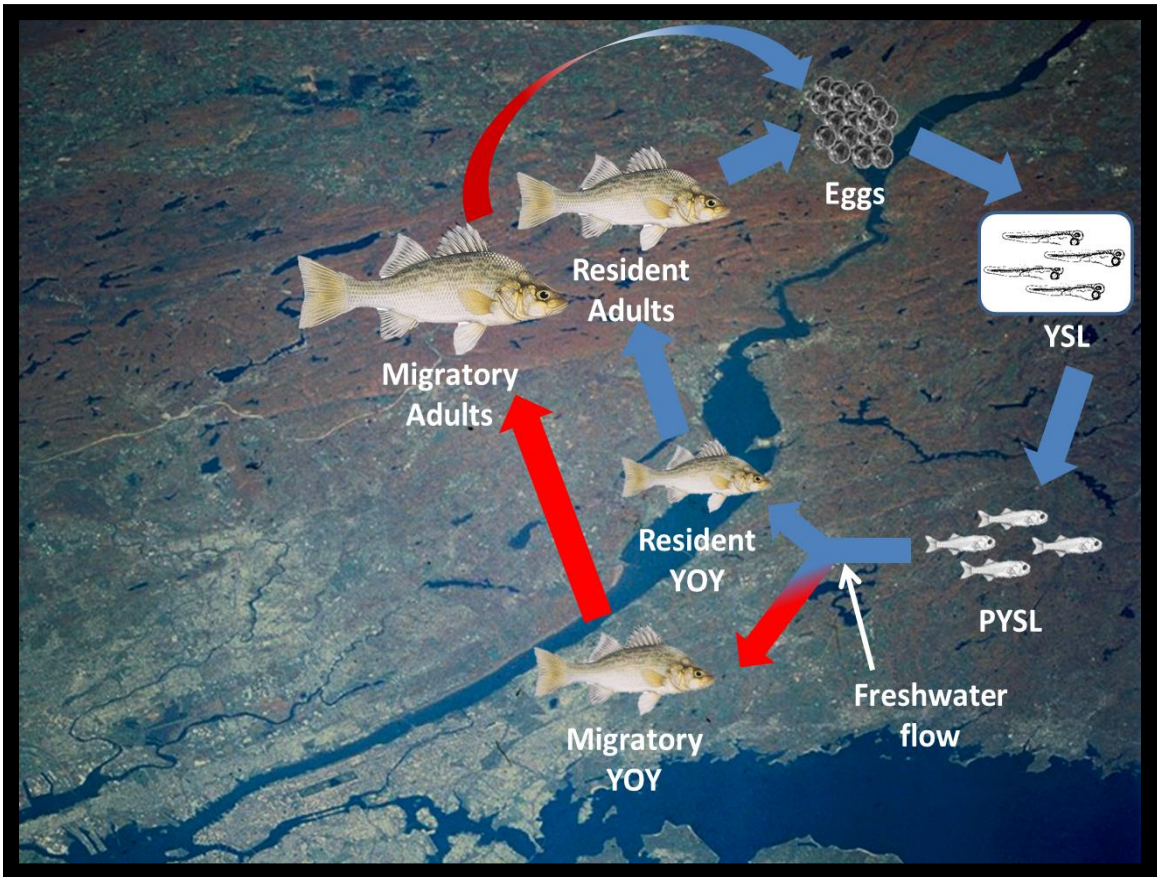

Table of Contents

Executive Summary

White perch, a dominant species within the Hudson River Estuary, responds to climate change through changes in their spatial distribution (Bailey and Secor 2016) and population demographics. We hypothesized that this distribution is underlain by partial migration whereby two "contingents," one of which remains resident to freshwater nursery areas and the other which disperses into down-estuary brackish habitats. We evaluated environmental influences on partial migration and white perch population dynamics (1) through a longitudinal life-history study of both contingents in a two year field study (2013-2014), and (2) over multiple generations through analysis of NY Utilities long-term dataset (1974-2013) on egg, larval, juvenile, and adult distributions and abundances. These two study components are summarized here and presented more fully in two attached manuscripts, which have been submitted for publication.

A third goal was to develop a stochastic age-structured model to simulate environmental effects on partial migration and population dynamics in white perch. This model has been coded in R and simulation runs conducted (appended to this report, p. 88: *Simulating the effects of contingent structure and long-term environmental change in white perch within the Hudson River Estuary*). However, because contingent abundances are strongly correlated the goal of using this model to examine consequences of partial migration on yield, persistence and stability was not further pursued. Rather we incorporated contingent-specific growth, mortality, and reproductive rates into a yield-per-recruit model to rank production and resilience to mortality of the two contingents and in comparison to Chesapeake Bay populations. We summarize this work and present the full methodology in the narrative of this final report.

(1) Effects of environmental conditions on white perch partial migration in the Hudson River Estuary: A field study (submitted paper: Gallagher, B.K., P.M. Piccoli, and D.H. Secor. In Review. Ecological carryover effects associated with partial migration in an estuarine fish. Oikos).

Otolith microchemistry analysis confirmed the existence of two white perch contingents (i.e., partial migration) for summer and fall juveniles (N=124) collected during 2013 and 2014. Sampling occurred from river km 48 (Tappan Zee) to river km 202 (Coxsakie), deploying seines for juveniles and gill nets for adults. During the early juvenile period, a large fraction of juveniles (33% and 49% in 2013 and 2014), dispersed into brackish waters, while the remainder remained resident to freshwater nursery habitats. The migratory contingent tended to hatch earlier and experienced cooler temperatures. Juvenile migratory behaviors persisted into adulthood for the majority (70%) of individuals. Adults that switched migration behaviors tended to do so during the first two years of life. As juveniles, the consequences of partial

migration appeared to be modified by river flow. In 2013, Tropical Storm Andrea impacted the Hudson River Estuary during the larval rearing period and was associated with high flow, reduced zooplankton stocks and depressed juvenile growth rate for both contingents. In 2014, a year with more typical spring flow, the migratory contingent exhibited higher juvenile growth. Migratory adults grew faster and attained a larger maximum size relative to the resident contingent, but may have experienced lower overall survival. The proportion of juveniles in the migratory contingent from 1999-2013 averaged 43% based on seine survey data, but retrospective analysis of surviving adults (N=229) from these same year-classes suggested that only 9% of individuals were migrants during their first year of life. Environmental conditions experienced during the larval period influenced the adoption of different migration behaviors as juveniles, which then had a substantial impact on growth characteristics later in life. Similar carryover effects have been described for Chesapeake Bay white perch. Partial migration dynamics in this dominant species is initiated during the juvenile period and will likely play an important role in determining the population persistence and resilience in response to predicted long-term changes in temperature and precipitation.

(2) Effect of climate variables and zebra mussel invasion on long-term changes in life-stage transitions and partial migration in Hudson River Estuary white perch (submitted paper: Gallagher, B.K. and D.H. Secor. In review. Intensified environmental and density-dependent regulation of white perch recruitment after an ecosystem shift in the Hudson River Estuary. Canadian Journal of Fisheries and Aquatic Science).

This study evaluated whether the zebra mussel invasion modified the relative influence of density-dependence and environmental conditions on the recruitment, growth, and migration dynamics of white perch within the Hudson River Estuary. A series of life-stage transition models developed from Utility survey data (1992-2013) were compared to earlier studies of white perch recruitment, growth, and spatial distribution to test whether the regime shift brought about by zebra mussel invasion changed functional relationships between distribution, abundance, flow, and other environmental variables. During the post-invasion period, standing stocks were estimated for white perch eggs, yolk-sac larvae (YSL), post yolk-sac larvae (PYSL), young-of-the-year (YOY) and adults, as well as indices of YOY growth and spatial distribution. Comparisons to pre-invasion observations (1974-1991), indicated that egg-YSL, PYSL-YOY and YOY-yearling transitions changed significantly after the invasion, while PYSL abundance developed a stronger negative effect on YOY growth. The PYSL-YOY transition became more sensitive to density-dependence and freshwater flow from 1992-2013, which is consistent with diminished abundance and increased environmental sensitivity of the forage base in the Hudson River Estuary following the zebra mussel invasion. The proportion of each contingent was fairly stable for the recent period, although the migrant fraction was positively correlated with annual availability of brackish littoral habitat. The increased sensitivity of the PYSL-YOY transition to density-dependence and freshwater flow is likely related to reductions in the food supply of white perch, and is generally consistent with riverwide declines in phytoplankton, pelagic zooplankton, and benthic invertebrates. Alterations in the abundance and environmental sensitivity of white perch in the Hudson River Estuary after the zebra mussel invasion will likely influence how the population responds to long-term increases in

temperature and precipitation. Similar changes may be detectable in other fish species in the Hudson River Estuary (e.g. striped bass, river herring, centrarchids).

(3) Demographic model to evaluate resilience of HRE white perch contingents to fishing and other anthropogenic sources of mortality

Summary

White perch are targeted by recreational fishers throughout the Hudson River Estuary (HRE), but little is known about their resilience to this source of mortality. Further, white perch tend to be smaller in the Hudson River than those observed for other estuarine systems (e.g., the Chesapeake Bay) prompting the speculation that the HRE population is "stunted." Condition, growth, mortality, and maturation data were compiled from the first component of this project (Gallagher et al. in review) and the literature (Klauda et al. 1988) to support yield-per-recruit and spawner-per-recruit analyses to (1) compare resilience of each contingent to fishing and other anthropogenic sources of mortality; and (2) compare HRE and Chesapeake Bay white perch production. Catch curve analysis provided an estimate of total mortality of 0.27 (23% yr^{-1}) for HRE fish collected during fall (Figure 2). The migratory contingent was two-fold greater in weight at age-2 (fully mature) and was predicted to mature approximately one year earlier than the freshwater contingent (Figure 3). Under the assumption of equal mortality rates, the migratory contingent can sustain 1.3-fold higher anthropogenic sources of mortality than the freshwater contingent (Figure 4; Table 1). In a second scenario in which the migratory contingent experiences 1.5-fold higher mortality than the freshwater contingent, sustainable anthropogenic mortality rates were similar.

White perch in the HRE are not stunted in the sense that they do not cease growing, but growth rates are substantially lower than their contingent counter-parts in the Patuxent River within the Chesapeake Bay. Modeled maximum size is about 27% less in the HRE than the Patuxent River for combined contingents (Figure 5; Table 2). There is an indication that lower growth rates may be related to the large fraction of resident white perch in the HRE in comparison to Chesapeake tributaries, which support higher proportions of the migratory contingent (Figure 6). Sustainable anthropogenic mortality rates were lower in the HRE than for Maryland Chesapeake Bay tributaries but somewhat higher than for Virginia Chesapeake Bay tributaries (Table 1).

Per-Recruit Model Parameterization

Klauda et al. (1988) reported mean length-at-age and maturity-at-age for male and female white perch in the Hudson River Estuary from 1975-1977 (n = 795). Female white perch tended to be slightly larger and mature slightly later than males, but these differences were small, with overlapping standard errors (Klauda et al. 1988). In addition, differences in growth between sexes were not evaluated in the current study. Therefore, length and maturity data were averaged across sexes and years, and a logistic function was fitted to these averages to describe the proportion of white perch that were mature as a function of total length (L), by the equation:

(1) $$Proportion\ Mature = \frac{1}{1+e^{-k(L-L_{50})}}$$

where the asymptote (i.e. the numerator) was fixed at 1, L_{50} is the point at which 50% maturity was reached and k is the rate at which the asymptote was approached. Parameters were estimated by minimizing the sum of squares using the Solver add-in in Microsoft Excel. The logistic function fit the data well (R^2 = 0.95; Figure 1a), and L_{50} was estimated to be 131 mm, while k was estimated at 0.08.

Juvenile and adult white perch captured in 2013 and 2014 were used to construct a length-weight relationship for the HRE population (n = 1,043) by the equation:

(2) $$W = \alpha L^{\beta}$$

where W is weight (in kg) α is the weight-length multiplier (in kg·mm^{-1}) and β is the exponent. Parameters were once again estimated by minimizing the sum of squares using the Solver add-in in Microsoft Excel. Length explained the vast majority of the variation in weight (R^2 = 0.98; Figure 1b) and α was estimated at $4.3 \cdot 10^{-9}$ kg·mm^{-1}, while β was estimated to be 3.2.

The instantaneous natural mortality rate (M) of adult white perch was estimated using a catch curve based on adult white perch captured in 2" mesh gillnets during fall 2014 (n = 216) by the regression equation:

(3) $$log_e(N_a) = b_0 - (a \times M)$$

where N_a is the catch at age a, b_0 is the intercept, and a is age. Data from ages 2-11 were used, and M was estimated to be 0.27 year^{-1} (Figure 2). Starting the catch curve at ages 3-5 yielded similar mortality estimates (range: 0.23-0.29). However, catch-at-age data were not adjusted for effort (i.e. gillnet soak time), so this mortality estimate should be viewed as preliminary.

Yield-Per-Recruit and SSB-Per-Recruit Models

Predicted length-at-age data from von Bertalanffy growth models for each contingent (Gallagher et al. in review) were used as inputs into equations 1 and 2 to calculate the maturity-at-age and weight-at-age for resident and migratory contingents from ages 1-13 (Figure 3). The baseline natural mortality rate was assumed to be 0.27 for both contingents. These data were used to conduct yield-per-recruit (YPR) and spawning stock biomass-per-recruit (SSBR) analyses and estimate biological reference points (BRPs) for each contingent for HRE white perch (see below).

Age-structured data were used to implement an YPR analysis, where the YPR was calculated by the equation:

(4) $$YPR = \sum_{a=1}^{13}(\frac{F_a}{Z_a} \times (1 - e^{-Z_a}) \times N_a \times W_a)$$

where F_a is the fishing mortality rate at age a, Z_a is the total mortality rate (F_a plus the natural mortality rate), N_a is the abundance at age a (N_1 is assumed to be equal to 1) and W_a is the weight at age a (Figure 3b). F_a values are typically obtained by multiplying a fixed fishing mortality rate by the age-specific selectivity (Hilborn and Walters 1992). However, there are currently no size limits on white perch caught recreationally in the HRE (NYSDEC 2016), and white perch begin to be harvested by anglers at sizes between 75 and 100 mm (Normandeau 2003). Therefore, white perch were assumed to be fully-selected (i.e. selectivity = 1) in all age-classes, similar to previous analyses of white perch in Virginia estuaries by Kerr and Secor (2008). Subsequently, the same data were used to conduct a SSBR analysis, which accounts for the maturity schedule, where SSBR was calculated by the equation:

(5) $$SSBR = \sum_{a=1}^{13} Mat_a \times N_a \times W_a$$

where Mat_a is the proportion mature at age a. SSBR is calculated both with and without fishing mortality and used to calculate the spawning potential ratio (SPR), by the equation:

(6) $$SPR = \frac{SSBR_F}{SSBR_{F=0}}$$

where $SSBR_F$ is the spawning stock biomass-per-recruit at a fishing mortality rate of F, and $SSBR_{F=0}$ is the spawning stock biomass-per-recruit when F is equal to 0.

Separate YPR and SSBR analyses were run for resident and migratory contingents of HRE white perch. In addition, two natural mortality scenarios were considered for the migratory contingent to explore the potential consequences of a higher mortality rate in this population segment (see Gallagher et al. in review). Specifically, the natural mortality rate of the migratory contingent was assumed to be either 0.27 (i.e. same as residents) or 0.41 (1.5x higher than residents), such that three YPR and SSBR analyses were conducted overall. YPR, SSBR and SPR were each plotted over a range of fishing mortality rates in each analysis (Figure 5). BRPs were estimated for each analysis, with F_{max} and $F_{40\%}$ reference points estimated for YPR and SSBR

analyses, respectively (Hilborn and Walters 1992; Table 1). F_{max} was estimated by maximizing YPR using the Solver add-in in Microsoft Excel, while $F_{40\%}$ was estimated by setting SPR to 0.4 using the Goal Seek function in Microsoft Excel. Fishery mortality rates exceeding F_{max} suggest that biomass is being removed faster than it can be replaced by somatic growth (i.e. growth overfishing), while $F_{40\%}$ is considered a more conservative reference point, above which individuals are removed faster than they can be replaced via recruitment processes (i.e. recruitment overfishing; Hilborn and Walters 1992). The YPR and SSBR associated with each BRP was calculated for each contingent and compared to previous estimates from Chesapeake Bay populations (Table 1; from Kerr and Secor 2008). To aid comparisons between populations, von Bertalanffy growth parameters (L_∞ and k; from Kerr and Secor 2008) and contingent proportions based on chemical analyses of the first-annulus of adult white perch otoliths (Kraus and Secor 2004a, Kerr and Secor 2011) were tabulated along with corresponding estimates for the HRE population (Table 2).

Table 1. Contingent-specific biological reference points (BRP; F_{max} and $F_{40\%}$) for fishing mortality in HRE white perch, and corresponding spawning stock biomass-per-recruit (SSBR) and yield-per-recruit (YPR). Migratory* denotes models where a higher mortality was used for the migratory contingent (M = 0.41; see text). Previous BRP estimates for white perch populations within six Chesapeake Bay tributaries (Upper Bay, Patuxent, Potomac, Nanticoke, York and James Rivers) from Kerr and Secor (2008) are shown for comparison.

River	Contingent	BRP	F	SSBR	YPR
Hudson	Migratory	F_{max}	0.38	0.07	0.02
	Migratory*	F_{max}	0.51	0.04	0.02
	Resident	F_{max}	0.31	0.04	0.01
James	Combined	F_{max}	0.27	0.12	0.02
York	Combined	F_{max}	0.24	0.21	0.04
Hudson	Migratory	$F_{40\%}$	0.24	0.10	0.02
	Migratory*	$F_{40\%}$	0.31	0.06	0.02
	Resident	$F_{40\%}$	0.20	0.07	0.01
Upper Bay	Combined	$F_{40\%}$	1.65	0.08	0.03
Patuxent	Combined	$F_{40\%}$	2.35	0.12	0.04
Potomac	Combined	$F_{40\%}$	0.53	0.09	0.01
Nanticoke	Combined	$F_{40\%}$	0.82	0.15	0.04
James	Combined	$F_{40\%}$	0.21	0.13	0.02
York	Combined	$F_{40\%}$	0.19	0.22	0.04

Table 2. Contingent proportions (M = migrant proportion; R = resident proportion; n_c = sample size) and von Bertalanffy growth parameters (n_g = sample size) for eight white perch populations. Note that the von Bertalanffy growth model for both contingents combined in the HRE included adults captured in the spring that were not used in the contingent-specific models (see Gallagher et al. in review).

		Contingent Proportions			**Growth**			
River	**Contingent**	**n_C**	**M**	**R**	**n_G**	**L_∞ mm**	**k**	**Source**
Upper Bay	Combined	75	0.31	0.69	59	240	0.46	Kerr and Secor (2008, 2012)
Choptank	Combined	78	0.55	0.45	75	225	0.48	Kerr and Secor (2008, 2012)
Potomac	Combined	45	0.35	0.65	70	258	0.26	Kerr and Secor (2008, 2012)
Nanticoke	Combined	75	0.81	0.19	88	254	0.35	Kerr and Secor (2008, 2012)
James	Combined	49	0.82	0.18	78	246	0.40	Kerr and Secor (2008, 2012)
York	Combined	75	0.68	0.32	61	269	0.35	Kerr and Secor (2008, 2012)
Patuxent	Combined	363	0.93	0.07	101	258	0.32	Kerr and Secor (2008, 2012)
	Resident	-	-	-	27	217	0.39	Kraus and Secor (2004)
	Migratory	-	-	-	336	217	0.69	Kraus and Secor (2004)
Hudson	Combined	229	0.09	0.91	263	188	0.62	Current study
	Resident	-	-	-	112	194	0.52	Current study
	Migratory	-	-	-	79	204	0.69	Current study

Figure 1. Length-maturity information (a) from Klauda et al. (1988) averaged for both sexes of HRE white perch from 1975-1977 (open circles), fitted by a logistic function (thick black line; R^2 = 0.95; see text) and length-weight information (b) from juvenile and adult white perch captured in 2013 and 2014 (open circles), fitted by a power model (thick black line; R^2 = 0.98; see text).

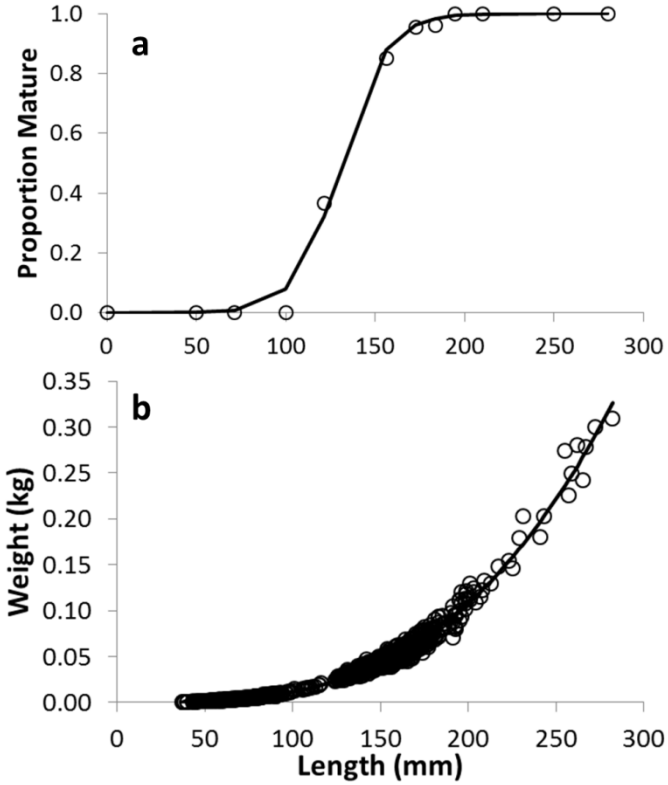

Figure 2. Preliminary catch curve constructed for adult white perch captured in 2" gillnets during fall 2014. Catch data were natural-log transformed and plotted as a function of age. The linear regression equation and model R^2 are shown in the top right corner, where the slope represents the natural mortality rate (M).

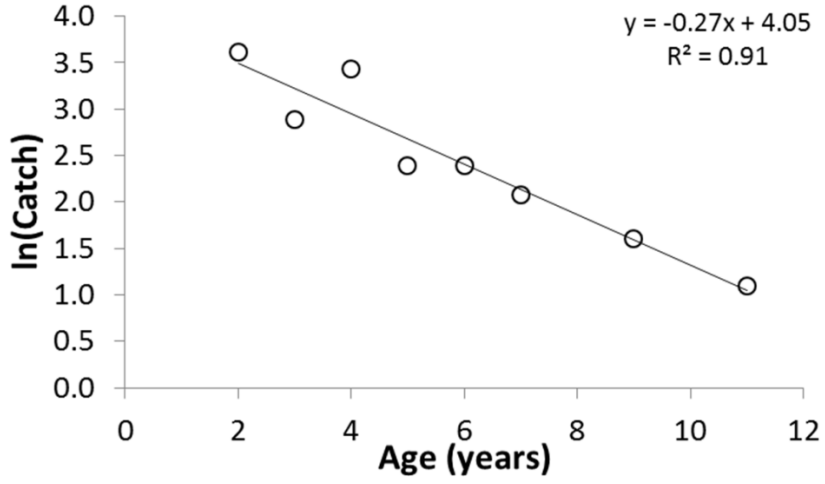

Figure 3. Maturity-at-age (a) and weight-at-age (b) for resident (blue) and migratory (red) contingents of white perch in the HRE.

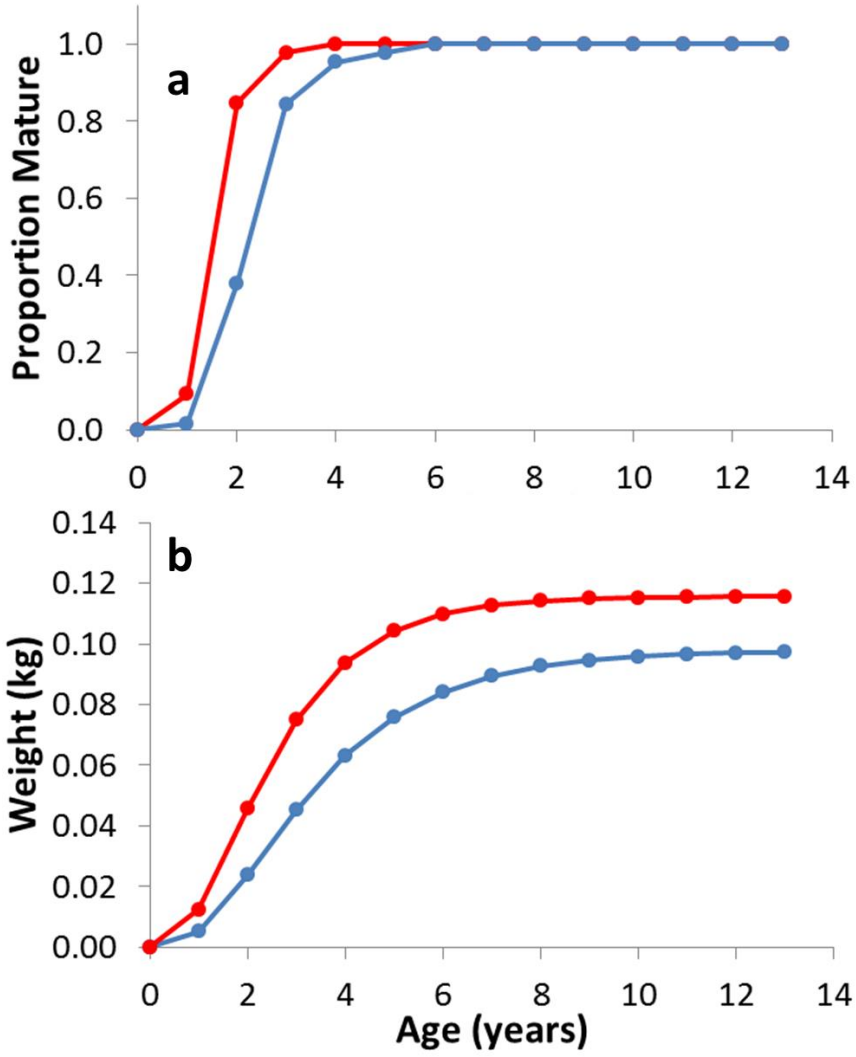

Figure 4. Yield-per-recruit (a), spawning stock biomass-per-recruit (b) and spawning potential ratio (c) plotted as a function of fishing mortality rate for the resident contingent (blue), migratory contingent (red) and the migratory contingent with a higher mortality rate (dark red).

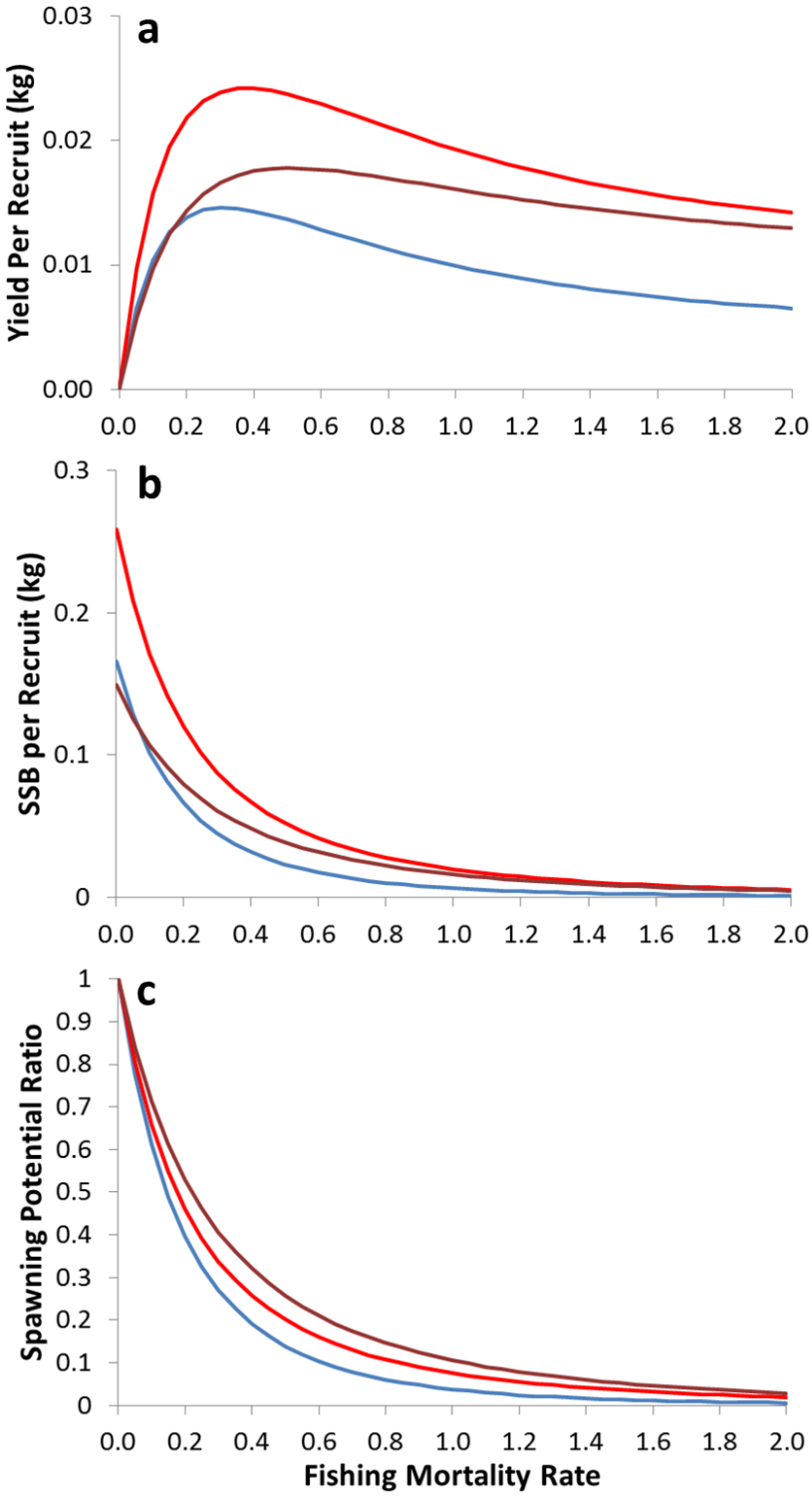
a
Yield Per Recruit (kg)
0.03
0.02
0.01
0.00
0.0 0.2 0.4 0.6 0.8 1.0 1.2 1.4 1.6 1.8 2.0
b
SSB per Recruit (kg)
0.3
0.2
0.1
0
0.0 0.2 0.4 0.6 0.8 1.0 1.2 1.4 1.6 1.8 2.0
c
Spawning Potential Ratio
1
0.9
0.8
0.7
0.6
0.5
0.4
0.3
0.2
0.1
0
0.0 0.2 0.4 0.6 0.8 1.0 1.2 1.4 1.6 1.8 2.0
Fishing Mortality Rate

Figure 5. Modeled von Bertalanffy growth curves for the Hudson River Estuary and the Chesapeake Bay (Kraus and Secor 2004), by contingent.

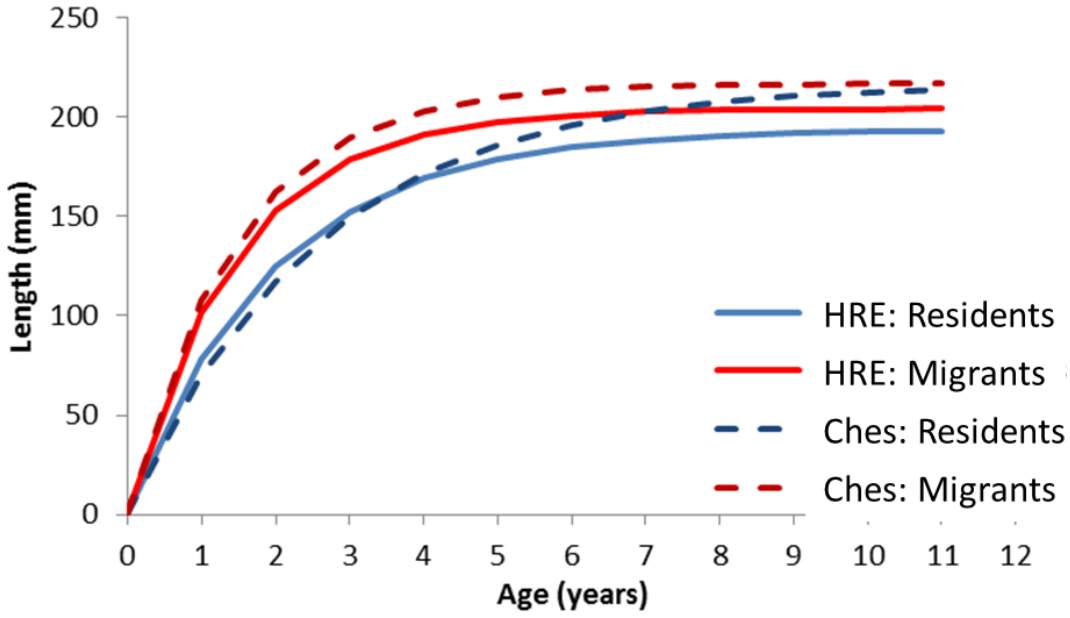

Figure 6. Estimated L_∞ (resident and migratory contingents combined) in eight white perch populations, plotted in relation to the fraction of the adult population that was migratory during the first year of life. Data for Chesapeake Bay tributaries were from Kerr and Secor (2008, 2011). Note that the relationship is marginally non-significant, and becomes much weaker if the Hudson River is removed (R^2 = 0.09). Estimated k had a non-significant negative relationship with migrant fraction (R^2 = 0.35; p = 0.12; data not shown). L_∞ estimates displayed a significant negative relationship with k estimates (R^2 = 0.86; p > 0.001; data not shown), even after removing the Hudson River.

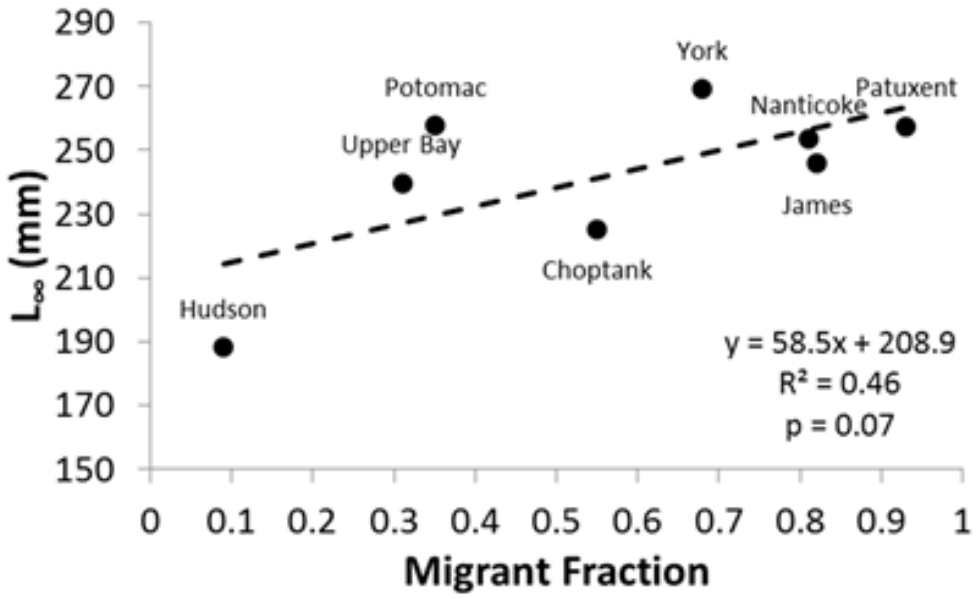

References

Bailey, H. and D.H. Secor. 2016. Coastal evacuations by fish during extreme weather events. Scientific Reports. 6:30280 | DOI: 10.1038/srep30280

Hilborn, R., and Walters, C. J. 1992. Quantitative fisheries stock assessment: choice, dynamics, and uncertainty. Chapman and Hall, London. 575 pp.

Kerr, L., and D. Secor. 2008. Demographic reference points for white perch in Chesapeake Bay. Final report to: National Oceanic and Atmospheric Administration (NOAA). Silver Spring, MD.

Kerr, L., and D. Secor. 2011. Partial migration across populations of white perch (*Morone americana*): a flexible life history strategy in a variable estuarine environment. Estuaries and Coasts 35(1): 227-236.

Klauda, R.J., J.B. McLaren, R.E. Schmidt and W.P. Dey. 1988. Life history of white perch in the Hudson River Estuary. *in*: L.W. Barnthouse, R.J. Klauda, D.S. Vaughan and R.L. Kendall (eds). Science, Law and Hudson River Power Plants. American Fisheries Society Monograph 4:69-88.

Kraus, R.T., and D.H. Secor. 2004a. Dynamics of white perch *Morone americana* population contingents in the Patuxent River estuary, Maryland, USA. Marine Ecology Progress Series. 279: 247-259.

Normandeau Associates, Inc. 2003. Assessment of Hudson River recreational fisheries. Final report to: New York State Department of Environmental Conservation (NYSDEC). New Paltz, NY.

NYSDEC (New York State Department of Environmental Conservation). 2016. Tidal Hudson River fishing regulations. Accessed August 20, 2016. Available: http://www.dec.ny.gov/outdoor/31427.html

List of papers, thesis, presentations and manuscripts

Thesis:

Gallagher, B.K. 2016. Influence of partial migration and environmental change on the population dynamics of white perch (*Morone americana*) within the Hudson River Estuary. MSc Degree in the Marine, Estuarine, and Environmental Studies Program (Univ. MD Center for Environmental Science). 174 p.

Presentations:

Gallagher, B.K., and D.H. Secor. 2016. Carryover effects of partial migration in white perch within the Hudson River Estuary. Ecological and Evolutionary Ethology of Fishes, 2016 Conference. Tallahassee. Winner, Young Investigator Award for best presentation.

Gallagher, B.K. and D.H. Secor. 2016. Revisiting the life history of white perch (*Morone americana*) within the Hudson River Estuary. AFS Tidewater Meeting, Edgewater, MD.

Gallagher, B.K., D.H. Secor and P.M. Piccoli. 2015. Intergenerational contingent structure in white perch (*Morone americana*) within the Hudson River Estuary. 145th AFS Annual Meeting. Portland, OR.

Gallagher, B.K., D.H. Secor and P.M. Piccoli. 2015. Partial migration in juvenile white perch (*Morone americana*) within the Hudson River Estuary. 2015 HRES Hudson River Symposium, New Paltz, NY.

Gallagher, B.K., D.H. Secor and P.M. Piccoli. 2015. Partial migration in juvenile white perch (*Morone americana*) within the Hudson River Estuary. 29th AFS Tidewater Meeting, Pine Knoll Shores, NC. Runner-up, Best student presentation.

Secor, D.H. 2014. Life cycle portfolios and resilience in coastal fishes. International Symposium on Weather and Climate Extremes, Food Security and Biodiversity. George Mason University, Fairfax, VA.

Manuscripts in review:

Gallagher, B.K., P.M. Piccoli, and D.H. Secor. In Review. Ecological carryover effects associated with partial migration in an estuarine fish. Oikos

Gallagher, B.K. and D.H. Secor. In review. Intensified environmental and density-dependent regulation of white perch recruitment after an ecosystem shift in the Hudson River Estuary. Canadian Journal of Fisheries and Aquatic Science

Ecological carryover effects associated with partial migration in an estuarine fish

By:

Brian K. Gallagher*[1,3], Philip M. Piccoli[2] and David H. Secor[1]

Footnotes:

*Corresponding author (e-mail: bkgallagher@vims.edu, phone: 804-684-7351)

[1]University of Maryland Center for Environmental Science, Chesapeake Biological Laboratory, P.O. Box 38, Solomons, MD 20688, USA

[2]Department of Geology, University of Maryland College Park, 237 Regents Drive, College Park, MD 20742, USA

[3]Present address: Virginia Institute of Marine Science, College of William and Mary, P.O. Box 1346, Gloucester Point, Virginia, 23062, USA

Abstract

Partial migration in complex life cycles allows environmental conditions experienced during one life-stage to interact with genetic thresholds and produce divergent spatial behaviors in the next stage. It has been hypothesized that complex life cycles and partial migration are adaptations that allow organisms to persist in non-stationary environments, but little is known about how these two life history features interact. We evaluated partial migration over the entire life cycle of a common estuarine fish (white perch, *Morone americana*) within the Hudson River Estuary, combining otolith microchemistry, population demographics and environmental data analysis. Ecological carryover effects were used as a framework to test how environmental variation during the larval period influenced migration behaviors and growth characteristics in subsequent life-stages. Two annual cohorts of juveniles were classified according to whether they persisted in natal habitats (freshwater resident contingent) or dispersed into non-natal habitats (brackish water migratory contingent) as juveniles. The migratory contingent tended to hatch earlier and experience cooler temperatures as larvae, while the availability of zooplankton prey during the larval period appeared to influence growth dynamics before and after metamorphosis. Juvenile migration behaviors were reversible but usually persisted into adulthood. As juveniles, the consequences of partial migration on growth appeared to be modified by flow, as demonstrated by the influence of a large storm event on feeding conditions in one of the study years. Migratory adults grew faster and attained larger maximum sizes, but may also experience higher rates of mortality. The interplay between life-stage transitions, conditional migration behaviors and habitat productivity throughout the life cycle shapes white perch population dynamics and will play an important role in responses to long-term environmental change.

Introduction

Many organisms exhibit complex life cycles, which feature rapid changes in body form and function as individuals progress from one life-stage to the next (Moran 1994). Complex life cycles often entail stage-specific movements to new habitats (Werner and Gilliam 1984). Here, differences in growth and dispersal capabilities between life-stages can potentially influence population dynamics and species interactions, but these effects tend to be modulated by the productivity and stability of each stage's habitat (Wilbur 1980, Petitgas et al. 2013). Complex life cycles are common among insects, amphibians, fishes and other taxa, and are broadly considered adaptations to enable these organisms to persist in highly variable environments (Wilbur 1980, Moran 1994, Stoks and Córdoba-Aguilar 2012).

The life cycles of fishes, especially during the egg and larval period, can be considered as a series of developmental stages, separated by thresholds in morphological and physiological attributes (i.e. saltatory development; Balon 1981). Most fish species produce very small offspring in great quantity, presumably to take advantage of highly abundant but patchily distributed planktonic prey (Winemiller and Rose 1993), which in turn generates variability in feeding success, predation risk and environmental conditions experienced during the larval period (Houde 1987). This variability in early life conditions, through its influence on growth, survival and dispersal, can carry over to the demographics and ecology of subsequent stages (Bertram and Chambers 1993, O'Connor and Cooke 2015), although there have been few

detailed studies examining such carryover effects within the life cycles of fishes (Pechenik 2006).

One pathway by which carryover effects can shape complex life cycles is through partial migration, where multiple groups - or contingents - with different spatial behaviors are contained within a single population (Secor 1999, Chapman et al. 2011a). Partial migration has been observed in a wide range of fish taxa (Chapman et al. 2012a), and is generally viewed as a conditional strategy, mediated by phenotypic plasticity, where individuals select a particular migration pathway early in life based on a combination of internal and external factors (Chapman et al. 2012b, Brodersen et al. 2014). Partial migration in fish populations has been proposed to be maintained through tradeoffs associated with each migration behavior in a given environment (Kaitala et al. 1993, Jonsson and Jonsson 1993), although the causes and consequences of partial migration are likely diverse and remain poorly understood for most species (Chapman et al. 2011a). Nonetheless, the ubiquity of partial migration across taxa and across aquatic environments led Secor (2015) to posit that partial migration may be a general phenomenon in fishes and may serve as a unifying concept in studies of fish movement and migration.

Partial migration can be viewed as a series of ecological carryover effects, which arise when conditions experienced during a particular life-stage alter individual physiology or behavior, which subsequently influence the phenotype or performance of the individual at a later time (Pechenik 2006, O'Connor et al. 2014). Partial migration is thought to arise through the "threshold model," which posits that individuals adopt a particular migration behavior based on whether or not a threshold size or condition level is attained early in life (Brodersen et al. 2008, Pulido 2011). This can be interpreted as a carryover effect, where early-life environmental conditions (e.g. temperature, food availability) directly influence individual growth rates, which consequently determine the frequency of specific migration behaviors (e.g. a resident freshwater contingent and migratory marine contingent). In addition to the threshold model, individual decisions to disperse or remain resident early in life may also be modulated by flow conditions (Conroy et al. 2015), predation risk (Skov et al. 2011), or personality traits (Chapman et al. 2011b). The resulting differences in environmental conditions and food webs encountered by each contingent can carry over to influence bioenergetics, growth, and maturity characteristics later in life (Morinville and Rasmussen 2002, Gillanders et al. 2015). Moreover, divergent life history characteristics may enable each contingent to uniquely contribute to aggregate population dynamics, which would ultimately carry over to influence productivity, stability and resilience at the population level (Kerr et al. 2010, Schindler et al. 2010, Secor 2015).

White perch (*Morone americana*) are a dominant fish species in rivers and estuaries along the east coast of North America. In estuarine white perch populations, adults undertake spawning migrations in the spring to deposit their eggs in tidal freshwater habitats over a period of 1-2 months (Mansueti 1964, Klauda et al. 1988). After hatching, pelagic larvae are typically retained in natal freshwater habitats, where their growth and survival is shaped by thermal conditions and densities of pelagic zooplankton prey (Limburg et al. 1998, Kerr and Secor 2010). Larvae metamorphose into fully-formed juveniles and settle in littoral habitats, where their diet shifts and becomes dominated by benthic and epibenthic invertebrates (Mansueti 1964, Bath and O'Connor 1985). In the Chesapeake Bay, environmental conditions experienced during the larval period have carryover effects on juvenile movement patterns, where shortly after metamorphosis, juveniles originating from earlier hatch dates tend to disperse from the natal habitat and begin utilizing brackish habitats down-estuary, while the remainder stay in freshwater (Kraus and

Secor 2004a, Kerr and Secor 2010). The migratory contingent exhibits slower growth during the larval period, but increased consumption rates and enhanced productivity in brackish water result in faster growth rates during the juvenile period compared to residents (Kerr and Secor 2009). Faster growth in the migratory contingent subsequently persists into adulthood (Kraus and Secor 2004a). Thus, white perch exhibit a complex life cycle, with an ontogenetic shift from pelagic to demersal habitats (Werner and Gilliam 1984), as well as conditional movements between freshwater and more productive brackish habitats mediated by partial migration (Kerr et al. 2009).

In this study, we tested ecological carryover effects associated with partial migration in white perch within the Hudson River Estuary (HRE). Previous studies have identified partial migration in other diadromous fish populations within the HRE, such as striped bass (Zlokovitz et al. 2003), blueback herring (Limburg and Turner 2016) and American eels (Morrison et al. 2003). Although white perch partial migration has been previously studied in the Chesapeake Bay, the HRE represents a substantially different system with respect to thermal regime (cooler, with longer winters), trophic status (less productive; Fisher et al. 1988), hydrology (lower residence times; Howarth et al. 2000), and ecosystem impacts owing to an invasive bivalve (Strayer et al. 2004). We hypothesized that resident and migratory contingents would be present in the HRE white perch population, and that contingent membership would be associated with differences in early life history characteristics such as hatch dates, environmental conditions and food availability. Furthermore, we hypothesized that migration behaviors would subsequently have significant carryover effects on growth in juveniles and adults. To test these hypotheses, we collected juvenile and adult white perch in the HRE, used otolith microchemistry to assign each individual to a contingent and employed analyses of otolith microstructure to estimate hatch dates, growth rates and early-life environmental histories for contingent comparisons.

Methods

Field Collections and Subsampling

Age-0 juvenile white perch were collected by the New York State Department of Environmental Conservation (NYSDEC) fall seine survey with a 30.5m×1.2m beach seine from September to November in 2013 and 2014. The 2014 year class was further sampled with a 15.2m×1.8m beach seine in September 2014. These collections both took place in freshwater (Coxsackie, Germantown, Staatsburg and Poughkeepsie), brackish water (Haverstraw and Tappan Zee) and transition-zone (Newburgh, near the salt front) regions (Figure 1). White perch yearlings (age-1) were also captured in seine samples during 2013 (n = 22) and 2014 (n = 16), and these fish were operationally classified as adults (both sexes begin to mature at age-1; Klauda et al. 1988). Adult white perch were collected using 30.5m×1.8m gillnets with 5.1cm and 7.6cm mesh panels in the spring (May) and fall (September) of 2014. Gillnets were soaked for 30-240 minutes in shoal areas (< 4 m depth). Collections of adult white perch in spring 2014 occurred only in the transition zone and freshwater portions of the estuary, consistent with their expected run upriver during the spawning season (Klauda et al. 1988); while fall collections of adults occurred in both freshwater and brackish water sites. All individuals were frozen upon capture and transported back to the laboratory for further analysis (Table A1).

Collected adults (n = 722; Table A1) were subsampled randomly based on total length, sample site, and season of capture. Adults were assigned to 20 mm length stanzas from 100-300

mm, and all fish > 180 mm were selected due to the rarity of large adults (n = 59) and their importance for contingent comparisons. As a result, the size distribution of subsampled adults was skewed slightly towards larger sizes relative to the entire adult sample (Gallagher 2016). Juveniles captured in 2014 (n = 226; Table A1) were also subsampled based on their location and date of capture to obtain a representative sample of each contingent. In total, 124 juvenile white perch otoliths (n = 67 in 2013, n = 57 in 2014) and 229 adult white perch otoliths were analyzed for age determination and movement trajectories (Table A1).

Otolith Processing and Age Determination

In the laboratory, otoliths (earstones) were removed via dissection, embedded in epoxy resin, sectioned transversely to a width of ~1 mm with a low-speed jewelers saw, and attached to glass slides using thermoplastic glue (Secor et al. 1991). Subsequently, each otolith was polished on a lapping wheel with 320, 600 and 1200 grit material until the core (earliest formed daily increment) was clearly visible. Otolith sections were then buffed on a microcloth with wetted 0.3μm alumina powder until most pits and abrasions were removed. Images of juvenile otolith sections were captured under transmitted light at 100× magnification. The number of increments present (representing daily age: Kraus and Secor 2004a) was enumerated, which was subtracted from the date of capture to obtain a hatch date. The error, bias and average percent error of age estimates from otolith increment counts were quantified in a subsample of juveniles and were deemed acceptably low (see Appendix).

Estimated ages for all juveniles ($a_{initial}$) were subsequently corrected for the effects of temperature on the formation of the first daily increment in white perch otoliths ($a_{corrected}$) by the equation:

$$a_{corrected} = a_{initial} + (9.03 - (0.32 \times T))$$

where T is the mean daily temperature at the hatch date calculated based on $a_{initial}$ (Houde and Morin 1990). Adjustments were small and ranged from 1-5 days. Temperature data were obtained from the IBM (International Business Machine Corporation) pumping station in Poughkeepsie located at river km 120, (USGS 2015a; http://waterdata.usgs.gov/nwis/uv?site_no=01372058). The biological intercept method was employed to back-calculate size-at-age data for age-0 juveniles (Campana 1990). The biological intercept method uses the proportionality between otolith radius (OR) and fish total length (TL) to reconstruct the length of each individual at any given age by the equation:

$$TL_a = TL_c + \frac{(OR_a - OR_c) \times (TL_c - TL_i)}{(OR_c - OR_i)}$$

where the subscripts *i*, *a* and *c* signify initial, at-age and at-capture values, respectively, of OR and TL. Kraus and Secor (2004a) estimated white perch OR_i and TL_i values of 3.2 μm and 3 mm, respectively, which were used as inputs.

Adult otoliths were similarly embedded and sectioned and the number of annuli in each otolith (representing annual ages; Casey et al. 1988) was counted at 40× magnification under transmitted light. A correction of 0.5 years (i.e. half of the growing season) was added to the age of adults captured in the fall to account for their additional ~3.5 months of growth relative to spring-captured adults.

Otolith Microchemistry

Contingent membership was determined for each individual using otolith strontium:calcium (Sr:Ca) profiles. Otolith sections were carbon-coated in a high vacuum

evaporator and analyzed via wavelength-dispersive X-ray spectrometry using an electron probe micro-analyzer (EPMA; JXA-8900R SuperProbe, JEOL USA Inc., Peabody, MA) at the University of Maryland NanoCenter. Before each analysis, the EPMA was calibrated using strontianite ($SrCO_3$) and calcite ($CaCO_3$) reference standards for Sr and Ca concentrations, respectively. For each juvenile otolith, Sr:Ca was analyzed over a profile of equally-spaced points (~20µm apart) from the core to the edge, with each point along the transect measuring an area of ~100µm^2 at the otolith surface, thus obtaining a longitudinal record of Sr:Ca for each individual (Figure A1a). Similarly, adult otoliths were analyzed in profiles, with ~25µm spacing, spanning the first year of life (i.e. from the core to the first annulus; Figure A1b). A consistent growth axis peripheral to the sulcul ridge was chosen for both juvenile and adult profiles. In addition to juvenile Sr:Ca profiles, lifetime Sr:Ca profiles were measured in a subsample of 49 adults to assess whether first-year migration behaviors persisted into adulthood (Figure A1b). In a previous study of white perch, salinity was found to be positively related to the ambient Sr:Ca ratio. Sr and Ca are then incorporated into the otolith matrix roughly in proportion to their ambient concentrations (Kraus and Secor 2004b). A similar relationship between otolith Sr:Ca and salinity in the HRE was verified in a subsample of YOY white perch captured in both years (see Appendix). For all analyses, a threshold Sr:Ca value of 2.0 mmol mol^{-1} was used to differentiate between freshwater (below; salinity < 3 ppt) and brackish water (above; salinity > 3 ppt) habitat use (Kraus and Secor 2004b; Figure A2).

Statistical Analyses

Differences in juvenile hatch date distributions were analyzed with a two-way analysis of variance (ANOVA) with contingent (resident and migratory), year (2013 and 2014) and their interaction as explanatory variables. Post-hoc contrasts via Tukey's HSD were subsequently employed to compare mean hatch dates across each year×contingent combination. Mean back-calculated total lengths at age 50 days, the approximate age of metamorphosis (Mansueti 1964) were compared between contingents and years using a two-way ANOVA and post-hoc contrasts. To aid interpretation, differences in back-calculated length at 50 days were also reported as differences in larval growth rates (integrated from ages 1-50d) using the formula $(TL_{50d} - TL_i) \times 50d^{-1}$, where TL_i is 3 mm (Kraus and Secor 2004a). To test contingent differences in juvenile growth rates, age-length relationships were compared using an analysis of covariance (ANCOVA) with length as the dependent variable, age as a covariate and contingent and year as categorical variables. Coefficients from the ANCOVA were subsequently used to perform contrasts to test whether intercepts and slopes (i.e. growth rates) were significantly different between contingents within year-classes (i.e. each year's juvenile cohort), and between year-classes within each contingent.

To explore factors influencing annual differences in larval and juvenile growth rates, we contrasted environmental conditions and food availability between 2013 and 2014. The mean temperature and freshwater flow experienced by each individual in their first 50 days of life were calculated for all individuals in each year-class, and both metrics were analyzed by a two-way ANOVA with contingent, year and their interaction as explanatory variables. Temperature data were obtained from the IBM pumping facility in Poughkeepsie (USGS 2015a), and freshwater flow data were obtained from Green Island in Troy, which is located at the head of the estuary and represents the majority of freshwater input into the HRE (Howarth et al. 2006; USGS 2015b; http://waterdata.usgs.gov/nwis/uv?site_no=01358000). Data on food availability included measures of primary (chlorophyll-a concentration) and secondary (copepod and cladoceran

densities) production in the HRE, which were obtained from the Cary Institute of Ecosystem Studies Hudson River Database (CIES 2015; http://www.caryinstitute.org/science-program/research-projects/hudson-river-ecosystem-study/hudson-river-ecosystem-study-data). Copepods and cladocerans are important prey items for larval white perch in the HRE (Limburg et al. 1997). Each metric was obtained from a bi-weekly survey conducted at a single station in the tidal freshwater portion of the HRE (Kingston; river km 146) over the course of the growing season (May-September) from 1992-2014.

To test which factors best predicted lifetime contingent membership in adult white perch, three separate logistic regression models were constructed and compared with predictors: salinity at capture, river kilometer at capture and first-year contingent classification. Each lifetime resident was coded as a 1, and each migrant as a 0, which served as the response variables (n = 49). The relative classification success of each predictor was subsequently evaluated by comparing effect sizes (Z-statistics) and deviance explained (%) among models.

von Bertalanffy growth curves were constructed separately for each contingent. Based on lifetime Sr:Ca profiles, the most reliable indicator of adult white perch contingent membership was location of capture during the fall (see Results). Therefore, adult white perch sampled during fall 2014 were assumed to be resident if they were captured in Germantown (freshwater; Table A1; n = 112) and migrants if they were captured in Haverstraw (brackish water; Table A1; n = 79). The von Bertalanffy growth model is commonly used to describe lifetime age-length data in fishes, by the equation:

$$L_t = L_\infty(1 - e^{-kt}) + \varepsilon$$

where L_t is the mean length at age t, L_∞ is the theoretical maximum length, k is the growth coefficient which determines how rapidly L_∞ is approached, and ε is a random error term assumed to be N (0, σ^2). The model typically is fitted with a theoretical age at which length is zero (t_0), which was not used here and assumed to be zero (after Kraus and Secor 2004a). Parameters were estimated by minimizing the negative log-likelihood using the SOLVER add-in in Microsoft Excel, and asymptotic standard errors were obtained for each parameter.

Relative mortality between contingents was assessed retrospectively by summing the number of adults assigned to each contingent (based on first-year Sr:Ca profiles) in each year-class (range = 1999-2012; based on age determination) within the adult sample. Frequencies were used to calculate the proportion of individuals in the migratory contingent for each year-class, as well as across year-classes. Mean standing stocks of age-0 juvenile white perch caught in freshwater (resident) and brackish water (migrant) portions of the HRE in seine surveys conducted by Applied Science Associates (ASA 2014) were used to calculate migrant proportions for the same set of years, by the equation:

$$Migrant\ Proportion = \frac{n_{brackish}}{n_{fresh} + n_{brackish}}$$

where $n_{brackish}$ is the mean standing stock of juvenile white perch captured below the salt front from weeks 28-40 each year and n_{fresh} is the mean standing stock above the salt front for the same set of weeks (ASA 2014; see Gallagher 2016 for details). Contingent proportion estimates based on standing stocks were subsequently compared to estimates from retrospective analysis of white perch adults using a series of Chi-square tests. This analysis assumes that 1) otolith ageing enables accurate assignment of adults to year-classes, 2) the adult white perch sample (n = 229) was representative of the population, and 3) the juvenile white perch standing stock estimates are not biased between freshwater and brackish regions of the HRE.

Results

Contingent Classification

Resident and migratory white perch were observed in both year-classes of juvenile white perch. The resident contingent had consistently low Sr:Ca values, indicative of freshwater habitat use, with infrequent excursions above the 2 mmol/mol threshold (Figure 2). These excursions likely related to instrumental error, as they varied substantially from profile trends. The migratory contingent was classified as initially low Sr:Ca values early in life, followed by a rapid increase in Sr:Ca, and then consistently high Sr:Ca values, signifying dispersal and subsequent brackish water habitat use (Figure 2). Of sampled age-0 juveniles, the 2013 year-class was composed of 67% residents and 33% migrants, while the 2014 year-class was almost evenly split, with 51% residents and 49% migrants (Table 1). Both contingents were also present in the adult sample (Figure 3a), which was dominated by first-year residents (86% in fall 2013; 95% in spring 2014; 88% in fall 2014) and displayed very few first-year migrants (n = 21 overall; Table 2a).

Lifetime Sr:Ca profiles indicated that first-year migratory behavior persisted to adulthood in 70% of adult white perch. First-year migrants switched to a lifetime resident behavior in 29% of individuals (Figure 3b; Table 2b), while 31% of first-year residents became migratory later in life (Figure 3c; Table 2b). Furthermore, lifetime Sr:Ca profiles suggested that location of capture during the fall (i.e. outside the spawning season) was the best predictor of lifetime contingent membership, as all fish captured in Germantown (freshwater; n = 16) were lifetime residents, and all but one fish caught in Haverstraw (brackish; n = 22) were lifetime migrants (Table 2b). This was corroborated by logistic regression models, which indicated river km, salinity, and first-year contingent explained 81%, 78%, and 10% of the deviance in lifetime contingent membership, respectively (data not shown). Out of 22 lifetime migrants, 12 individuals (55%) dispersed at age-0, 6 dispersed at age-1 (27%), 3 dispersed at age-2 (14%) and one individual dispersed at age-7 (4%; data not shown).

Juvenile Contingent Comparisons

Juvenile white perch hatch dates were significantly influenced by contingent and year-class (F-test: $p < 0.001$), but not their interaction ($p > 0.1$; Table 3). Resident white perch hatched significantly later (Tukey: $p < 0.001$), while hatch dates were earlier on average in 2014 ($p < 0.01$; Figure 4a). A significant effect of year was observed on white perch length at 50 days (F-test: $p < 0.001$), but contingent and the interaction term were not significant ($p > 0.3$; Table 3). Contrasts indicated that white perch were significantly smaller at 50 days in 2013 relative to 2014 (Tukey: $p < 0.001$; Figure 4b). As a result of differences in hatch dates, mean temperature exposure during the first 50 days of life was significantly affected by contingent and year-class (F-test: $p < 0.003$), but not their interaction ($p > 0.2$; Table 3). Resident white perch were exposed to warmer temperatures across both year-classes (Tukey: $p < 0.001$), while temperatures were cooler on average in 2014 ($p < 0.01$; Figure 4c). Mean freshwater flow exposure during the first 50 days of life was significantly influenced by year (F-test: $p < 0.001$), while contingent and the interaction term had no effect ($p > 0.05$; Table 3). Contrasts showed that freshwater flow during this period was significantly higher in 2013 than in 2014 (Tukey: $p < 0.001$; Figure 4d).

Measures of primary and secondary production indicated that white perch prey availability during the larval period was generally diminished in 2013 relative to 2014 and the long-term average (1992-2012; Figure 5). Chlorophyll concentrations peaked earlier in 2013 than

2014 (Figure 5a), while copepod densities were slightly below average in both years (Figure 5b) and cladoceran densities (Figure 5c) were substantially lower in 2013. All three metrics, especially cladoceran density, were below-average late in the white perch larval period (weeks 24-28) during 2013, which followed a high freshwater flow event associated with the passing of Tropical Storm Andrea in June. This storm event was also responsible for the higher freshwater flows experienced by white perch larvae in 2013 than 2014 (Figure 4d).

Comparisons of juvenile white perch age-length relationships indicated that migrants displayed a significantly lower intercept (t-test: $p < 0.01$) and a significantly faster growth rate (> 1.5×) than residents in 2013 ($p < 0.01$; Table 4; Figure 6a). In contrast, there were no significant differences in intercepts or slopes between contingents in 2014 ($p > 0.6$; Table 4; Figure 6b). Using contrasts to compare each contingent across year-classes suggested that resident white perch had a significantly lower intercept (t-test: $p < 0.03$) and a significantly faster growth rate (> 2×) in 2014 relative to 2013 ($p < 0.02$), while there were no significant differences between years for the migratory contingent ($p > 0.5$; Table 4).

Adult Contingent Comparisons

Parameter estimates for von Bertalanffy growth models indicated that migratory adults grew faster ($k = 0.69$) and attained a larger maximum size ($L_\infty = 204$ mm) than the resident contingent ($k = 0.52$; $L_\infty = 194$ mm; Figure 6c). The 95% confidence intervals for each parameter estimate did not overlap between contingents, which indicate that observed differences in adult growth characteristics were statistically significant (Table 5).

Retrospective analysis of contingent representation based on first-year Sr:Ca profiles showed that residents were dominant in nearly all year-classes from 1999 to 2013. The percentage of each year-class in the migratory contingent ranged from 0% to 40%, and was approximately 9% across all year-classes (Table 6). In contrast, seine survey data suggested that the percentage of juvenile white perch in the migratory contingent each year ranged from 12% to 60%, and the overall percentage across years from 1999-2012 was 43% (Table 6). Chi-square tests indicated that differences in contingent proportions between retrospective and survey-based data sets were statistically significant in 6 out of 12 year-classes ($p < 0.05$), as well as across all year-classes ($p < 0.001$; Table 6). Thus, the representation of first-year migrants was significantly lower in adult samples assessed retrospectively compared to direct estimates based on field observations.

Discussion

Our analyses highlight the importance of ecological carryover effects in the life cycle of HRE white perch, as environmental conditions experienced early in life influence juvenile migration behaviors, which persisted into adulthood and significantly impacted lifetime growth, maturity and mortality. Formation of the two contingents followed from a larval carryover effect: across the two years studied, earlier hatch dates and exposure to cooler temperatures during the larval period were associated with migratory behavior, especially in 2013. Still, expected differences in larval growth between contingents were not detected. As age-0 juveniles, migrants exhibited faster growth rates in 2013, but there was no difference between contingents in 2014. Although differences in juvenile growth were inconsistent, migratory adults grew faster and attained a larger maximum size than residents, indicating that migratory behavior was associated with increased per-capita production. In addition, first-year migrants were underrepresented in the adult sample compared to expectations based on survey data, which may be indicative of

higher mortality rates in the migratory contingent. Overall, results suggest a strong latency in the influence of partial migration, with carryover effects throughout the life cycle of HRE white perch.

Carryover Effects of Early Life History

Reproductive timing, represented here by hatch date, is well-known to carry over to early life feeding, starvation, predation and associated vital rates in fishes and other taxa (Cushing 1975, Saino et al. 2011). Here, we build on limited set of discoveries that reproductive timing and environmental variability also influence systems of partial migration in temperate ecosystems (Pulido and Berthold 2010, Brodersen et al. 2011). Similar to results reported here, Kerr and Secor (2010) showed that resident white perch from a Chesapeake Bay tributary tended to originate from later hatch dates relative to migrants, which coincided with higher temperatures and zooplankton densities during the larval period (Kerr and Secor 2010). In the HRE, resident white perch experienced warmer temperatures and lower freshwater flows as larvae, which are positively associated with primary and secondary productivity in the HRE (Gladden et al. 1988, Cole and Caraco 2006). These differences were much more pronounced in the 2013 year-class, although the resident contingent in 2014 was still skewed towards later hatch dates, higher temperatures and lower flows.

In accordance with the threshold model for partial migration, we predicted that the migratory contingent would display lower larval growth rates than the resident contingent, which was not observed. Differences in larval growth rates between resident and migratory contingents in Chesapeake Bay white perch were small (0.10 mm d^{-1}; Kraus and Secor 2004a), but nonetheless greater than those observed in this study (0.02 mm d^{-1} in 2013; 0.04 mm d^{-1} in 2014). It is worth noting that we used a proxy for larval growth (otolith back-calculations; Campana 1990) rather than directly observing larval growth (e.g. larval size-at-age; Limburg 1999), which might have better resolved contingent growth differences.

Substantially reduced larval growth rates observed in 2013 (0.33 mm d^{-1} vs. 0.59 mm d^{-1} in 2014) were likely influenced by Tropical Storm Andrea, which made landfall and impacted the Hudson River watershed from June 5-8 (National Hurricane Center: http://www.nhc.noaa.gov/archive/2013/ANDREA.shtml) and caused an abrupt increase in freshwater flow in the middle of the white perch larval period (Figure 4d). The large pulse in flow was associated with subsequent declines in measures of primary and secondary productivity, especially cladoceran density, which persisted for a month or more after the storm (Figure 5). Interestingly, persistent declines in phytoplankton and zooplankton biomass were also observed after Hurricane Floyd and Tropical Storms Irene and Lee dramatically increased freshwater flow and turbidity in the HRE in 1999 and 2011 (Strayer et al. 2014). Limburg et al. (1999) concluded that seasonal peaks in copepod and cladoceran densities were the most important determinants of larval white perch growth and survival in the HRE, which is supported by our analysis (Figure 5).

Overall, this study provides some, albeit inconsistent, evidence that growth and energetic thresholds are important determinants of migration behavior in juvenile white perch, as predicted by the threshold model (Brodersen et al. 2008, Pulido 2011). However, the carryover effects of early-life characteristics on juvenile migration behaviors in fishes are likely shaped by ecosystem productivity and inter-annual variability in environmental conditions, and the nature of this environmental influence merits further research in other systems and over longer time periods than the two year-classes examined in this study.

Consequences of Partial Migration

Regardless of the cause of divergent migration behaviors, early life resident and migratory behaviors had lifelong consequences in HRE white perch. First-year migration behaviors persisted into adulthood in the majority (~70%) of individuals analyzed. In addition, multiple lines of evidence indicated that differences in habitat use between resident and migratory contingents carried over to influence lifetime growth characteristics (Figures 6a and 6c). On the other hand, we observed that a moderate number (31%) of first-year residents switched to become lifetime migrants later in life and vice-versa (29% of first-year migrants switched to become lifetime residents; Table 2b). Most lifetime migrants dispersed downriver in their first or second year of life, and the distribution of ages at dispersal was remarkably similar to previous observations by Kerr et al. (2011) in the Patuxent River. In contrast, Kerr et al. (2011) found no instances of migratory individuals reverting to resident behavior. The causes of this behavioral switching in white perch remain unknown, but may be related to energetic status, trade-offs between foraging opportunities and predation risk, or individual variation in behavioral plasticity (Secor 1999, Brodersen et al. 2014).

Dispersal to brackish habitats in the HRE was associated with increased growth in juvenile white perch in 2013, but not in 2014 (Figure 6a and 6b). This is similar to previous observations by Kraus and Secor (2004a), where seine survey data (10 years from July-September) indicated that juvenile white perch captured in brackish water were significantly larger than those in freshwater during some years, but not others. Inter-annual differences in contingent growth characteristics may have been driven by variability in the productivity gradient along the brackish-freshwater axis of the estuary, which would presumably influence food availability in the littoral habitats utilized by juvenile white perch (Klauda et al. 1988). For example, reduced growth in the resident contingent in 2013 compared to 2014 may have been related to lower food availability in the freshwater portion of the HRE as a result of high discharge levels (Strayer et al. 2008; Figure 4d). Faster growth in the migratory contingent observed in 2013 might suggest that the reduction in food availability may have been less severe in brackish habitats, as the HRE broadens and shoals in Haverstraw Bay, which tends to reduce water velocities (Gladden et al. 1988). Alternatively, differences between year-classes may be due to compensatory growth (Bertram and Chambers 1993, Kerr and Secor 2009). Suppressed larval growth rates in 2013 may have elicited compensatory growth during the juvenile period, and the migratory contingent may have exhibited stronger compensation than residents due to their exposure to lower temperatures and higher flow as larvae (Figure 4). These differences in environmental conditions between contingents were considerably dampened in 2014 (Figure 4), which may have reduced the potential for compensatory growth in this year-class.

More so than for juveniles, contingent membership had carryover effects on growth characteristics of adults. Migratory adults grew faster and reached larger sizes than residents, although there was considerable overlap in individual size-at-age between contingents, especially at older ages (Figure 6c). Enhanced growth in brackish habitats is consistent with previous surveys of HRE white perch, where from 1983 to 1988, adults were skewed towards larger sizes in the brackish portion of the estuary (LMS 1989). Similarly, Kraus and Secor (2005a) observed faster adult growth rates in migratory white perch in the Patuxent River ($k = 0.67$ for migrants; $k = 0.39$ for residents). Lifetime growth differences between contingents may be a result of higher productivity in the brackish portion of the HRE (Howarth et al. 2006), higher consumption rates and scope for growth in the migratory contingent (Kerr and Secor 2009), or some combination of

both. Interestingly, white perch in the Patuxent River attained larger maximum sizes than in the HRE (L_∞ = 217 mm; Kraus and Secor 2005a), which may reflect higher productivity in Chesapeake Bay (Fisher et al. 1988), especially after the zebra mussel invasion in the HRE (Cole and Caraco 2006). Enhanced growth in the migratory contingent likely translates to faster maturation and higher fecundity, as both metrics increase with body size in HRE white perch (Klauda et al. 1988), which may potentially carry over to influence reproductive success and population dynamics.

Retrospective analysis of contingent proportions across year-classes of adult white perch suggested that the migratory contingent was underrepresented compared to expectations based on seine survey data (Table 6). These differences might be attributed to higher morality in the migratory contingent if adult ages were accurate, seine survey data were not biased and our adult sample was representative of the population. Counting otolith annuli to age adult white perch has previously been validated by Casey et al. (1988) through the use of tetracycline marking. The seine survey data used to calculate expected contingent proportions samples the entire spatial extent of the HRE on a bi-weekly basis (ASA 2014; see Gallagher 2016) and is therefore unlikely to be biased between freshwater or brackish regions. However, due to the short duration and small spatial extent of our sampling efforts for adults (8-12 gillnet deployments within 3 sampling areas and over a period of 3 days in both spring and fall of 2014), biased contingent representation in the adult sample cannot be ruled out. Nonetheless, the difference in the relative abundance of the migratory contingent across year-classes was larger than expected (9% based on adult otoliths vs. 43% based on direct sampling). If the migratory contingent does experience higher mortality rates, this may be a consequence of compensatory growth. Kerr and Secor (2009) speculated that there could potentially be a trade-off between compensatory growth and mortality in migratory white perch, a trade-off reported in many fishes and other taxa (Mangel and Stamps 2001). Alternatively, increased predation owing to higher abundance of marine predators (e.g. adult bluefish and striped bass) could contribute to higher mortality rates in the migratory contingent (Limburg 2001, Heimbuch 2008).

As a result of larger size-at-age during the yearling and adult stages, it would seem likely that the migratory contingent contributes more production to the population on a per-capita basis than the resident contingent. However, if migratory white perch exhibit a higher mortality rate than residents, overall contributions to production could be substantially diminished. The dominance of first-year resident individuals in the adult sample suggests that this segment of the population has been important for maintaining overall abundance levels within the HRE, at least over the time period analyzed (1999-2013). Future modeling work (after Kerr et al. 2010) could elucidate whether the migratory contingent contributes to or diminishes overall population productivity.

Population responses to climate change in HRE white perch will likely be modified by the features of partial migration uncovered in this study. This study showed that seasonal and inter-annual variability in environmental conditions influence the carryover effects of early life history on partial migration in juvenile white perch, which in turn may impact population responses to climate change. Freshwater flow is projected to increase in the US Mid-Atlantic region (including the HRE) by 10-15% over the next century (Najjar et al. 2009), which will likely have significant impacts on ecosystem productivity (Strayer et al. 2014). Moreover, increased intensity or changed seasonality of flow could ultimately change zooplankton densities encountered by white perch larvae, which may alter the prevalence of juvenile migration behaviors, as well as the bioenergetics and growth characteristics of each contingent. Through

these mechanisms, partial migration dynamics, which are largely initiated during the first year of life, will likely play an important role in determining the persistence and resilience of the HRE white perch population in response to long-term increases in temperature and precipitation due to climate change. Similar interactions between environmental change and life-cycle characteristics should be considered when attempting to predict future population status in other temperate vertebrates (e.g. Pulido and Berthold 2010, Petitgas et al. 2013).

Conclusions

Partial migration in white perch within the HRE involved a sequence of ecological carryover effects throughout the life cycle, which likely have important effects at the population level. Environmental conditions experienced during the larval period influenced the adoption of different migration behaviors as juveniles, which then had a substantial impact on growth characteristics later in life. Similar carryover effects are likely to exist in other fishes, and deserve further study. This may be especially vital in populations that are impacted by human activities such as habitat loss, eutrophication, fishing and climate change, where carryover effects have the potential to obscure responses to these anthropogenic impacts and thereby reduce the success of conservation and management efforts (O'Connor and Cooke 2015, Secor 2015).

Acknowledgements

We thank John Young, the Hudson River Estuary Monitoring Program and Applied Science Associates for allowing us to access white perch standing stocks from Year-Class Reports, as well as David Strayer and the Cary Institute of Ecosystem Studies for their assistance with acquiring and analyzing Hudson River monitoring data. Steve Nack, Matt Siskey, Gray Redding and Alex Atkinson assisted with field collections and otolith processing. Jeremy Testa and Helen Bailey both provided constructive comments which improved a previous draft of this manuscript. This research was funded by the Hudson River Foundation under grant number 31479.

References

Applied Science Associates, Inc (ASA). 2014. 2013 Year class report for the Hudson River Estuary monitoring program and Central Hudson Gas and Electrical Corporation. New Hampton, NY.

Balon, E.K. 1981. Saltatory processes and altricial to precocial forms in the ontogeny of fishes. American Zoologist. 21(2): 573-596.

Bath, D.W., and O'Connor, J.M. 1985. Food preferences of white perch in the Hudson River estuary. New York Fish and Game Journal 32: 63-70.

Bertram, D.F., and R.C. Chambers. 1993. Negative correlations between larval and juvenile growth rates in winter flounder: implications of compensatory growth for variation in size-at-age. Marine Ecology Progress Series 96: 209-209.

Brodersen, J, P.A. Nilsson, L.A. Hansson, and C. Skov. 2008. Condition-dependent individual decision-making determines cyprinid partial migration. Ecology 89(5): 1195-1200.

Brodersen, J., A. Nicolle, P.A. Nilsson, C. Skov, C. Brönmark, and L.A. Hansson. 2011. Interplay between temperature, fish partial migration and trophic dynamics. Oikos, 120(12): 1838-1846.

Brodersen, J., B. Chapman, P. Nilsson, C. Skov, L.-A. Hansson, and C. Brönmark. 2014. Fixed and flexible: coexistence of obligate and facultative migratory strategies in a freshwater fish. PLoS ONE 9(3): e90294.

Campana, S.E. 1990. How reliable are growth back-calculations based on otoliths? Canadian Journal of Fisheries and Aquatic and Aquatic Sciences 47(11): 2219-2227.

Cary Institute of Ecosystem Studies (CIES). 2015. Hudson River Data. Accessed November 17, 2015. Available: http://www.caryinstitute.org/science-program/research-projects/hudson-river-ecosystem-study/hudson-river-ecosystem-study-data

Casey J.F., Minkkinen S.P., Solo J.B. 1988. Characterization of Choptank River populations of white, *Morone americana*, and yellow, *Perca flavescens*, perch. Final Report FY1986, Maryland Department of Natural Resources, Annapolis, MD.

Chapman, B.B., C. Brönmark, J.-Å Nilsson, and L.A. Hansson. 2011a. The ecology and evolution of partial migration. Oikos, 120: 1764–1775.

Chapman, B.B., K. Hulthén, D.R. Blomqvist, L.A. Hansson, J.Å. Nilsson, J. Brodersen, P. Anders Nilsson, C. Skov and C. Brönmark. 2011b. To boldly go: individual differences in boldness influence migratory tendency. Ecology Letters 14(9): 871-876.

Chapman, B., C. Skov, K. Hulthén, J. Brodersen, P. Nilsson, L.A. Hansson, and C. Brönmark. 2012a. Partial migration in fishes: definitions, methodologies and taxonomic distribution. Journal of Fish Biology 81: 479–499.

Chapman, B., K. Hulthén, J. Brodersen, P. Nilsson, C. Skov, L.A. Hansson, and C. Brönmark. 2012b. Partial migration in fishes: causes and consequences. Journal of Fish Biology 81: 456–478.

Cole, J. J., and Caraco, N. F. 2006. Primary production and its regulation in the tidal-freshwater Hudson River. *in:* J.S. Levinton and J.R. Waldman (eds). The Hudson River Estuary. Cambridge University Press, New York, NY. 107-120.

Conroy, C. W., P.M. Piccoli and D.H. Secor. 2015. Carryover effects of early growth and river flow on partial migration in striped bass *Morone saxatilis*. Marine Ecology Progress Series 541: 179-194.

Cooper, J., F. Cantelmo, and C. Newton. 1988. Overview of the Hudson River Estuary. *in*: L.W. Barnthouse, R.J. Klauda, D.S. Vaughan and R.L. Kendall (eds). Science, Law and Hudson River Power Plants. American Fisheries Society Monograph 4: 11-24.

Cushing D.H. 1975. Marine ecology and fisheries. Cambridge University Press, Cambridge, England. 292 pp.

Fisher, T., L. Harding, D. Stanley, and L. Ward. 1988. Phytoplankton, nutrients, and turbidity in the Chesapeake, Delaware, and Hudson estuaries. Estuarine, Coastal and Shelf Science 27: 61-93.

Gallagher, B.K. 2016. Influence of partial migration and environmental change on the population dynamics of white perch (*Morone americana*) within the Hudson River Estuary. M.S. Thesis, University of Maryland, College Park, MD.

Gillanders, B., C. Izzo, Z. Doubleday, and Q. Ye. 2015. Partial migration: growth varies between resident and migratory fish. Biology Letters 11(3):20140850.

Gladden, J., F. Cantelmo, J. Croom and R. Shapot. 1988. Evaluation of the Hudson River ecosystem in relation to the dynamics of fish populations. *in*: L.W. Barnthouse, R.J. Klauda, D.S. Vaughan and R.L. Kendall (eds). Science, Law and Hudson River Power Plants. American Fisheries Society Monograph 4: 69-88.

Heimbuch, D.G. 2008. Potential effects of striped bass predation on juvenile fish in the Hudson River. Transactions of the American Fisheries Society 137(6): 1591-1605

Houde, E. D. 1987. Fish early life dynamics and recruitment variability. *in*: R. D. Hoyt (ed). 10th Annual Larval Fish Conference. American Fisheries Society Symposium 2: 17-29.

Houde E.D., Morin L. 1990 Temperature effects on otolith daily increment deposition in striped bass and white perch larvae. *in:* International Council for the Exploration of the Sea, Copenhagen, Denmark, Council Meeting 1000: 5.

Howarth, R., D. Swaney, T. Butler, and R. Marino. 2000. Rapid communication: Climatic control on eutrophication of the Hudson River Estuary. Ecosystems 3: 210–215.

Howarth, R, R. Marino, D. Swaney and E. Boyer. 2006. Wasterwater and watershed influences on primary productivity and oxygen dynamics in the Lower Hudson River Estuary. *in:* J.S. Levinton and J.R. Waldman (eds). The Hudson River Estuary. Cambridge University Press, New York, NY, 121-136.

Jonsson, B., and N. Jonsson. 1993. Partial migration: niche shift versus sexual maturation in fishes. Reviews in Fish Biology and Fisheries 3: 348–365.

Kaitala, A., V. Kaitala, and P. Lundberg. 1993. A theory of partial migration. American Naturalist 142(1): 59-81.

Kerr, L., and D. Secor. 2009. Bioenergetic trajectories underlying partial migration in Patuxent River (Chesapeake Bay) white perch (*Morone americana*). Canadian Journal of Fisheries and Aquatic Sciences 66(4): 602-612.

Kerr, L., and D. Secor. 2010. Latent effects of early life history on partial migration for an estuarine-dependent fish. Environmental Biology of Fishes 89: 479–492.

Kerr, L., and D. Secor. 2011. Partial migration across populations of white perch (*Morone americana*): a flexible life history strategy in a variable estuarine environment. Estuaries and Coasts 35(1): 227-236.

Kerr, L., D. Secor, and P. Piccoli. 2009. Partial migration of fishes as exemplified by the estuarine-dependent white perch. Fisheries 34(3): 114-123.

Kerr, L.A., S.X. Cadrin, and D.H. Secor. 2010. The role of spatial dynamics in the stability, resilience, and productivity of an estuarine fish population. Ecological Applications 20(2): 497-507.

Klauda, R.J., J.B. McLaren, R.E. Schmidt and W.P. Dey. 1988. Life history of white perch in the Hudson River Estuary. *in*: L.W. Barnthouse, R.J. Klauda, D.S. Vaughan and R.L. Kendall (eds). Science, Law and Hudson River Power Plants. American Fisheries Society Monograph 4: 69-88.

Kraus, R.T., and D.H. Secor. 2004a. Dynamics of white perch *Morone americana* population contingents in the Patuxent River estuary, Maryland, USA. Marine Ecology Progress Series. 279: 247-259.

Kraus, R.T., and D.H. Secor. 2004b. Incorporation of strontium into otoliths of an estuarine fish. Journal of Experimental Marine Biology and Ecology 302(1): 85- 106.

Kraus, R.T., and D.H. Secor. 2005. Connectivity in estuarine white perch populations of Chesapeake Bay: evidence from historical fisheries data. Estuarine, Coastal and Shelf Science 64(1): 108-118.

Limburg, K. E. 2001. Through the gauntlet again: demographic restructuring of American shad by migration. Ecology 82(6): 1584-1596.

Limburg, K.E. and S.M. Turner. 2016. How common is "Non-textbook" migration in Hudson River blueback herring? Estuaries and Coasts: 39(4): 1262–1270.

Limburg, K.E., M.L. Pace, D. Fischer and K.K. Arend. 1997. Consumption, selectivity, and use of zooplankton by larval striped bass and white perch in a seasonally pulsed estuary. Transactions of the American Fisheries Society 126(4): 607-621.

Limburg, K.E., M.L. Pace, and K.K. Arend. 1998. Growth, mortality, and recruitment of larval *Morone* spp. in relation to food availability and temperature in the Hudson River. Fishery Bulletin 97: 80–91.

LMS (Lawler, Matusky and Skelly Engineers, Inc). 1989. Hudson River Estuary white perch adult and subadult stock assessment study: fall 1988. Final report to: Orange and Rockland Utilities, Inc. Pearl River, NY.

Mangel, M., and J. Stamps. 2001. Trade-offs between growth and mortality and the maintenance of individual variation in growth. Evolutionary Ecology Research 3: 583–593.

Mansueti, R.J. 1964. Eggs, larvae, and young of the white perch, *Roccus americanus*, with comments on its ecology in the estuary. Chesapeake Science 5(1-2): 3-45.

Morinville, G., and J. Rasmussen. 2003. Early juvenile bioenergetic differences between anadromous and resident brook trout (*Salvelinus fontinalis*). Canadian Journal of Fisheries and Aquatic Sciences 60: 401–410.

Morrison, W., and D. Secor. 2003. Demographic attributes of yellow-phase American eels (*Anguilla rostrata*) in the Hudson River estuary. Canadian Journal of Fisheries and Aquatic Sciences 60: 1487–1501.

Morrison W.E., Secor D.H. and Piccoli P.M. 2003. Estuarine habitat use by Hudson river American eels as determined by otolith strontium:calcium ratios. *in:* D.A. Dixon (ed). Biology, management and protection of catadromous eels. American Fisheries Society Symposium 33: 87-100.

Najjar, R., L. Patterson, and S. Graham. 2009. Climate simulations of major estuarine watersheds in the Mid-Atlantic region of the US. Climatic Change 95: 139–168.

O'Connor, and S. Cooke. 2015. Ecological carryover effects complicate conservation. Ambio 44: 582–591.

O'Connor, C., D. Norris, G. Crossin, and S. Cooke. 2014. Biological carryover effects: linking common concepts and mechanisms in ecology and evolution. Ecosphere 5(3): 1-11.

Pechenik, J. 2006. Larval experience and latent effects- metamorphosis is not a new beginning. Integrative and Comparative Biology 46: 323–333.

Petitgas, P., A.D. Rijnsdorp, M. Dickey-Collas, G.H. Engelhard, M.A. Peck, J.K. Pinnegar, K. Drinkwater, M. Huret, and R.D.M. Nash. 2013. Impacts of climate change on the complex life cycles of fish. Fisheries Oceanography 22(2): 121-139.

Pulido, F. 2011. Evolutionary genetics of partial migration– the threshold model of migration revis(it)ed. Oikos 120: 1776–1783.

Pulido, F., and P. Berthold. 2010. Current selection for lower migratory activity will drive the evolution of residency in a migratory bird population. Proceedings of the National Academy of Sciences 107(16): 7341-7346.

Saino, N., R. Ambrosini, D. Rubolini, J. von Hardenberg, A. Provenzale, K. Hüppop, O. Hüppop and 6 others. 2011. Climate warming, ecological mismatch at arrival and population decline in migratory birds. Proceedings of the Royal Society of London B: Biological Sciences 278(1707): 835-842.

Schindler, D., R. Hilborn, B. Chasco, C. Boatright, T. Quinn, L. Rogers, and M. Webster. 2010. Population diversity and the portfolio effect in an exploited species. Nature 465: 609-612.

Secor, D.H. 1999. Specifying divergent migrations in the concept of stock: the contingent hypothesis. Fisheries Research 43(1): 13-34.

Secor, D.H. 2015. Migration ecology of marine fishes. Johns Hopkins University Press, Baltimore, MD. 304 pp.

Secor, D.H., Dean, J.M., and Laban, E.H. 1991. Otolith removal and preparation for microstructural examination: a user's manual. The Electronic Power Research Institute and the Bell W. Baruch Institute for Marine and Coastal Sciences, Columbia, SC.

Skov, C., H. Baktoft, J. Brodersen, C. Bronmark, B. Chapman, L. Hansson, and P. Nilsson. 2010. Sizing up your enemy: individual predation vulnerability predicts migratory probability. Proceedings of the Royal Society B: Biological Sciences 278: 1414-1418.

Stoks, R., and A. Córdoba-Aguilar. 2012. Evolutionary ecology of Odonata: a complex life cycle perspective. Annual Review of Entomology 57: 249-265.

Strayer, D., K. Hattala, and A. Kahnle. 2004. Effects of an invasive bivalve (*Dreissena polymorpha*) on fish in the Hudson River estuary. Canadian Journal of Fisheries and Aquatic Sciences 61: 924-941.

Strayer, D.L., M.L. Pace, N.F. Caraco, J.J. Cole, and S. Findlay. 2008. Hydrology and grazing jointly control a large-river food web. Ecology. 89(1): 12-18.

Strayer, D., J. Cole, S. Findlay, D. Fischer, J. Gephart, H. Malcom, M. Pace, and E. Rosi-Marshall. 2014. Decadal-scale change in a large-river ecosystem. BioScience 64: 496-510.

United States Geological Survey (USGS). 2015a. National Water Information System data available on the World Wide Web (USGS Water Data for the Nation). Accessed June 9, 2015. Available: http://waterdata.usgs.gov/nwis/uv?site_no=01372058

United States Geological Survey (USGS). 2015b. National Water Information System data available on the World Wide Web (USGS Water Data for the Nation). Accessed June 9, 2015. Available: http://waterdata.usgs.gov/nwis/uv?site_no=01358000

Werner, E. E., and J. F. Gilliam. 1984. The ontogenetic niche and species interactions in size structured populations. Annual review of ecology and systematics. 393-425.

Wilbur, H.M. 1980. Complex life cycles. Annual review of Ecology and Systematics. 67-93.

Winemiller, K.O., and K. A. Rose. 1993. Why do most fish produce so many tiny offspring? American Naturalist 142: 585–603.

Zlokovitz, E., D. Secor, and P. Piccoli. 2003. Patterns of migration in Hudson River striped bass as determined by otolith microchemistry. Fisheries Research 63: 245-259.

Tables

Table 1. Numbers of juvenile white perch in each contingent from 2013 and 2014 year-classes (proportions in parentheses). The mean salinity observed at each location over the course of the sampling season (August-October) is shown for reference.

		Fall 2013			Fall 2014		
Location	**River km**	**Salinity**	**Residents**	**Migrants**	**Salinity**	**Residents**	**Migrants**
Coxsackie	202	0.16	29 (1.00)	0 (0.00)	0.13	7 (1.00)	0 (0.00)
Germantown	173	-	-	-	0.10	12 (1.00)	0 (0.00)
Poughkeepsie	120	0.14	2 (1.00)	0 (0.00)	-	-	-
Newburgh	93	1.26	14 (0.82)	3 (0.18)	0.15	10 (0.91)	1 (0.09)
Haverstraw	58	4.60	0 (0.00)	14 (1.00)	3.92	0 (0.00)	17 (1.00)
Tappan Zee	48	6.54	0 (0.00)	5 (1.00)	4.42	0 (0.00)	10 (1.00)
Total	-	-	45 (0.67)	22 (0.33)	-	29 (0.51)	28 (0.49)

Table 2. Numbers of adult white perch in each contingent based on first-year Sr:Ca profiles (a; proportions in parentheses) and lifetime Sr:Ca profiles (b) from fall 2013, spring 2014 and fall 2014 samples.

a

Location	River km	Fall 2013		Spring 2014		Fall 2014	
		First-Year Residents	First-Year Migrants	First-Year Residents	First-Year Migrants	First-Year Residents	First-Year Migrants
Germantown	173	1 (1.00)	0 (0.00)	37 (0.97)	1 (0.03)	60 (0.98)	1 (0.02)
Staatsburg	142	-	-	22 (1.00)	0 (0.00)	2 (1.00)	0 (0.00)
Poughkeepsie	120	6 (1.00)	0 (0.00)	-	-	-	-
Newburgh	93	4 (0.67)	2 (0.33)	32 (0.89)	4 (0.11)	-	-
Haverstraw	58	1 (1.00)	0 (0.00)	-	-	43 (0.77)	13 (0.23)
Total	-	12 (0.86)	2 (0.14)	91 (0.95)	5 (0.05)	105 (0.88)	14 (0.12)

b

First-Year Contingent	Location	River km	Season	Salinity	Lifetime Residents	Lifetime Migrants
Resident	Germantown	173	Fall	0.10	15 (1.00)	0 (0.00)
	Newburgh	93	Spring	0.20	6 (1.00)	0 (0.00)
	Haverstraw	58	Fall	4.13	1 (0.09)	10 (0.91)
	Total	-	-	-	22 (0.69)	10 (0.31)
Migrant	Germantown	173	Fall	0.10	1 (1.00)	0 (0.00)
	Newburgh	93	Spring	0.20	3 (1.00)	0 (0.00)
	Newburgh	93	Fall	1.26	1 (0.50)	1 (0.50)
	Haverstraw	58	Fall	4.13	0 (0.00)	11 (1.00)
	Total	-	-	-	5 (0.29)	12 (0.71)

Table 3. ANOVA results comparing white perch early-life characteristics between contingents and years. Temperature and flow are based on means calculated for the first 50 days of life for each individual (see text). Statistically significant p-values ($p < 0.05$) are denoted by an asterisk (*).

Response	Predictor	df	SS	MS	F-ratio	p-value
Hatch Date	Contingent	1	2824	2824	16.35	<0.001*
(ordinal day)	Year	1	6560	6560	37.98	<0.001*
	Interaction	1	327	327	1.89	0.172
	Error	120	20725	173		
Length at 50d	Contingent	1	14	14	0.72	0.399
(mm)	Year	1	5308	5308	274.94	<0.001*
	Interaction	1	4	4	0.21	0.647
	Error	120	2317	19		
Mean Temperature	Contingent	1	58.1	58.05	14.30	<0.001*
(°C)	Year	1	39.5	39.49	9.73	0.002*
	Interaction	1	6.2	6.25	1.54	0.217
	Error	120	487.2	4.06		
Mean Flow	Contingent	1	17668	17668	1.17	0.280
($m^3s^{-1}d^{-1}$)	Year	1	1819257	1819257	120.91	<0.001*
	Interaction	1	46313	46313	3.08	0.082
	Error	120	1805498	15046		

Table 4. ANCOVA coefficients and contrasts comparing intercepts and slopes from white perch age-length relationships across contingents and years. Note that year contrasts are 2013 vs. 2014 and contingent contrasts are resident vs. migratory. Statistically significant p-values ($p < 0.05$) are denoted by an asterisk (*).

Year	Contingent	Intercept	SE	t-statistic	p-value	Slope	SE	t-statistic	p-value
2013	Resident	30.42	16.69	1.82	0.071	0.33	0.14	2.34	0.021*
	Migratory	-10.59	10.93	-0.97	0.335	0.67	0.09	7.33	<0.001*
	Contingent Contrast	41.00	12.61	3.25	0.002*	-0.34	0.11	-3.20	0.002*
2014	Resident	-6.32	23.14	-0.27	0.785	0.68	0.20	3.36	0.001*
	Migratory	-11.16	16.68	-0.67	0.505	0.74	0.14	5.14	<0.001*
	Contingent Contrast	4.84	16.03	0.30	0.763	-0.06	0.14	-0.42	0.672
Year Contrast	Resident	36.74	16.03	2.29	0.024*	-0.35	0.14	-2.40	0.018*
	Migratory	0.58	12.60	0.05	0.964	-0.07	0.11	-0.60	0.553

Table 5. Parameter estimates, standard errors and 95% confidence intervals for von Bertalanffy growth models constructed for resident and migratory adult white perch. Each model was fit to data from fall-captured adults, with residents caught in Germantown, and migrants caught in Haverstraw (see text).

Contingent	n	Model R^2	Parameter	Estimate	SE	95% CI
Resident	112	0.78	k	0.52	0.02	0.48-0.56
			L_∞	194	1.35	191-196
Migratory	79	0.59	k	0.69	0.04	0.62-0.76
			L_∞	204	1.43	201-207

Table 6. Estimated proportions of age-0 juvenile white perch in the migratory contingent based on retrospective analyses of adult white perch otoliths (see text) and seine survey data where juveniles were sampled directly (ASA 2014; Chapter 2) from 1999-2012. Chi-square statistics and p-values are shown for each comparison of contingent proportions. Statistically significant p-values ($p < 0.05$) are denoted by an asterisk (*).

Year	Retrospective Proportion	Survey Proportion	χ^2	p-value
1999	0.00	0.47	0.00	0.950
2001	0.00	0.43	0.02	0.885
2003	0.40	0.35	0.05	0.816
2004	0.00	0.12	1.39	0.238
2005	0.00	0.49	9.43	0.002*
2006	0.00	0.59	3.47	0.062
2007	0.06	0.41	7.16	0.007*
2008	0.00	0.50	32.56	<0.001*
2009	0.00	0.60	32.70	<0.001*
2010	0.17	0.51	21.13	<0.001*
2011	0.21	0.16	0.10	0.757
2012	0.10	0.46	23.67	<0.001*
Total	0.09	0.43	99.06	<0.001*

Figures

Figure 1. Map of the Hudson River Estuary, with white perch sampling locations in freshwater (blue circles), brackish water (red circles) and transition zone (purple circles) regions.

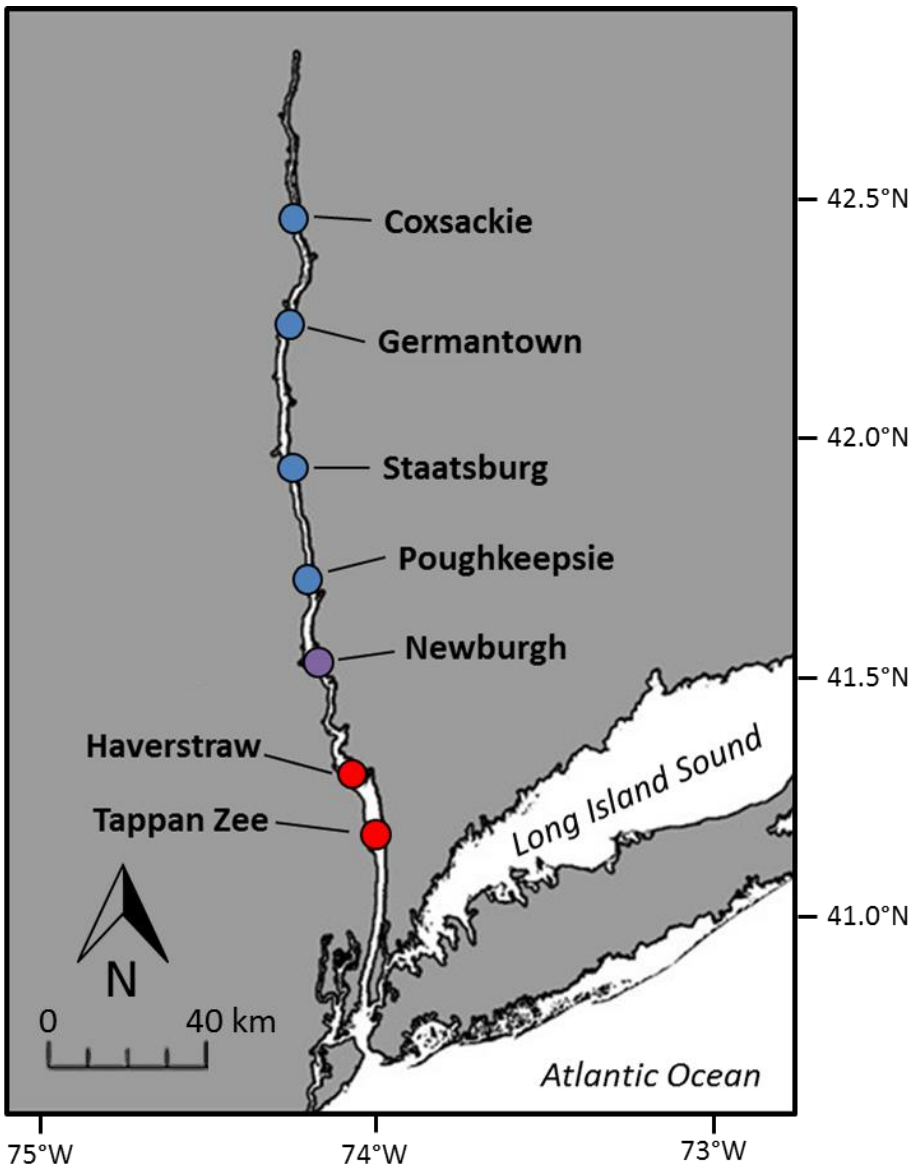

Figure 2. Otolith Sr:Ca profiles as a function of back-calculated total length from resident (blue) and migratory (red) juvenile white perch collected in 2013 and 2014. The 2 mmol mol^{-1} Sr:Ca threshold is displayed for reference (thick black line).

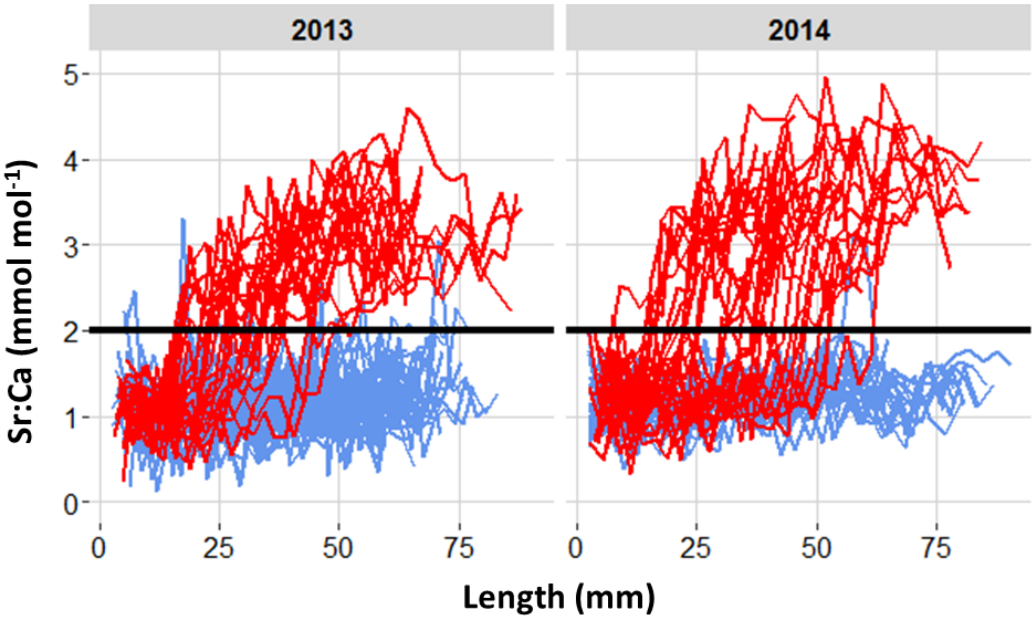

Figure 3. Sr:Ca profiles from migratory (red; left) and resident (blue; right) adult white perch based on first-year (a) and lifetime (b and c) transects. Lifetime profiles are grouped into first-year migrants (b) and first-year residents (c). Note the different x-axes in each plot, with (a) standardized to the proportion of the first annulus, while (b) and (c) are plotted over age with the first year excluded. The 2 mmol mol^{-1} Sr:Ca threshold is displayed for reference (thick black line).

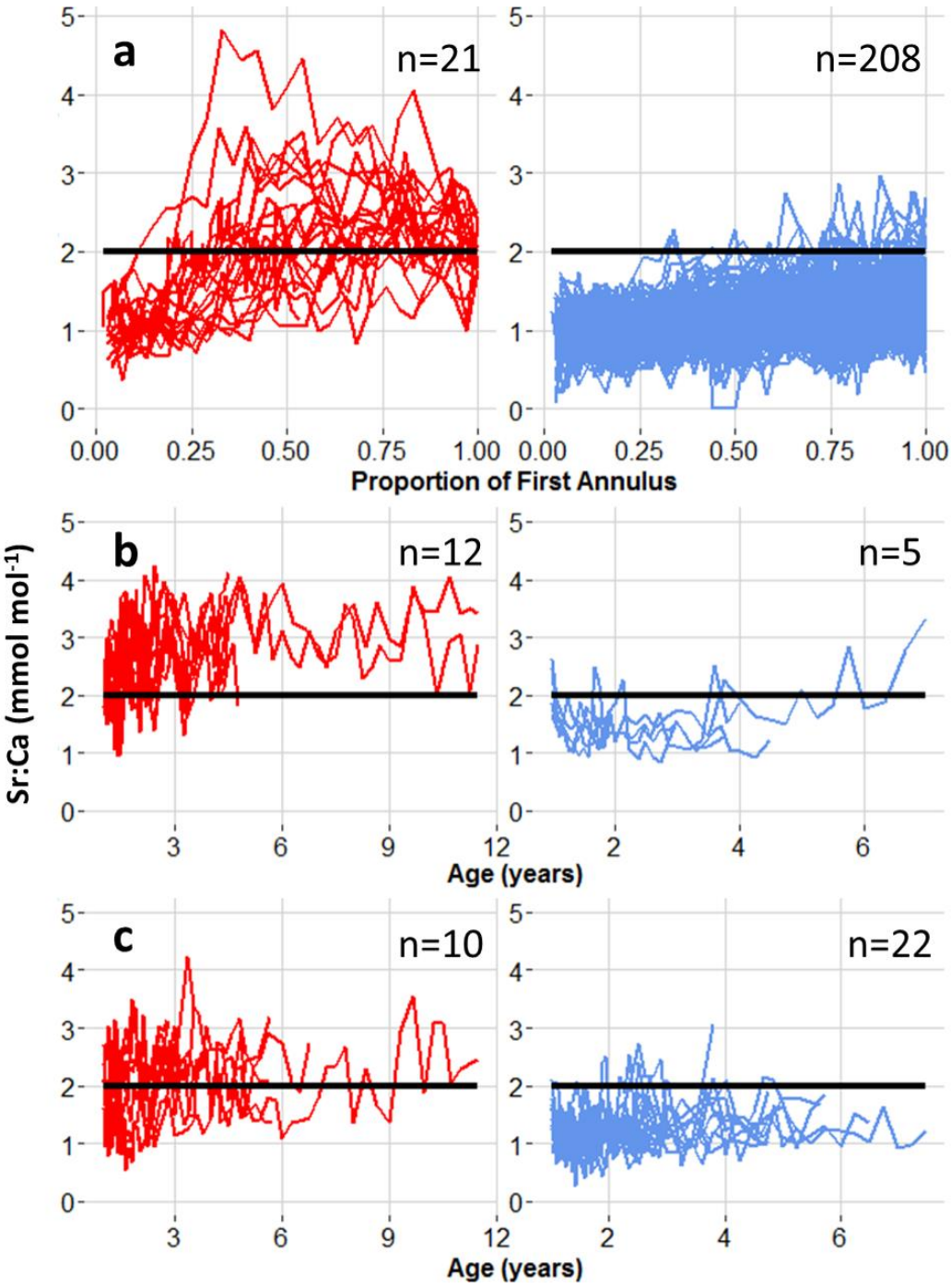

Figure 4. Box-whisker plots of hatch date (a), back-calculated length at an age of 50 days (b), and mean temperature (c) and freshwater flow (d) experienced by individuals during the first 50 days of life for resident (blue) and migratory (red) white perch in 2013 and 2014. The thick bar within each box represents the median, the edges of each box are the 25th and 75th percentiles, the whiskers are the 10th and 90th percentiles, and the open circles are data points outside this range. The letters above each box reflect whether means in each category were significantly different based on Tukey's HSD ($p < 0.05$).

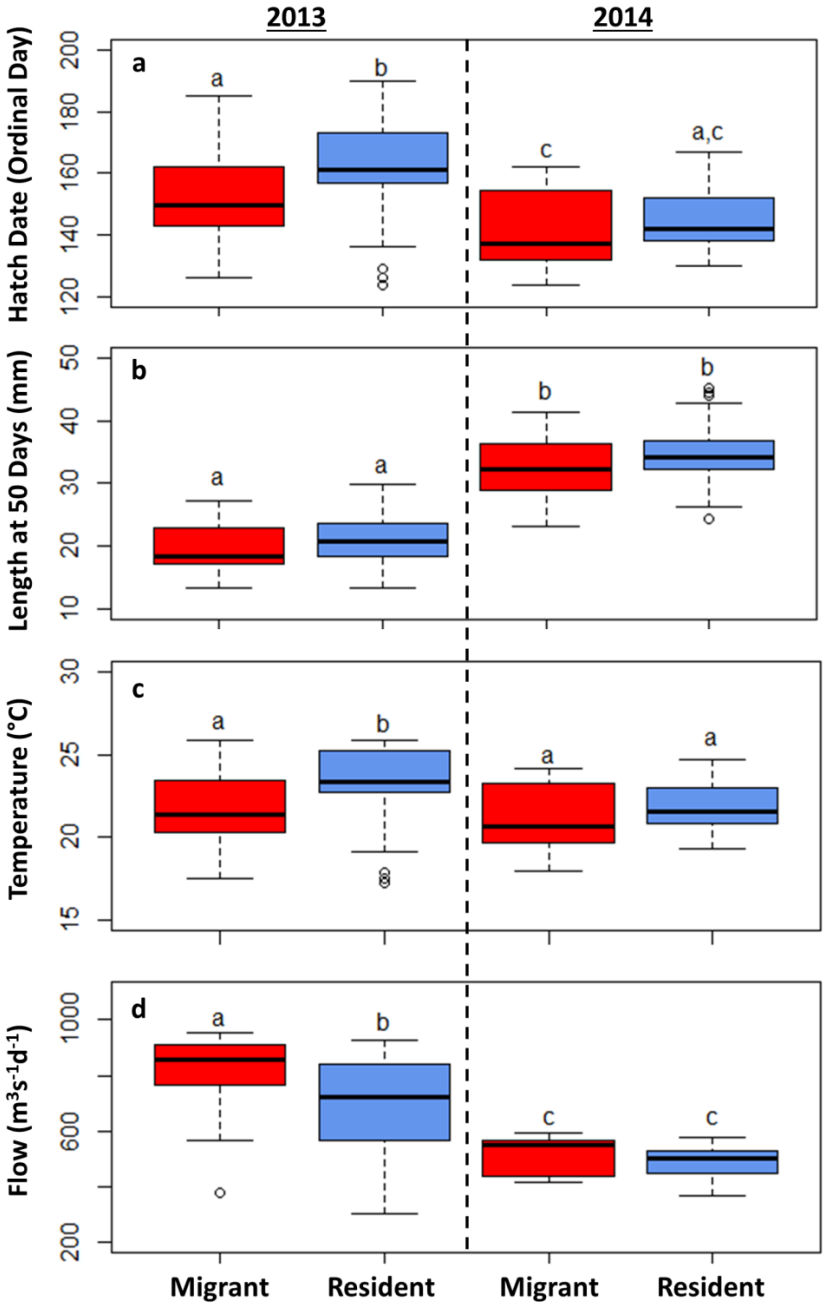

Figure 5. Plots showing bi-weekly chlorophyll-a concentration (a), copepod density (b) and cladoceran density (c) in 2013 (dark red line) and 2014 (dark blue line) in relation to long-term averages (thick black line) and 95% confidence intervals (dark gray shaded region) after the invasion of zebra mussels (1992-2012). The light gray shaded region highlights weeks 19-28, when white perch post yolk-sac larvae are most abundant (ASA 2014), and the dashed line denotes week 23 (June 5-8), when Hurricane Andrea impacted the HRE in 2013.

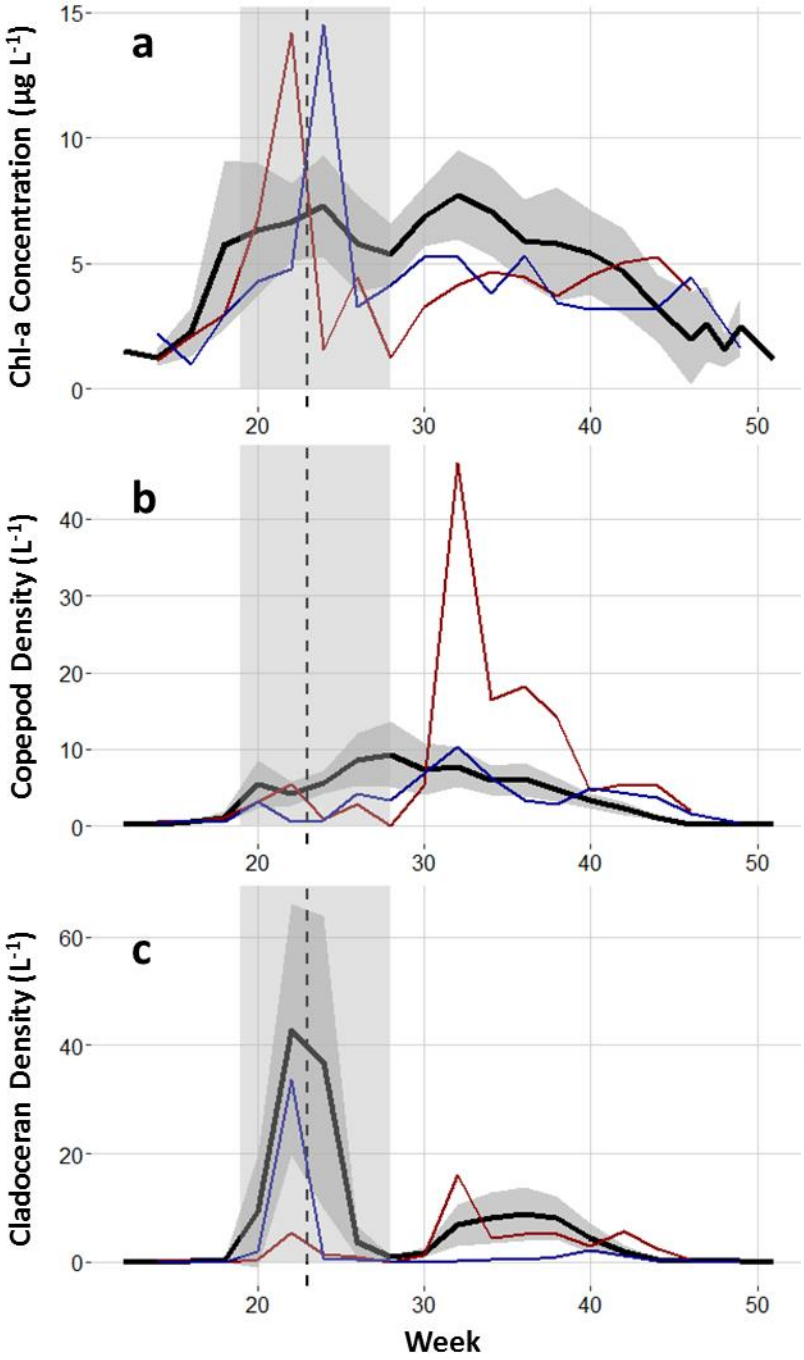

Figure 6. Age-length relationships plotted for resident (blue) and migratory (red) contingents of juveniles captured in 2013 (a), juveniles captured in 2014 (b) and adults captured in fall 2014 (c). The dashed black line in (c) denotes a length of 190 mm; when white perch in the HRE are fully mature (Klauda et al. 1988).

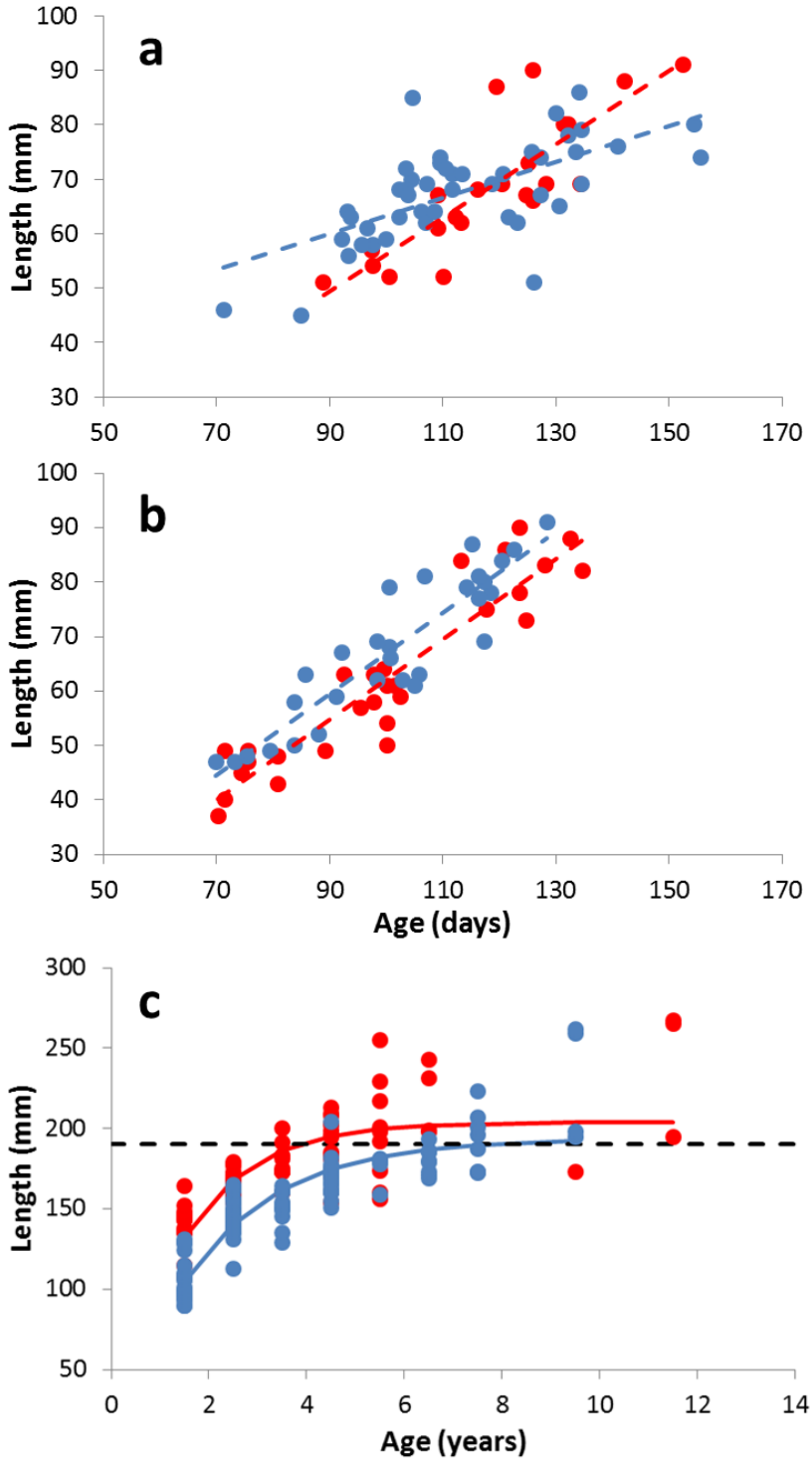

Appendix

Age Precision and Sr:Ca Verification

Before the rest of the sample was aged, a subsample of juvenile white perch otoliths (n = 31 in 2013, n = 25 in 2014) was analyzed in each year-class to ensure that ageing techniques were consistent. Each otolith in the subsample was aged three times so that precision, bias and average percent error between readings could be estimated. We calculated the error and bias between the first and second and between the second and third readings of each otolith in each year-class. In addition, the average percent error (APE) across all three readings was estimated for each otolith and averaged within each year-class. These metrics were calculated by the formulae:

$$Error = \sum_{j=1}^{n} \left| a_{ij} - a_{(i+1)j} \right|$$

$$Bias = \sum_{j=1}^{n} a_{ij} - a_{(i+1)j}$$

$$APE_j = \frac{\sum_{i=1}^{3} \left(\frac{\left| a_{ij} - a_{mean} \right|}{a_{mean}} \right)}{3} \times 100$$

where a_{ij} and $a_{(i+1)j}$ are the estimated ages obtained from otolith *j* in readings *i* and *i+1*, respectively, and a_{mean} is the mean age of otolith *j* across all three readings. To determine whether bias was statistically significant, we performed paired t-tests comparing the ages from the first and second readings and the second and third readings for each year-class. Error was less than 7 days for each reading and year-class (range: 2.2 - 6.0 days), and the mean APE across individuals was 3.5% (range: 0.5 - 8.4%) and 5.6% (range: 0.8 - 12.7%) in 2013 and 2014, respectively. There was a significant positive age bias ($p < 0.05$) between the first and second readings in both year classes (3.0 days in 2013; 2.6 days in 2014), but bias became non-significant ($p > 0.30$) when comparing the second and third readings (1.3 days in 2013; 0.6 days in 2014). Therefore, the third reading was used to estimate ages of each individual in the subsample for all subsequent analyses (see Statistical Analyses section in the Methods).

To verify the relationship between Sr:Ca and salinity, a subsample of juvenile fish otoliths in each year class (n = 28 in 2013, n = 20 in 2014) was selected and Sr:Ca measurements were taken at four or five locations along the edge each otolith, so that the mean Sr:Ca at the edge of the otolith could be related to salinity-at-capture (after Kraus and Secor 2004b). To estimate the relationship between otolith Sr:Ca and salinity, data from both year-classes were combined and an analysis of variance (ANOVA) was performed to test whether mean Sr:Ca at the edge of the otolith was significantly different between five salinity categories (0-1ppt, 2-3ppt, 3-4ppt, 4-5ppt and 6-7ppt) and post-hoc contrasts using Tukey's honestly significant difference

(HSD) were subsequently employed to compare Sr:Ca means across salinity levels. A positive relationship was expected to exist between salinity and Sr:Ca, similar to previous observations in white perch and congeneric striped bass (Secor et al. 1995, Kraus and Secor 2004b). The ANOVA detected significant differences in mean Sr:Ca across salinity categories ($p < 0.001$), and contrasts revealed that, as expected, Sr:Ca was significantly lower at salinities < 3 ppt compared to those at higher salinities ($p < 0.001$; Figure A2).

References

Kraus, R.T., and D.H. Secor. 2004b. Incorporation of strontium into otoliths of an estuarine fish. Journal of Experimental Marine Biology and Ecology 302(1): 85-106.

Secor, D. H., A. Henderson-Arzapalo and P.M. Piccoli. 1995. Can otolith microchemistry chart patterns of migration and habitat utilization in anadromous fishes? Journal of Experimental Marine Biology and Ecology 192(1): 15-33.

Table A1. Numbers of age-0 juvenile and adult (age-1 and older) white perch collected in each HRE sampling location and season. The number of fish used in analyses of otolith microstructure and microchemistry are displayed in parentheses. River km is distance from the mouth of the HRE.

			Fall 2013		Spring 2014	Fall 2014	
Location	**River km**	**Region**	**Juvenile**	**Adult**	**Adult**	**Juvenile**	**Adult**
Coxsackie	202	Fresh	38 (29)	1 (1)	-	16 (7)	-
Germantown	173	Fresh	-	-	120 (38)	99 (12)	296 (61)
Staatsburg	142	Fresh	-	-	70 (22)	15 (0)	6 (2)
Poughkeepsie	120	Fresh	9 (2)	11 (6)	-	-	-
Newburgh	93	Transition	31 (17)	7 (6)	122 (36)	30 (11)	-
Haverstraw	58	Brackish	24 (13)	2 (1)	-	53 (17)	86 (56)
Tappan Zee	48	Brackish	7 (5)	1 (0)	-	13 (10)	-
Total	-	-	109 (67)	22 (14)	312 (96)	226 (57)	388 (119)

Figure A1. Example electron micrographs of a juvenile (a) and adult (b) white perch otolith after each were analyzed for Sr:Ca profiles. The white squares in each image are microprobe points, where Sr:Ca was measured (see text). The core and sulcul regions were used as points of reference when determining the transect location in each otolith. Note the different regions used in analyses of adult Sr:Ca within the first year of life (First annulus) and after the first year of life (Lifetime).

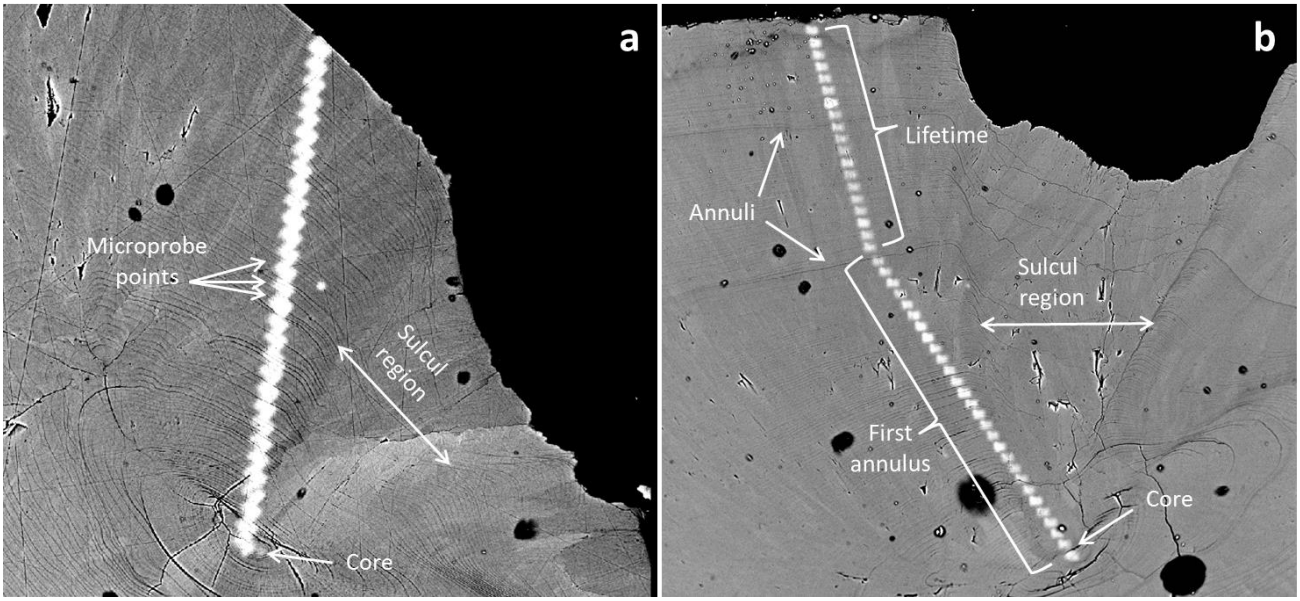

Figure A2. Box plots of mean Sr:Ca at the edge of juvenile white perch otoliths within five salinity-at-capture bins, with sample sizes displayed for each bin. The 2 mmol/mol Sr:Ca threshold is shown for reference (dashed black line). The thick bar within each box represents the median, the edges of each box are the 25th and 75th percentiles, the whiskers are the 10th and 90th percentiles, and the open circles are data points outside this range. The letters above each box reflect whether means in each category were significantly different based on Tukey's HSD ($p < 0.05$).

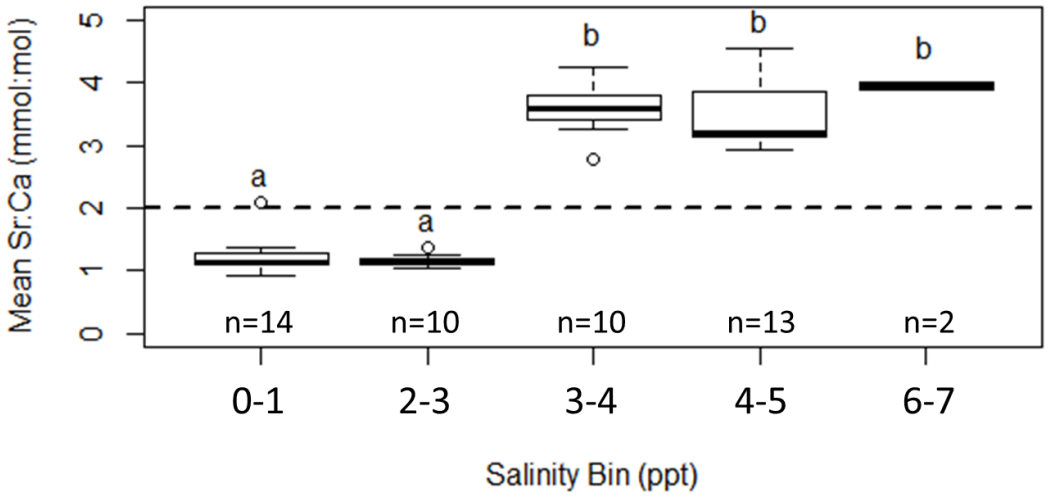

Intensified environmental and density-dependent regulation of white perch recruitment after an ecosystem shift in the Hudson River Estuary

By:

Brian K. Gallagher[1,2] and David H. Secor*

University of Maryland Center for Environmental Science, Chesapeake Biological Laboratory, P.O. Box 38, Solomons, MD 20688, USA

Footnotes:

[1]Corresponding author (e-mail: bkgallagher@vims.edu, phone: 804-684-7351)

[2]Present address: Virginia Institute of Marine Science, College of William and Mary, P.O. Box 1346, Gloucester Point, Virginia, 23062, USA

*e-mail: secor@umces.edu

Abstract

Long-term monitoring data were used to test whether the invasion of zebra mussels in the Hudson River Estuary (HRE) in 1991 altered the influence of density-dependence and environmental conditions on life-stage transitions, growth and partial migration in white perch (*Morone americana*). During the post-invasion period (1992-2013), we estimated standing stocks of white perch eggs, yolk-sac larvae (YSL), post yolk-sac larvae (PYSL), young-of-the-year (YOY) and adults, as well as indices of YOY growth and spatial distribution. A series of linear and nonlinear functions were employed to model life-stage transitions, while the effects of six environmental and density-dependent variables on YOY growth and partial migration were quantified. Comparisons to pre-invasion observations (1974-1991), indicated that egg-YSL, PYSL-YOY and YOY-yearling transitions changed significantly after the invasion, while PYSL abundance developed a stronger negative effect on YOY growth. The PYSL-YOY transition became more sensitive to density-dependence and freshwater flow from 1992-2013, which is consistent with diminished abundance and increased environmental sensitivity of the forage base in the HRE reported after the zebra mussel invasion.

Introduction

Examining the potential of regime shifts to intensify, dampen or reverse population responses to environmental change is an important and broadly relevant problem in fisheries research. Regime shifts in aquatic ecosystems alter ecosystem characteristics, species interactions, as well as the population dynamics of individual species within the system (Hare and Mantua 2000, Collie et al. 2004). Threshold changes can drive ecosystems into alternative stable states, which control how populations and communities interact and respond to environmental conditions and external forcing (Strayer et al. 2008, Planque et al. 2010), and can thereby confound traditional management strategies that depend on stationarity (Folke et al. 2004).

Important consequences of regime shifts and long-term environmental change include alterations in primary and secondary production, which influence the productivity and spatial distribution of fish populations. In particular, reductions in prey availability have the potential to intensify density-dependence in growth and recruitment. For example, grazing pressure from the invasive overbite clam (*Potamocorbula amurensis*) played an important role in shifting the abundance and composition of the zooplankton community in the San Francisco Estuary (Kimmerer et al. 1994), which contributed to food limitation and subsequent declines in delta smelt (*Hypomesus transpacificus*), threadfin shad (*Dorosoma petenense*) and striped bass (*Morone saxatilis*) abundance (Feyrer et al. 2007). For striped bass, these changes in the forage base were associated with a density-dependent reduction in carrying capacity, leading to long-term declines in recruitment to age-3 (Kimmerer et al. 2000). In addition to changing density-dependent processes, shifts in population state brought about by regime shifts, climate

oscillations or fishing pressure can potentially alter how populations respond to environmental variability (Planque et al. 2010). For example, truncated age structure of Barents Sea cod (*Gadus morhua*) due to fishing resulted in a strengthening of the correlation between temperature and recruitment (Ottersen et al. 2006). Similarly, Brander (2005) reported that recruitment across six European cod stocks from 1963-2001 was more strongly influenced by the winter North Atlantic Oscillation when spawning stock biomass was low. Thus, determining whether regime shifts alter the state of a population and, subsequently, change the responses of one or more life-stages to density-dependence or environmental conditions is a key step in incorporating species responses to climate change into assessment and management frameworks (Collie et al. 2004).

Due to the availability of extensive long-term monitoring data that overlaps with considerable changes in the ecosystem, the Hudson River Estuary (HRE) represents a model system to study the effects of regime shifts and long-term environmental change on population dynamics (Strayer et al. 2014a). The HRE is a large (243 km in length) estuary that receives most of its freshwater input from the Troy Dam at the head of the estuary (Figure 1; Cooper et al. 1988). Through its effects on turbidity and advection, freshwater flow strongly controls primary production in the HRE, with conditions of low flow resulting in increased water clarity and residence time and generally leading to higher rates of primary and secondary productivity (Gladden et al. 1988, Howarth et al. 2000). Freshwater flow and temperature have both increased in the HRE since 1950 (Seekell and Pace 2011, Strayer et al. 2014a) and are projected to continue increasing over the next century (Najjar et al. 2009). In addition to these long-term changes, the zebra mussel (*Dreissena polymorpha*) invaded the tidal freshwater portion of the HRE in 1991, which triggered rapid and extensive changes in the HRE ecosystem. Grazing pressure increased exponentially, greatly reducing the biomass of phytoplankton, pelagic zooplankton and benthic invertebrates (Caraco et al. 1997, Pace et al. 1998, Strayer and Smith 2001). As a consequence of their role in reducing the forage base, zebra mussels had demonstrable impacts on many fishes, with pelagic species generally displaying reduced abundance and growth rates after the invasion, as well as downriver shifts in their spatial distribution (Strayer et al. 2004). However, increased water clarity after the invasion enhanced primary and secondary production in littoral habitats, resulting in increased abundance, higher growth rates and upriver distributional shifts in many littoral fishes (e.g. centrarchids; Strayer et al. 2004). Importantly, the zebra mussel invasion also increased the sensitivity of the abundance of many organisms to freshwater flow. For example, the abundance of littoral benthic invertebrates and littoral fishes has developed a stronger inverse relationship with freshwater flow than was observed before the invasion (Strayer et al. 2008). More recently, the abundance and size of zebra mussels in the HRE have decreased (Strayer and Malcom 2006), allowing some recovery of zooplankton and benthic invertebrate stocks (Pace et al. 2010, Strayer et al. 2011), which in turn has alleviated the reduction in growth rates previously observed in some fish species (Strayer et al. 2014b).

White perch (*Morone americana*) is a dominant fish species in the HRE which completes its entire life-cycle within the estuary, and is therefore likely to be sensitive to large-scale changes in the HRE ecosystem. Furthermore, because white perch larvae are pelagic, but subsequently become demersal and select littoral habitats as juveniles (Mansueti 1964), different life-stages are likely to respond to ecosystem change in distinct ways. Life history characteristics of white perch have been shown to be sensitive to ecosystem attributes (Tuckett et al. 2013). For example, white perch recruitment in several Chesapeake Bay tributaries is positively associated with freshwater flow (Kraus and Secor 2005), likely due to a strengthening of the estuarine

turbidity maximum in high flow years, which enhances larval retention and feeding success (North and Houde 2003). Similarly, first-year growth in Oneida Lake white perch is positively influenced by summer water temperatures and measures of primary and secondary productivity (VanDeValk et al. 2016). Previous studies of young-of-the year (YOY) white perch growth and recruitment in the HRE suggested that growth is unrelated to YOY abundance, but positively influenced by water temperature (Klauda et al. 1988), while recruitment to the YOY stage was unrelated to larval abundance, temperature or flow (Pace et al. 1993).

Estuarine white perch display partial migration, characterized by a resident contingent that remains in natal freshwater habitats throughout life, and a migratory contingent, which disperses from the natal habitat and primarily uses brackish water (Kraus and Secor 2004, Kerr and Secor 2011). Inter-annual variability in the numerical dominance of each contingent is modulated by freshwater flow in Chesapeake Bay tributaries, such that residents dominate in drought conditions and migrants dominate in wetter years (Kraus and Secor 2004). Recent evidence confirmed that white perch in the HRE also display partial migration (Gallagher 2016) and that the resident (freshwater) contingent is consistently more abundant. Migratory white perch in the HRE grow and mature faster than residents (Gallagher 2016), and therefore may contribute disproportionately to the productivity of the population in a similar manner to Chesapeake Bay populations (Kerr et al. 2010). Although white perch recruitment, growth and migration dynamics have been well-documented in the HRE and elsewhere, the influence of density-dependence, temperature and freshwater flow on these early life characteristics may have been altered by the zebra mussel invasion. Such changes, if present, could potentially impact the status of the population in the future, as temperature and precipitation are both projected to increase (by 4°C and 7% on average, respectively) in the HRE over the next century (Najjar et al. 2009).

Our objective was to evaluate whether the zebra mussel invasion modified the relative influence of density-dependence and environmental conditions on the recruitment, growth, and migration dynamics of YOY white perch in the HRE. We focused on three questions: 1.) Are white perch early life-stage abundances related to the abundance and environmental conditions experienced by their previous life-stage? 2.) Do density-dependence and environmental variables affect growth and partial migration dynamics in YOY white perch? and 3.) Has the zebra mussel invasion altered the responses of white perch life-stage transitions, growth and partial migration to density-dependent and environmental factors? To address these questions, we applied a series of stage-structured models and exploratory statistical analyses to an extensive set of environmental and biological monitoring data collected after the invasion of zebra mussels (1992-2013). These findings were then compared to previous studies of YOY white perch recruitment (Pace et al. 1993), growth (Klauda et al. 1988, LMS 1989) and spatial distribution (LMS 1989) before the zebra mussel invasion, to test whether the regime shift brought about by the invasion has altered these early-life characteristics in white perch through changed functional relationships with abundance, flow, and other environmental variables.

Methods

Study area

The HRE is a large, partially mixed estuary characterized by unusually low sinuosity and strong tidal influence compared to many estuaries, with a watershed spanning approximately 12,900 km^2 (Figure 1; Geyer and Chant 2006). The grand mean temperature and flow in the HRE

from 1951-2013 are 12.5°C and 402 $m^3s^{-1}d^{-1}$, respectively, although both metrics have a positive trend over this time period, with accelerated rates of increase since 1990 (Figure 2). In addition, the position of the salt front in the HRE is strongly influenced by freshwater flow (Cooper et al. 1988) and can vary by 20-60 km on a seasonal basis (Geyer and Chant 2006). The position of the salt front controls the salinity distribution within the river, which directly influences spatial variation in the abundance and composition of zooplankton, benthic invertebrate and fish communities (Gladden et al. 1988, Strayer and Smith 2001, Daniels et al. 2005).

White perch abundance, growth and migration data

Standing stock abundance estimates were obtained from annual reports prepared by Applied Science Associates, Inc. (ASA 2014) for white perch eggs, yolk-sac larvae (YSL), post yolk-sac larvae (PYSL), young-of-the-year juveniles (YOY) and adults (yearling and older) from 1992-2013. These data are collected in "Year-class Reports" for the Hudson River Estuary Monitoring Program, an extensive survey funded by four utility companies which has been in place since 1974. Data were drawn from three separate surveys, which targeted different life-stages. Egg, YSL and PYSL standing stocks were estimated from the Longitudinal River Survey (LRS); YOY standing stock was estimated from the Utilities Beach Seine Survey (UBSS) and adult white perch standing stock was based on the Fall Juvenile Survey (FJS). Each of these surveys follows a random sampling design, stratified by depth zones. A summary of the depth strata, time-span, gear and mesh sizes used in each of the three surveys can be found in Table S.1. The spatial and temporal resolution of each survey is relatively high and consistent (~1000 samples × $year^{-1}$), with fish sampling occurring in the same 13 river sections, spanning from Albany to New York City (Figure 1), on weekly or bi-weekly intervals depending on the survey and time of year.

For each life-stage in each survey, mean densities (number × m^{-3}) within each stratum and river section were calculated each sampling week. These densities were subsequently converted into river-wide standing stock estimates by multiplying the density by the stratum volume in each river section, and summing across strata and river sections (ASA 2014). Time periods chosen for averaging the standing stocks of each life-stage were based upon the mean (weekly mean > 1% of the grand mean) and coefficient of variation (CV < 2) of standing stocks during each week across years from 1992-2013, in order to select periods of relatively high and stable abundances. For white perch life-stages sampled in the LRS, the time periods selected were weeks 17-25, 18-26 and 19-28 for eggs, YSL and PYSL, respectively, while weeks 28-40 and 27-41 were used in analyses of YOY (from the UBSS) and adults (from the FJS), respectively (Table S.1). Due to likely differences in sampling efficiency (e.g. extrusion from nets) and stage duration between early life-stages, standing stocks of each life-stage should be interpreted as indices of abundance, rather than estimates of the absolute abundance of each stage in the HRE.

YOY white perch standing stocks were analyzed in relation to the position of the salt front to separate resident and migratory contingents during each year. Daily salt front positions in the HRE have been computed by the US Geological Survey (USGS) since 1991 (USGS 2015a; http://ny.water.usgs.gov/projects/dialer_plots/saltfront.html). Data were not available for most of 2012, and in this year daily salt front positions were estimated using a multiple regression model from Cooper et al. (1988), with lagged freshwater flow and tidal amplitude data as the independent variables. The predicted daily salt front positions from the regression model were proportional to observed values reported by the USGS from January-February in 2012

(slope = 0.97; R^2 = 0.45; data not shown). Based upon the mean salt front position each week, river sections were designated as freshwater (above) or brackish water (below). Associated freshwater and brackish water standing stocks were then averaged over weeks 28-40. The proportion of YOY that were in the migratory (i.e. brackish) contingent was calculated each year (hereafter migrant fraction) and used as an index of migratory contingent prevalence. In addition, mean YOY total length at the end of the growing season (hereafter YOY length) was calculated each year as the mean river-wide size reported during the last two sampling weeks of the UBSS (first and third weeks of October; weeks 40 and 42). These mean lengths served as an index of YOY white perch somatic growth.

In addition to standing stock estimates, we also utilized a set of annual abundance indices for white perch eggs, YSL, PYSL, YOY and yearlings reported from 1974-2013 in Year-class Reports. These indices were calculated from the same surveys as the standing stock estimates and show high correlations to the annual mean standing stocks from 1992-2013 ($R^2 > 0.90$ in all cases; data not shown). However, in order to account for differences in sampling duration between early (1974-1987) and recent (1988-2013) survey time periods, the calculation of each index utilized a different set of sampling weeks than the mean standing stocks (see above), with YOY and yearling indices drawn from weeks 33-40; while egg, YSL and PYSL indices relied on a different set of 7-week periods each year, depending on the week in which the cumulative density reached 5% of the annual sum of densities over all sampling weeks (ASA 2014). Despite these discrepancies, the strong correlation of each annual abundance index to the annual mean standing stock and the longer duration of the index data set supported quantitative comparisons of white perch life-stage transitions before (1974-1991) and after (1992-2013) the zebra mussel invasion (see Statistical Analyses below).

Environmental and biological variables

Daily temperature and freshwater flow records were obtained respectively from a pumping station in Poughkeepsie at river km 120, (USGS 2015b; http://waterdata.usgs.gov/nwis/uv?site_no=01372058) and the Green Island monitoring site at the head of the estuary in Troy, NY (USGS 2015c; http://waterdata.usgs.gov/nwis/uv?site_no=01358000). In addition to being the richest data set, freshwater flow at Green Island represents approximately 70% of freshwater input into the HRE (Howarth et al. 2006). Daily temperature and flow values were averaged during spring (April-June) and summer (July-September) months to calculate seasonal means for each year. In addition, estimates of annual mean zebra mussel filtration rates during the growing season (May-September) from 1992-2013 were received from the Cary Institute of Ecosystem Studies (D. Strayer, personal communication; see Strayer and Malcom 2006 for details) and used to examine possible effects of zebra mussels on white perch early life-stages. Descriptive statistics for all white perch early life-history, biological and environmental variables can be found in Table 1.

Statistical analyses

A life-cycle analysis was employed to model the transitions across early life-history stages of HRE white perch. We used the methods developed by Paulik (1973) to decompose the stock-recruitment relationship of HRE white perch (in this study, the relationship between adult and YOY standing stocks) into a series of life-stage transitions leading up to the YOY stage. Similar life-cycle analyses have been successfully applied to describe the life-stage transitions in North Sea herring (Nash and Dickey-Collas 2005) and assess changes in these transitions over

time (Payne et al. 2009). Transitions were modeled in two possible ways, depending on whether the relationship was linear or non-linear. For linear transitions, the mean standing stock of life-stage *s* (N_s) was modeled as a proportion of the mean standing stock of one or more previous life-stages (N_{s-1}) by the equation:

$$(1) \qquad N_s = \alpha(N_{s-1})$$

where α is a density-independent multiplier. We estimated α using simple linear regression with the intercept fixed at 0, reflecting traditional assumptions in stock-recruit theory (Quinn and Deriso 1999). Similarly, non-linear transitions were modeled using a Ricker stock-recruitment function by the equation:

$$(2) \qquad N_s = \alpha(N_{s-1})e^{-\beta(N_{s-1})}$$

where α is once again the density-independent multiplier, and β is the density-dependent parameter, equal to the inverse of the value of N_{s-1} which corresponds to the maximum value of N_s (Quinn and Deriso 1999). To test for environmental effects on non-linear transitions, additional Ricker models including each combination of temperature, freshwater flow (both from the time-period over which N_{s-1} was averaged) and annual mean zebra mussel filtration rates as covariates were constructed by the equation:

$$(3) \qquad N_s = \alpha(N_{s-1})e^{-\beta(N_{s-1})-\sum\gamma_E(E)}$$

where Σ is a summation term for all environmental variables (E) in a given model, and γ_E represent the coefficients corresponding to each environmental variable. All models (n=7) were then compared and the best model was selected using Akaike's information criterion corrected for small sample sizes (AICc; Burnham and Anderson 2002). Ricker models were linearized to the form $\log_e(N_s \times N_{s-1}^{-1}) = \log_e(\alpha) - \beta(N_{s-1})$ (equation 2) or $\log_e(N_s \times N_{s-1}^{-1}) = \log_e(\alpha) - \beta(N_{s-1}) - \Sigma\,\gamma_E(E)$ (equation 3) and the parameters were estimated using simple linear regression (two parameters) or multiple regression (three or more parameters).

The effects of environmental and density-dependent factors on YOY white perch growth and partial migration from 1992-2013 were explored using a Pearson correlation analysis. The response variables of interest were YOY length (a proxy for growth) and the migrant fraction (an index of migratory contingent prevalence), while the predictors in both analyses were the mean summer temperature and flow, annual mean zebra mussel filtration rates (environmental factors), as well as the mean standing stocks of white perch YOY and PYSL (density-dependent factors). In addition, because the availability of brackish habitat in the HRE may influence white perch growth and migration, the mean proportion of the total HRE shoal volume in the brackish portion of the estuary during the summer was calculated and used as a predictor (hereafter termed brackish shoal proportion). This proportion was calculated by assigning the 13 river sections (Figure 1) into freshwater and brackish regions based on the mean summer salt front position, summing the shoal volumes of all brackish sections (depth < 6 m; reported in ASA 2014) and dividing by the total shoal volume of the HRE (~345 million m^3). For comparison, correlations reported in previous studies of YOY white perch growth and spatial distribution in the 1970s and 80s (Klauda et al. 1988, LMS 1989) were compiled and compared to estimated correlations from 1992-2013. These previous studies selected a Type-I error rate of 0.05 and did not adjust p-values of their correlations for multiple comparisons. Therefore, for the 12 correlations analyzed in the more recent period, we selected the same Type-I error rate and did not make any adjustments to ensure that correlations were comparable across time periods.

Indices of white perch egg, YSL, PYSL, YOY and yearling (age-1) abundance were compared between pre-invasion (1974-1991) and post-invasion (1992-2013) periods. Two-sample t-tests assuming unequal variance were performed to test for differences in the mean

index of abundance between these two time periods. Subsequently, life-stage transitions during each time period were modeled using the functional relationships described previously (equations 1, 2 and 3). Differences in parameter estimates between pre-invasion and post-invasion periods were analyzed using analysis of covariance (ANCOVA) and post-hoc contrasts. The relationships between the egg index and the YOY index, as well as the yearling index and the YOY index from the previous year were also modeled for both time periods.

Results

Life cycle analysis

The stock-recruitment (adult-YOY) relationship for white perch in the HRE from 1992-2013 (Figure 3) was described by a Ricker model with freshwater flow during the PYSL period as a covariate ($\log_e(\alpha) = 0.91$; $\beta = 5.61 \times 10^{-4}$; $\gamma_{flow} = 2.18 \times 10^{-3}$; Table 2). Paulik diagrams decomposing the stock-recruitment relationship into a series of life-cycle transitions (Figure 3) illustrated that the shape of the stock-recruitment relationship was primarily driven by the transition from PYSL to YOY (Figure 3; $\log_e(\alpha) = -4.72$; $\beta = 2.21 \times 10^{-6}$; $\gamma_{flow} = 1.89 \times 10^{-3}$; Table 2). The standing stock of eggs, YSL and PYSL were proportional to the standing stock of their previous life-stages in a density-independent manner ($p < 0.001$; Table 2). The standing stocks of white perch YSL and PYSL were also proportional to the adult standing stock. While each α estimate for linear transitions was positive and statistically significant, it is important to emphasize that the standing stocks of each life-stage are indices of abundance, and therefore α estimates do not represent the actual proportionality between life-stage abundances.

Comparisons of seven linearized Ricker model structures describing adult-YOY and PYSL-YOY relationships resulted in the selection of the model including freshwater flow during the PYSL period for both transitions ($\Delta AICc > 2$ for all other models; Table 3). In addition, flow during the PYSL period had a significant negative effect on $log_e(YOY \times adult^{-1})$ and $log_e(YOY \times PYSL^{-1})$ in each model configuration where it was included ($p < 0.05$; Table 3), while the effects of temperature during the PYSL period and zebra mussel filtration rates were not significant ($p > 0.25$; Table 3). Similarly, the density-dependent term in both relationships (i.e. adult standing stock for $log_e(YOY \times adult^{-1})$ and PYSL standing stock for $log_e(YOY \times PYSL^{-1})$ had a significant negative effect on transition responses in each model tested ($p < 0.001$; Table 3).

Somatic growth and contingent structure

For the period 1992-2013, YOY length at the end of the growth season was positively associated with mean summer water temperature ($r = 0.70$; $p < 0.01$) and negatively correlated to summer flow ($r = -0.50$; $p < 0.05$) and the PYSL standing stock ($r = -0.46$; $p < 0.05$; Table 4; Figure 4). In addition, the abundance of the migratory contingent of YOY was closely related to the abundance of the resident contingent from 1992-2013 ($R^2 = 0.81$; Figure 5), with the migrant fraction ranging from 0.12 to 0.60, (mean = 0.42; Figure 5). The migrant fraction was unrelated to any of the environmental or density-dependent variables analyzed ($p > 0.15$), but was positively correlated to the brackish shoal proportion from July-September ($r = 0.67$; $p < 0.01$; Table 4), although this trend was largely driven by two years (2004 and 2011) when the migrant fraction and brackish shoal proportion were both relatively low (Figure 4d).

Pre- vs. post-invasion indices of abundance

Post-invasion (1992-2013) indices of white perch abundance were significantly lower than pre-invasion (1974-1991) indices for eggs ($p < 0.02$), YOY ($p < 0.01$) and yearlings ($p < 0.01$; Table 5). In the post-invasion time period, abundance indices declined by approximately 50%, 40% and 60% of their pre-invasion means for eggs, YOY and yearlings, respectively (Table 5). Each life-stage transition differed between the two time periods, although these differences varied in magnitude (Figures 6 and 7). The egg-YSL transition exhibited a significantly steeper slope ($p < 0.001$) in the post-invasion time period ($\alpha = 0.94$) than before the invasion ($\alpha = 0.41$) (Table 6). Change in the YSL-PYSL transition between the two time-periods was not statistically significant ($p > 0.15$), but showed a slightly flatter slope after the invasion ($\alpha = 5.62$) relative to the pre-invasion period ($\alpha = 6.53$) (Table 6). The PYSL-YOY transition during the post-invasion period exhibited a reduced YOY maximum and increased influence of freshwater flow during the PYSL period ($log_e(\alpha) = 2.59$; $\beta = 0.57$; $\gamma_{flow} = 1.43 \times 10^{-3}$) relative to estimates before the zebra mussel invasion ($log_e(\alpha) = 2.08$; $\beta = 0.32$; $\gamma_{flow} = 2.68 \times 10^{-4}$) (Table 6; Figure 7), although contrasts performed on the linearized model coefficients indicated that none of these changes were statistically significant ($p > 0.05$). Similarly, contrasts indicated that the egg-YOY transition showed a significantly enhanced effect of density-dependence after the invasion ($\beta_{post} = 3.61$; $\beta_{pre} = 1.34$; $p > 0.001$), as well as a strong, but marginally non-significant, increase in the effect of freshwater flow ($\gamma_{post} = 1.57 \times 10^{-3}$; $\gamma_{pre} = -4.86 \times 10^{-4}$; $p = 0.097$) (Table 6). Finally, the linear relationship between the yearling index of abundance and the YOY index from the previous year exhibited a significantly flatter slope ($p < 0.05$) after the zebra mussel invasion ($\alpha = 0.21$) than was observed during the pre-invasion time period ($\alpha = 0.32$) (Table 6; Figure 7).

Discussion

In accordance with expected effects of the zebra mussel invasion on the early life history of white perch in the HRE, our analyses revealed substantial alterations in life-stage transitions after the zebra mussel invasion. Following the invasion, the PYSL-YOY transition became more sensitive to PYSL abundance (i.e. density-dependence) and freshwater flow experienced during the PYSL period. In addition, declines in yearling abundance and egg production after the zebra mussel invasion suggests that the adult population has been negatively impacted, which has not been reported in previous studies (Strayer et al. 2004). These shifts in white perch abundance and life-stage transitions are generally consistent with broader changes in the abundance and flow sensitivity of the forage base in the HRE after the zebra mussel invasion (Strayer et al. 2004, 2008). In contrast, the effects of density-dependence and environmental conditions on YOY white perch growth and partial migration were generally similar before and after the zebra mussel invasion.

Environmental and density-dependent effects

Standing stock of white perch eggs, YSL and PYSL were directly proportional to adult abundance, while the standing stock of YOY showed density-dependence, regulated by PYSL abundance and negatively influenced by freshwater flow during the PYSL period (Figure 3). The reduced abundance of YOY white perch in years with high PYSL abundance is consistent with density-dependent mortality of YOY after settlement in littoral habitats. This density-dependent mortality is probably most intense shortly after peak settlement, when the abundance of newly metamorphosed YOY is highest. Upon settlement, YOY white perch likely experience high levels of mortality due to predation, which is in turn regulated by density and habitat type

(Juanes 2007). Density-dependent prey limitation could also cause mortality either directly through starvation or indirectly by exposing juveniles to a prolonged period of size-dependent predation (Walters and Juanes 1993). Lower survival between the PYSL-YOY transition during high flow years (Figure 3) could relate to the findings of Strayer et al. (2008), who observed an inverse relationship between flow and the abundance of littoral benthic invertebrates (prey items for YOY white perch) in the HRE. Reduced pelagic forage availability during the PYSL stage may also be contributing to lower YOY abundances during high flow years. Densities of principal zooplankton prey are known to affect white perch recruitment (Limburg et al. 1999), while cladocerans and (to a lesser degree) copepods have been observed to be negatively influenced by flow (Strayer et al. 2008). Contrary to this study, North and Houde (2003) reported that the stock-recruitment relationships of white perch and congeneric striped bass in the Upper Chesapeake Bay were best described when incorporating a positive effect of freshwater discharge. Interestingly, differences in the direction of the flow effect on the white perch stock-recruitment function in the Hudson River (negative) and Chesapeake Bay (positive) are generally consistent with observed effects of freshwater flow on primary and secondary production in both systems (Howarth et al. 2000, Strayer et al. 2008, Testa et al. 2008).

YOY white perch growth displayed a strong positive relationship with summer temperature, and moderate negative correlations with summer flow and PYSL abundance from 1992-2013 (Table 4; Figure 4). The positive effect of temperature on YOY white perch growth is not surprising, and has been observed in several other systems (Kerr and Secor 2010, VanDeValk et al. 2016). The negative influence of freshwater flow on white perch growth is consistent with previous reports that low flows coincide with increased water clarity and residence times in the HRE (Gladden et al. 1988, Howarth et al. 2000), which may increase primary and secondary production, particularly in littoral habitats utilized by juvenile white perch (Strayer et al. 2008). The negative effect of the PYSL standing stock on YOY growth is more difficult to interpret, especially since growth was unrelated to YOY abundance (Table 4), in contrast to other studies that have documented density-dependent growth in white perch (VanDeValk et al. 2016) and striped bass (Martino and Houde 2010). The effect of larval abundance on YOY growth (Figure 4c) may be related to the density-dependent mortality observed during the PYSL-YOY transition (see above); such that competition for food in newly settled YOY may increase in years of high larval abundance, potentially reducing growth rates early in the YOY period, which carry over to influence length at the end of the growing season.

The production of YOY in the migratory contingent was proportional to total YOY abundance from 1992-2013 ($R^2 = 0.87$; Figure 5), with a migrant fraction of approximately 40% on average, which was positively correlated with habitat availability in the brackish portion of the HRE. While the migrant fraction was not significantly correlated with freshwater flow during the summer ($r = -0.30$; Table 4), summer flow was highly correlated with the brackish shoal proportion ($r = -0.83$; data not shown). Thus, in years with exceptionally high freshwater flow during the summer (2 out of the 22 years analyzed), the salt front was pushed down-estuary and subsequently restricted the availability of favorable habitat in the brackish portion of the HRE, thereby limiting the abundance of the migratory contingent. The relatively constant proportionality between migrant abundance and total YOY abundance implies that years with high recruitment (i.e. moderate PYSL abundance and low flow; Figure 3) will produce higher numbers of migrants with associated higher growth rates (Gallagher 2016), which may further enhance population productivity (Kerr et al. 2010). In contrast, a previous study of YOY white perch in the Patuxent River observed that the resident contingent dominated in years

characterized by low flow and diminished recruitment, while years with moderate to high flow favored stronger year-classes and greater representation of the migratory contingent (Kraus and Secor 2004).

Impacts of the zebra mussel invasion

Indices of abundance from pre-invasion (1974-1991) and post-invasion (1992-2013) time periods demonstrated, for the first time, that the abundance of white perch eggs and yearlings declined after zebra mussels invaded the HRE (Table 5), while also confirming the reduction of YOY standing stocks reported in previous studies (Strayer et al. 2004, 2014b). Our analysis of life-stage transitions from egg to YSL to PYSL prior to the zebra mussel invasion largely mirrored previous research. Pace et al. (1993) analyzed the egg-YSL, YSL-PYSL and PYSL-YOY life-stage transitions during the pre-invasion period from 1974-1990, and found that YSL and PYSL abundances were related to the abundance of their previous life-stages in a density-independent manner, similar to our analyses of egg-YSL and YSL-PYSL transitions from 1992-2013 (Figure 3; Table 2). However, the indices of white perch abundance indicated that the slope of egg-YSL transition became steeper during the post-invasion time period (Table 6), resulting in similar YSL abundance between the two time periods despite declines in egg production (Figure 6; Table 5). This pattern suggests that a compensatory increase in hatching success and early larval survival may have occurred after the invasion.

In contrast to our findings, Pace et al. (1993) reported that the relationship between PYSL and YOY abundance was relatively flat, and unrelated to annual variations in temperature and flow, whereas the PYSL-YOY relationship reported here (1992-2013) exhibited strong density-dependence and a significant negative effect of freshwater flow during the PYSL period (Figure 3; Table 3a). This change in the PYSL-YOY transition after the zebra mussel invasion was further corroborated by the index-based Ricker models describing the transition, which showed increases in the effect size of β ($\beta_{post} = 0.57$, $p < 0.001$; $\beta_{pre} = 0.32$, $p = 0.077$) and γ_{flow} ($\gamma_{post} = 1.43 \times 10^{-3}$, $p = 0.070$; $\gamma_{pre} = 2.68 \times 10^{-4}$, $p = 0.872$) (Table 6) during the post-invasion time-period. Although contrasts indicated that the differences between Ricker model parameters in the pre-invasion and post-invasion time periods were not statistically significant (Table 6), we argue that the significant reduction in YOY abundance after the invasion, the consistent negative effect of flow on the post-invasion adult-YOY and PYSL-YOY transitions (Table 3), and substantial differences in the shape of the YOY-PYSL relationship between time periods (Figure 6) suggest that these differences are ecologically significant.

The increased sensitivity of the PYSL-YOY transition to density-dependence and freshwater flow is likely related to reductions in the food supply of white perch, and is generally consistent with riverwide declines in phytoplankton (Caraco et al. 1997), pelagic zooplankton (Pace et al. 1998) and benthic invertebrate (Strayer and Smith 2001) densities and the strong negative relationship of littoral benthic invertebrate density with flow (Strayer et al. 2008) observed in the first 10-15 years after the zebra mussel invasion. In addition, the increased sensitivity to freshwater flow has probably contributed to the diminished production of YOY observed after the zebra mussel invasion, as flow during the PYSL period (from weeks 19-28) increased at a rate of 1.9% $year^{-1}$ on average in the HRE from 1992 to 2013 (Figure 8).

White perch in the HRE begin to mature as yearlings (Klauda et al. 1988), which raises the possibility that the reduction in yearling abundance after the zebra mussel invasion has depleted the overall spawning stock abundance of the population. Declines in yearling abundance after the zebra mussel invasion were likely driven by reduced YOY abundance (Table

5) and a flattened slope in the transition between YOY and yearlings (Figure 7), both of which would be expected to decrease the number of yearlings. If the diminished abundance of yearling white perch in the HRE carries over to subsequent age-classes, this would explain the significant reduction in egg production observed after the invasion (Table 5). Reduced post-invasion abundance of adult white perch may also provide one explanation for the negative temporal trends observed in adult, YSL and PYSL standing stocks from 1992-2013 (Table 1). Overall, these comparative analyses suggest that the zebra mussel invasion has forced the HRE white perch population into an alternate state, characterized by lower spawning stock abundance and curtailed juvenile production that is more sensitive to environmental variability, which can in turn be attributed to differences in life-cycle transitions before and after the invasion.

YOY white perch growth showed increased density-dependence after the zebra mussel invasion, but no change in its relationship to environmental conditions. While YOY growth was negatively correlated to PYSL abundance in the post-invasion period (Figure 4c), there was no relationship between these variables before the invasion ($r = 0.06$; Table S.2), suggesting that reductions in food availability may have intensified density-dependent growth in newly settled YOY. Using a model averaging approach, Strayer et al (2004) reported that temperature and flow had positive and negative effects (similar to those reported here), respectively on YOY white perch growth from 1974-1999, but also found evidence of reduced growth after the zebra mussel invasion. Klauda et al. (1988) reported a significant positive correlation between mean water temperature in June and July and growth rates of early juvenile white perch from 1973-1979, while white perch condition (i.e. weight at a length of 70mm) was negatively associated with flow and YOY abundance (Table S.2). Similarly, in white perch stock assessment studies from 1971-1988, LMS (1989) indicated that YOY length in November was positively related to mean summer water temperature and negatively correlated to mean summer flow (Table S.2).

We detected no change in the migrant fraction of the population associated with the zebra mussel invasion, nor did we observe appreciable change in the effects of density-dependence and environmental conditions. Two previous analyses both concluded that the spatial center of abundance in YOY white perch was not significantly altered by the zebra mussel invasion or a subsequent recovery of the forage base after 2005 (Strayer et al. 2004, 2014b). Data from 1983-1988 (LMS 1989) suggested that the center of abundance of YOY white perch (distance up-estuary) from late-September to November was negatively associated with freshwater flow from July-September, but unrelated to temperature or YOY abundance (Table S.2), similar to our findings from the post-invasion period (Table 4).

Regime shift-climate change interactions

The HRE white perch population has been perturbed to an alternate state through the complex interactions of two large-scale phenomena: an abrupt regime shift and long-term increases in flow associated with climate change. Precipitation in the HRE watershed is projected to increase by 7% on average over the next century, which should result in a 10-15% increase in freshwater flow (Najjar et al. 2009), and this long-term change will likely be overlain by substantial decadal-scale variability that will affect the productivity of white perch and the HRE ecosystem as a whole (Strayer et al. 2014a). The response of HRE white perch to long-term changes in flow will be further complicated by concurrent increases in water temperature, which Najjar et al. (2009) projected to increase by approximately 4°C on average by 2100. The effects of rising temperatures on the HRE ecosystem are likely to be modest over decadal timescales (Strayer et al. 2014a), but the increased biological rates (e.g. zooplankton productivity, white

perch growth) that would accompany temperatures at the end of the century could potentially interact with higher freshwater flow (which favors lower primary production; Howarth et al. 2000) in unpredictable ways.

Regime shifts are typically abrupt (1-3 years), and can be triggered by overfishing (Daskalov et al. 2007), invasive species (Shiganova et al. 1998), eutrophication (Österblom et al. 2007), climate oscillations (Francis and Hare 1994), gradual changes in temperature and precipitation (Smol et al. 2005), or some combination of these factors (e.g. Weijerman et al. 2005, Möllmann et al. 2008). Regardless of the cause, abrupt regime shifts in aquatic ecosystems will inevitably lead to changes in the abundance and population dynamics of many constituent species (Collie et al. 2004). Further comparisons of fish population characteristics across various stages of ecosystem disturbance and recovery in multiple systems (e.g. nutrient remediation; Kemp et al. 2009) can potentially uncover more diverse mechanisms by which populations have responded to changes in ecosystem structure in the past. Further research is warranted to develop a more comprehensive understanding of the interactive effects of regime shifts and climate change on fish populations in systems where adequate environmental and biological monitoring data are available.

Conclusions

This research highlights the importance of abrupt and long-term changes in ecosystem characteristics to the dynamics of the HRE white perch population. Alterations in the abundance and environmental sensitivity of white perch in the HRE after the zebra mussel invasion will likely influence how the population responds to long-term increases in temperature and precipitation in the HRE. Similar changes in the shape of early life-stage transitions may be detectable in other fish species in the HRE (e.g. striped bass, river herring, centrarchids) and other marine ecosystems subjected to regime shifts, especially those characterized by intense modifications of the forage base. Improved knowledge of the causes and consequences of state shifts in fish populations, such as those highlighted here, can facilitate the implementation of stock assessment and fisheries management practices that more comprehensively account for such changes.

Acknowledgements

We thank J. Young, the Hudson River Estuary Monitoring Program and Applied Science Associates for allowing us to access data from Year-Class Reports, as well as D. Strayer and the Cary Institute of Ecosystem Studies for sharing zebra mussel filtration rates. We acknowledge J. Testa and H. Bailey for providing insights and comments which improved a previous draft of this manuscript. This research was funded by the Hudson River Foundation under grant number 31479.

References

Applied Science Associates, Inc (ASA). 2014. 2013 Year class report for the Hudson River Estuary monitoring program and Central Hudson Gas and Electrical Corporation. New Hampton, NY.

Brander, K.M. 2005. Cod recruitment is strongly affected by climate when stock biomass is low. ICES Journal of Marine Science 62: 339-343.

Burnham, K. P. and D. R. Anderson. 2002. Model selection and multimodel inference: Apractical information-theoretic approach. Springer-Verlag:New York.

Caraco, NF, JJ Cole, PA Raymond, and DL Strayer. 1997. Zebra mussel invasion in a large, turbid river: phytoplankton response to increased grazing. Ecology 78(2): 588-602.

Collie, J., K. Richardson, and J. Steele. 2004. Regime shifts: Can ecological theory illuminate the mechanisms? Progress in Oceanography 60: 281-302.

Cooper, J., F. Cantelmo, and C. Newton. 1988. Overview of the Hudson River Estuary. in: L.W. Barnthouse, R.J. Klauda, D.S. Vaughan and R.L. Kendall (eds). Science, Law and Hudson River Power Plants. American Fisheries Society Monograph 4: 11-24.

Daniels, R.A., Limburg, K.E., and Schmidt, R.E. 2005. Changes in fish assemblages in the tidal Hudson River, New York. American Fisheries Society Symposium 45: 471-503.

Daskalov G.M., A.N. Grishin, S. Rodionov, and V. Mihneva. 2007. Trophic cascades triggered by overfishing reveal possible mechanisms of ecosystem regime shifts. Proceedings of the National Academy of Sciences 104(25): 10518-10523.

Feyrer, F., M. Nobriga, and T. Sommer. 2007. Multidecadal trends for three declining fish species: habitat patterns and mechanisms in the San Francisco Estuary, California, USA. Canadian Journal of Fisheries and Aquatic Sciences 64: 723–734.

Folke, C., S. Carpenter, B. Walker, M. Scheffer, T. Elmqvist, L. Gunderson and C.S. Holling. 2004. Regime shifts, resilience, and biodiversity in ecosystem management. Annual Review of Ecology, Evolution, and Systematics 35: 557-581.

Francis, R.C. and S.R. Hare. 1994. Decadal-scale regime shifts in the large marine ecosystems of the North-east Pacific: A case for historical science. Fisheries Oceanography 3(4): 279-291.

Gallagher, B.K. 2016. Influence of partial migration and environmental change on the population dynamics of white perch (*Morone americana*) within the Hudson River Estuary. M.S. Thesis, University of Maryland, College Park, MD.

Geyer, W.R. and R. Chant. 2006. The physical oceanography processes in the Hudson River Estuary. in: J.S. Levinton and J.R. Waldman (eds). The Hudson River Estuary. Cambridge University Press, New York, NY, 121-136.

Gladden, J., F. Cantelmo, J. Croom and R. Shapot. 1988. Evaluation of the Hudson River ecosystem in relation to the dynamics of fish populations. in: L.W. Barnthouse, R.J. Klauda, D.S. Vaughan and R.L. Kendall (eds). Science, Law and Hudson River Power Plants. American Fisheries Society Monograph 4: 69-88.

Hare, S.R. and Mantua, N.J. 2000. Empirical evidence for North Pacific regime shifts in 1977 and 1989. Progress in Oceanography, 47(2): 103-145.

Howarth, R., D. Swaney, T. Butler, and R. Marino. 2000. Rapid Communication: Climatic control on eutrophication of the Hudson River Estuary. Ecosystems 3: 210-215.

Howarth, R, R. Marino, D. Swaney and E. Boyer. 2006. Wasterwater and watershed influences on primary productivity and oxygen dynamics in the Lower Hudson River Estuary. in: J.S. Levinton and J.R. Waldman (eds). The Hudson River Estuary. Cambridge University Press, New York, NY, 121-136.

Juanes, F. 2007. Role of habitat in mediating mortality during the post-settlement transition phase of temperate marine fishes. Journal of Fish Biology 70(3): 661-677.

Kemp, W. M., J.M. Testa, D.J. Conley, D. Gilbert, and J.D. Hagy. 2009. Temporal responses of coastal hypoxia to nutrient loading and physical controls. Biogeosciences 6(12): 2985-3008.

Kerr, L., and D. Secor. 2010. Latent effects of early life history on partial migration for an estuarine-dependent fish. Environmental Biology of Fishes 89: 479–492.

Kerr, L., and D. Secor. 2011. Partial migration across populations of white perch (*Morone americana*): A flexible life history strategy in a variable estuarine environment. Estuaries and Coasts 35(1): 227-236.

Kerr, L.A., S.X. Cadrin, and D.H. Secor. 2010. The role of spatial dynamics in the stability, resilience, and productivity of an estuarine fish population. Ecological Applications 20(2): 497-507.

Kimmerer, W., E. Gartside, and J. Orsi. 1994. Predation by an introduced clam as the likely cause of substantial declines in zooplankton of San Francisco Bay. Marine Ecology Progress Series 113: 81-93.

Kimmerer, W., J. Cowan, L. Miller, and K. Rose. 2000. Analysis of an estuarine striped bass (*Morone saxatilis*) population: influence of density-dependent mortality between

metamorphosis and recruitment. Canadian Journal of Fisheries and Aquatic Sciences 57: 478–486.

Klauda, R.J., J.B. McLaren, R.E. Schmidt and W.P. Dey. 1988. Life history of white perch in the Hudson River Estuary. in: L.W. Barnthouse, R.J. Klauda, D.S. Vaughan and R.L. Kendall (eds). Science, Law and Hudson River Power Plants. American Fisheries Society Monograph 4: 69-88.

Kraus, R., and D. Secor. 2004a. Dynamics of white perch *Morone americana* population contingents in the Patuxent River estuary, Maryland, USA. Marine Ecology Progress Series 279: 247–259.

Kraus, R., and D. Secor. 2005. Connectivity in estuarine white perch populations of Chesapeake Bay: evidence from historical fisheries data. Estuarine, Coastal and Shelf Science 64(1): 108-118.

Limburg, K.E., M.L. Pace, D. Fischer and K.K. Arend. 1997. Consumption, selectivity, and use of zooplankton by larval striped bass and white perch in a seasonally pulsed estuary. Transactions of the American Fisheries Society 126(4): 607-621.

Limburg, K.E., M.L. Pace, and K.K. Arend. 1998. Growth, mortality, and recruitment of larval Morone spp. in relation to food availability and temperature in the Hudson River. Fishery Bulletin 97: 80–91.

Lawler, Matusky and Skelly Engineers, Inc (LMS). 1989. Hudson River Estuary white perch adult and subadult stock assessment study: fall 1988. Final report to: Orange and Rockland Utilities, Inc. Pearl River, NY.

Mansueti, R.J. 1964. Eggs, larvae, and young of the white perch, *Roccus americanus*, with comments on its ecology in the estuary. Chesapeake Science. 5(1-2): 3-45.

Martino, E.J., and E.D. Houde. 2012. Density-dependent regulation of year-class strength in age-0 juvenile striped bass (*Morone saxatilis*). Canadian Journal of Fisheries and Aquatic Sciences 69(3): 430-446.

Möllmann, C., B. Müller-Karulis, G. Kornilovs, and M.A. St John. 2008. Effects of climate and overfishing on zooplankton dynamics and ecosystem structure: regime shifts, trophic cascade, and feedback loops in a simple ecosystem. ICES Journal of Marine Science 65(3): 302-310.

Najjar, R., L. Patterson, and S. Graham. 2009. Climate simulations of major estuarine watersheds in the Mid-Atlantic region of the US. Climatic Change 95: 139–168.

Nash, R., and M. Dickey-Collas. 2005. The influence of life history dynamics and environment on the determination of year class strength in North Sea herring (*Clupea harengus L.*). Fisheries Oceanography 14: 279–291.

North, E. W., and E. D. Houde. 2003. Linking ETM physics, zooplankton prey, and fish early-life histories to striped bass *Morone saxatilis* and white perch *M. americana* recruitment. Marine Ecology Progress Series 260: 219–236.

Österblom H, Hansson S, Larsson U, Hjerne O, F. Wulff, R. Elmgren, and C. Folke. 2007. Human-induced trophic cascades and ecological regime shifts in the Baltic Sea. Ecosystems 10(6): 877-89.

Ottersen, G., D.O. Hjermann, and N.C. Stenseth. 2010. Changes in spawning stock structure strengthen the link between climate and recruitment in a heavily fished cod (*Gadus morhua*) stock. Fisheries Oceanography 15(3): 230–243.

Pace, M., S. Baines, H. Cyr, and J. Downing. 1993. Relationships among early life stages of *Morone americana* and *Morone saxatilis* from long-term monitoring of the Hudson River Estuary. Canadian Journal of Fisheries and Aquatic Sciences 50: 1976-1985.

Pace, M., S. Findlay, and D. Fischer. 1998. Effects of an invasive bivalve on the zooplankton community of the Hudson River. Freshwater Biology 39: 103-116.

Pace, M., D. Strayer, D. Fischer, and H. Malcom. 2010. Recovery of native zooplankton associated with increased mortality of an invasive mussel. Ecosphere 1: 1-10.

Paulik, G. J. 1973. Studies of the possible form of the stock-recruitment curve. Rapports et Procès-Verbaux des Réunions du Conseil International pour l'Exploration de la Mer 164: 302–315.

Payne, M., E. Hatfield, M. Dickey-Collas, T. Falkenhaug, A. Gallego, J. Gröger, P. Licandro, M. Llope, P. Munk, C. Röckmann, J. Schmidt, and R. Nash. 2009. Recruitment in a changing environment: the 2000s North Sea herring recruitment failure. ICES Journal of Marine Science 66: 272-277.

Planque, B., J. Fromentin, P. Cury, K.F. Drinkwater, S. Jennings, R.I. Perry, and S. Kifani. 2010. How does fishing alter marine populations and ecosystems sensitivity to climate? Journal of Marine Systems 79: 403–417.

Quinn J.T. and R.B. Deriso. 1999. Quantitative fish dynamics. Oxford University Press.

Seekell, D., and M. Pace. 2011. Climate change drives warming in the Hudson River Estuary, New York (USA). Journal of Environmental Monitoring 13: 2321–2327.

Shiganova, T. A. 1998. Invasion of the Black Sea by the ctenophore *Mnemiopsis leidyi* and recent changes in pelagic community structure. Fisheries Oceanography 7(3-4): 305-310.

Smol, J.P., A.P. Wolfe, H.J.B. Birks, M.S. Douglas, V.J. Jones, and 21 others. 2005. Climate-driven regime shifts in the biological communities of arctic lakes. Proceedings of the National Academy of Sciences of the United States of America 102(12): 4397-4402.

Strayer, D.L., and L.C. Smith. 2001. The zoobenthos of the freshwater tidal Hudson River and its response to the zebra mussel (*Dreissena polymorpha*) invasion. Archiv Fur Hydrobiologie-Supplement 139: 1-52.

Strayer, D., K. Hattala, and A. Kahnle. 2004. Effects of an invasive bivalve (*Dreissena polymorpha*) on fish in the Hudson River estuary. Canadian Journal of Fisheries and Aquatic Sciences 61: 924-941.

Strayer, D., and H. Malcom. 2006. Long-term demography of a zebra mussel (*Dreissena polymorpha*) population. Freshwater Biology 51: 117-130.

Strayer, DL, ML Pace, NF Caraco, JJ Cole, and S. Findlay. 2008. Hydrology and grazing jointly control a large-river food web. Ecology 89(1): 12-18.

Strayer, D. L., N. Cid, and H.M. Malcom. 2011. Long-term changes in a population of an invasive bivalve and its effects. Oecologia 165(4): 1063-1072.

Strayer, D., J. Cole, S. Findlay, D. Fischer, J. Gephart, H. Malcom, M. Pace, and E. Rosi-Marshall. 2014a. Decadal-Scale Change in a Large-River Ecosystem. BioScience 64: 496-510.

Strayer, D., K. Hattala, A. Kahnle, R. Adams, and A. Fisk. 2014b. Has the Hudson River fish community recovered from the zebra mussel invasion along with its forage base? Canadian Journal of Fisheries and Aquatic Sciences 71: 1146-1157.

Testa, J., M. Kemp, W. Boynton, and J. Hagy. 2008. Long-term changes in water quality and productivity in the Patuxent River Estuary: 1985 to 2003. Estuaries and Coasts 31(6): 1021-1037.

Tuckett, Q., K. Simon, J. Saros, D. Halliwell, and M. Kinnison. 2013. Fish trophic divergence along a lake productivity gradient revealed by historic patterns of invasion and eutrophication. Freshwater Biology 58: 2517-2531.

United States Geological Survey (USGS). 2015a. National Water Information System data available on the World Wide Web (USGS Water Data for the Nation). Accessed June 9, 2015. Available: http://ny.water.usgs.gov/projects/dialer_plots/saltfront.html

United States Geological Survey (USGS). 2015b. National Water Information System data available on the World Wide Web (USGS Water Data for the Nation). Accessed June 9, 2015. Available: http://waterdata.usgs.gov/nwis/uv?site_no=01372058

United States Geological Survey (USGS). 2015c. National Water Information System data available on the World Wide Web (USGS Water Data for the Nation). Accessed June 9, 2015. Available: http://waterdata.usgs.gov/nwis/uv?site_no=01358000

VanDeValk, A.J., J.L. Forney, T.E. Brooking, J.R. Jackson, and L.G. Rudstam. 2016. First-year density and growth as they relate to recruitment of white perch to the adult stock in Oneida Lake, New York, 1968–2011. Transactions of the American Fisheries Society 145(2): 416-426.

Walters, C.J., and F. Juanes. 1993. Recruitment limitation as a consequence of natural selection for use of restricted feeding habitats and predation risk taking by juvenile fishes. Canadian Journal of Fisheries and Aquatic Sciences 50(10): 2058-2070.

Weijerman, M., H. Lindeboom, and A.F. Zuur. 2005. Regime shifts in marine ecosystems of the North Sea and Wadden Sea. Marine Ecology Progress Series 298: 21-39.

Tables

Table 1. List of 13 primary variables analyzed in this study, with descriptive statistics (mean, minimum, maximum and correlation coefficient with year) for each variable from 1992-2013. Statistically significant temporal correlations are marked with an asterisk (*).

Variable	Units	Type	Source	Mean	Min	Max	r_{year}
Mean adult standing crop	Millions	White Perch	ASA (2014)	2.54	0.89	5.89	-0.30
Mean YOY standing crop	Millions	White Perch	ASA (2014)	0.71	0.05	2.35	0.13
Mean PYSL standing crop	Millions	White Perch	ASA (2014)	709	340	1529	-0.65*
Mean YSL standing crop	Millions	White Perch	ASA (2014)	105	32	257	-0.47*
Mean Egg standing crop	Millions	White Perch	ASA (2014)	123	22	351	-0.17
Proportion of migratory YOY	Unitless	White Perch	ASA (2014)	0.42	0.12	0.60	0.07
Mean YOY length in October	mm	White Perch	ASA (2014)	73.9	62.8	82.3	0.14
Mean zebra mussel filtration rate	$m^3m^{-2}day^{-1}$	Biological	D. Strayer	3.76	0.06	8.28	-0.59*
Mean summer salt front position	km from Battery	Environmental	USGS (2015a)	99	74	118	0.16
Mean spring temperature	°Celsius	Environmental	USGS (2015b)	14.7	13.2	17.2	0.22
Mean summer temperature	°Celsius	Environmental	USGS (2015b)	24.5	23.2	26.4	0.32
Mean spring flow	$m^3sec^{-1}day^{-1}$	Environmental	USGS (2015c)	587	181	857	-0.01
Mean summer flow	$m^3sec^{-1}day^{-1}$	Environmental	USGS (2015c)	234	98	546	0.43*

Table 2. Parameter estimates (with standard errors in parentheses) for each white perch life-stage transition based on mean standing stocks from 1992-2013. The α estimates, model R^2 and p-values for Ricker models (denoted by ‡) are for the linearized equations, where $\alpha = \log_e(\alpha)$ (see Methods).

Life-Stage Transition	α	β	γ_{flow}	Model R^2	Model p-value
Adult-Egg	46.40 (4.56)	-	-	0.38	<0.001
Adult-YSL	40.41 (3.19)	-	-	0.53	<0.001
Adult-PYSL	258.25 (21.59)	-	-	0.39	<0.001
Egg-YSL	0.76 (0.08)	-	-	0.36	<0.001
Egg-PYSL	4.87 (0.53)	-	-	0.28	<0.001
YSL-PYSL	6.07 (0.47)	-	-	0.55	<0.001
Adult-YOY‡	0.91 (0.49)	$5.61\ 10^{-4}$ ($1.24\ 10^{-4}$)	$2.18\ 10^{-3}$ ($8.61\ 10^{-4}$)	0.59	<0.001
PYSL-YOY‡	-4.72 (0.47)	$2.21\ 10^{-6}$ ($4.44\ 10^{-7}$)	$1.89\ 10^{-3}$ ($8.07\ 10^{-4}$)	0.62	<0.001

Table 3. Parameter estimates, R^2, AICc and ΔAICc values for seven linearized Ricker model configurations for white perch describing the PYSL-YOY transition (a) and the adult-YOY transition (b) with each combination of temperature, flow (both during the PYSL period) and zebra mussel filtration rates. Parameters that were significantly different than 0 ($p < 0.05$) are marked with an asterisk (*). Model 3 had the lowest AICc in both cases (bold italic text).

a

Model	Intercept	Adult	Temperature	Flow	Filtration	R-square	AICc	ΔAICc
1	0.02	-0.57*	-	-	-	0.46	57.5	3.4
2	-1.95	-0.56*	0.10	-	-	0.46	60.2	6.1
3	***0.91***	***-0.56****	***-***	***$-2.19\ 10^{-3}$****	***-***	***0.59***	***54.1***	***0.0***
4	-0.03	-0.58*	-	-	0.02	0.46	60.5	6.3
5	1.68	-0.56*	-0.04	$-2.26\ 10^{-3}$*	-	0.59	57.5	3.3
6	1.13	-0.54*	-	$-2.40\ 10^{-3}$*	-0.05	0.60	57.0	2.9
7	2.90	-0.54*	-0.09	$-2.40\ 10^{-3}$*	-0.06	0.61	60.6	6.5

b

Model	Intercept	PYSL	Temperature	Flow	Filtration	R-square	AICc	ΔAICc
1	-5.48*	$-2.29\ 10^{-3}$*	-	-	-	0.51	53.8	2.6
2	-5.41	$-2.28\ 10^{-3}$*	0.00	-	-	0.51	56.8	5.6
3	***-4.72****	***$-2.20\ 10^{-3}$****	***-***	***$-1.91\ 10^{-3}$****	***-***	***0.62***	***51.2***	***0.0***
4	-5.51*	$-2.31\ 10^{-3}$*	-	-	0.01	0.51	56.8	5.6
5	-1.51	$-2.39\ 10^{-3}$*	-0.16	$-2.15\ 10^{-3}$*	-	0.64	53.7	2.5
6	-4.49*	$-2.11\ 10^{-3}$*	-	$-2.15\ 10^{-3}$*	-0.06	0.64	53.9	2.7
7	-0.30	$-2.30\ 10^{-3}$*	-0.20	$-2.58\ 10^{-3}$*	-0.07	0.66	56.3	5.0

Table 4. Correlations between migrant fraction and YOY length and six predictor variables of interest from 1992-2013. Statistically significant ($p < 0.05$) correlations are marked with an asterisk (*).

			Response	
Predictor	**Type**	**Time Period**	**Migrant Fraction**	**YOY Length**
PYSL Standing Stock	Density-dependent	May-Jul	-0.16	-0.46*
YOY Standing Stock	Density-dependent	Jul-Sep	-0.05	0.19
Summer Temperature	Environmental	Jul-Sep	0.24	0.70*
Summer Flow	Environmental	Jul-Sep	-0.30	-0.50*
Zebra Mussel Filtration	Biological	May-Oct	-0.03	-0.06
Brackish Shoal Proportion	Habitat availability	Jul-Sep	0.67*	0.37

Table 5. Statistical comparisons of mean post-invasion (1992-2013) and pre-invasion (1974-1991) indices of abundance for white perch eggs, YSL, PYSL, YOY and yearlings. The % Difference metric is calculated as $(Mean_{post}\text{-}Mean_{pre}) \times Mean_{pre}^{-1} \times 100$. Statistically significant p-values are denoted by an asterisk (*).

Life-Stage	Post-Invasion Mean	Pre-Invasion Mean	t-Statistic	% Difference	p-value
Egg	0.41	0.89	-2.66	-54	0.02*
YSL	0.45	0.46	-0.06	-1	0.95
PYSL	2.85	3.50	-1.30	-19	0.20
YOY	4.82	8.08	-2.83	-40	0.01*
Yearling	1.21	3.26	-3.95	-63	<0.01*

Table 6. Parameter estimates (with standard errors in parentheses) and p-values for life-stage transitions based on white perch indices of abundance shown in Figures 6 and 7. The % Difference metric is calculated as ($Estimate_{post}$-$Estimate_{pre}$) × $Estimate_{pre}^{-1}$ × 100. The contrast t-statistics and p-values are for ($Estimate_{post}$-$Estimate_{pre}$) contrasts performed on each parameter using ANCOVA (estimates for PYSL-YOY and egg-YOY transitions are from linearized Ricker models; see Methods). Statistically significant p-values are denoted by an asterisk (*).

Life-Stage Transition	Parameter	Post-Invasion Estimate	Post-Invasion p-value	Pre-Invasion Estimate	Pre-Invasion p-value	Contrast t-Statistic	% Difference	Contrast p-value
Egg-YSL	α	0.94 (0.12)	< 0.001*	0.41 (0.06)	< 0.001*	3.81	129	< 0.001*
YSL-PYSL	α	5.62 (0.48)	< 0.001*	6.53 (0.49)	< 0.001*	-1.31	-14	0.199
YOY-Yearling	α	0.21 (0.04)	< 0.001*	0.32 (0.03)	< 0.001*	-2.33	-34	0.026*
PYSL-YOY	$\log_e(\alpha)$	2.59 (0.46)	< 0.001*	2.08 (0.88)	0.025*	0.68	25	0.503
	β	0.57 (0.10)	< 0.001*	0.32 (0.17)	0.077	1.84	78	0.074
	γ_{flow}	$1.43\ 10^{-3}$ ($9.31\ 10^{-4}$)	0.070	$2.68\ 10^{-4}$ ($7.18\ 10^{-4}$)	0.872	0.97	508	0.34
Egg-YOY	$\log_e(\alpha)$	4.47 (0.35)	< 0.001*	3.49 (0.37)	< 0.001*	1.88	28	0.069
	β	3.61 (0.60)	< 0.001*	1.34 (0.20)	< 0.001*	3.60	169	< 0.001*
	γ_{flow}	$1.57\ 10^{-3}$ ($7.94\ 10^{-4}$)	0.056	$-4.86\ 10^{-4}$ ($9.08\ 10^{-4}$)	0.596	1.71	-423	0.097

Figures

Figure 1. Map of the Hudson River Estuary (HRE), with the 13 river sections sampled by the Hudson River Estuary Monitoring Program outlined, and markers denoting approximate locations of monitoring stations for temperature (Poughkeepsie) and freshwater flow (Troy; see text).

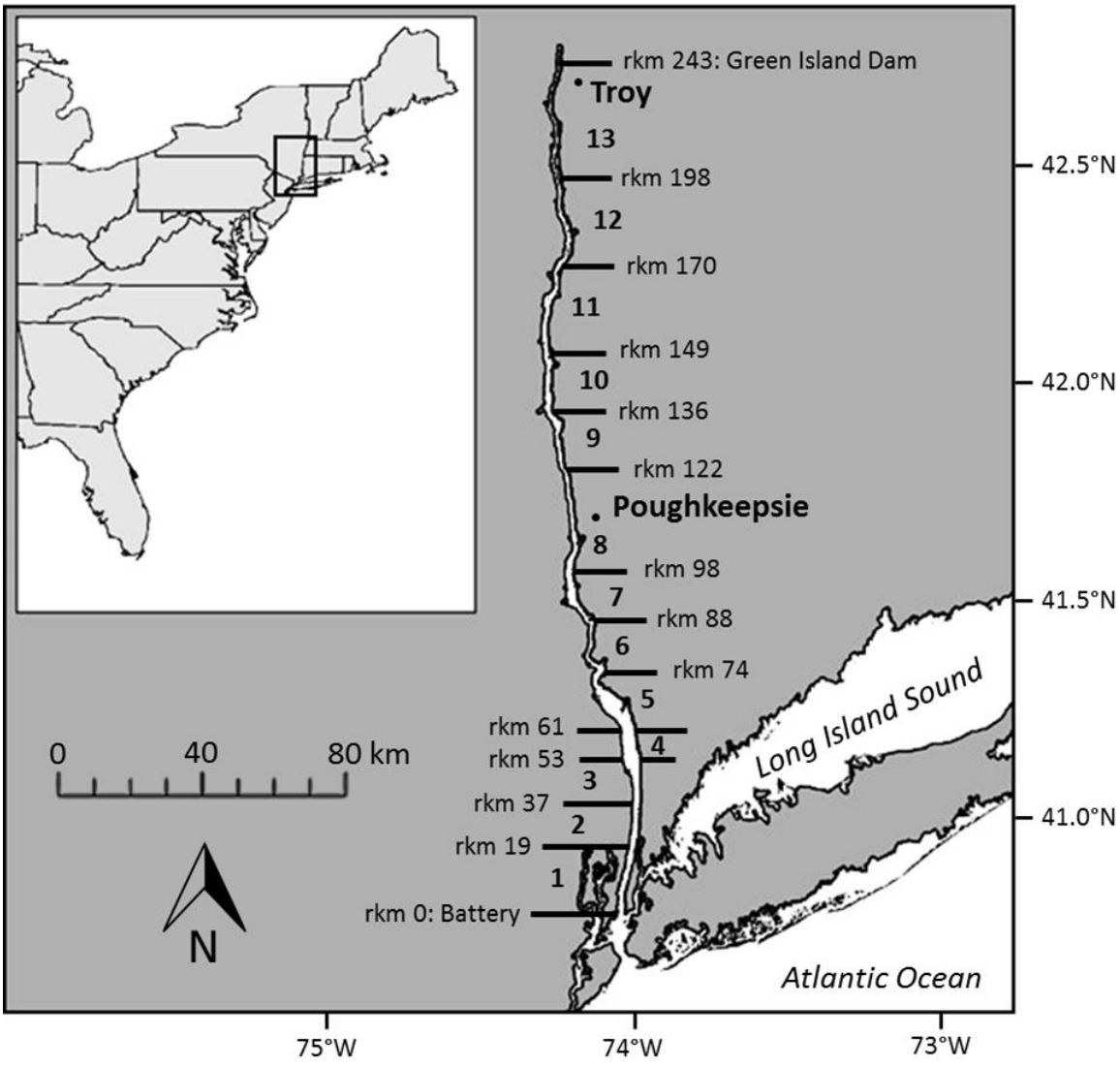

Figure 2. Plots of annual mean temperature (a) and freshwater flow (b) in the HRE from 1951-2013, each plotted with a locally weighted regression (thin black line; LOESS quadratic smoother with a span of 0.5) to show long-term patterns. The dashed grey lines on each plot denote the year 1991, when zebra mussels invaded the HRE (see text). Temperature data were reported in ASA (2014) and freshwater flow data were acquired from USGS (2015c).

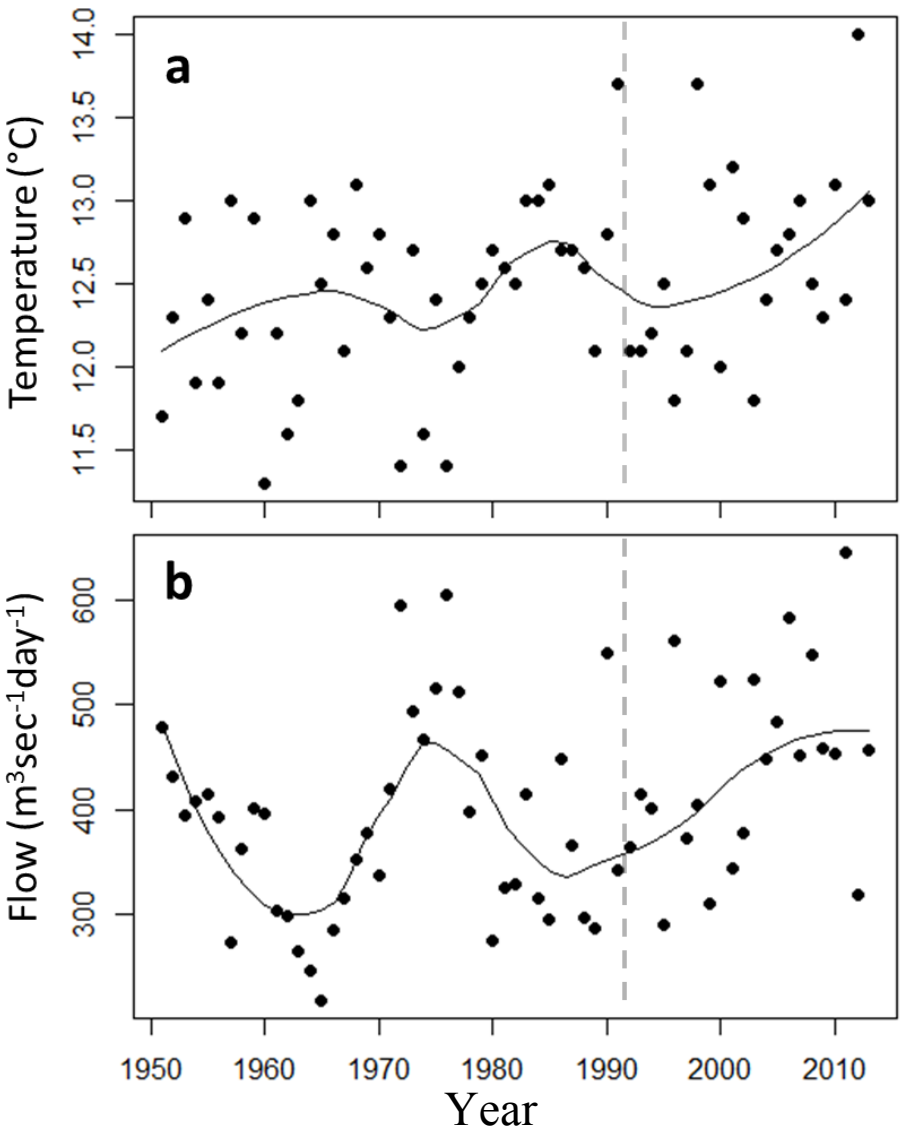

Figure 3. Paulik diagram depicting (clockwise from top right) adult-YOY, adult-YSL, YSL-PYSL and PYSL-YOY life-stage transitions based on mean standing stocks from 1992-2013. Note that all four plots within the diagram have a common origin. Ricker models are plotted both with (dashed lines) and without (solid lines) freshwater flow during the PYSL period as a covariate (see Methods).

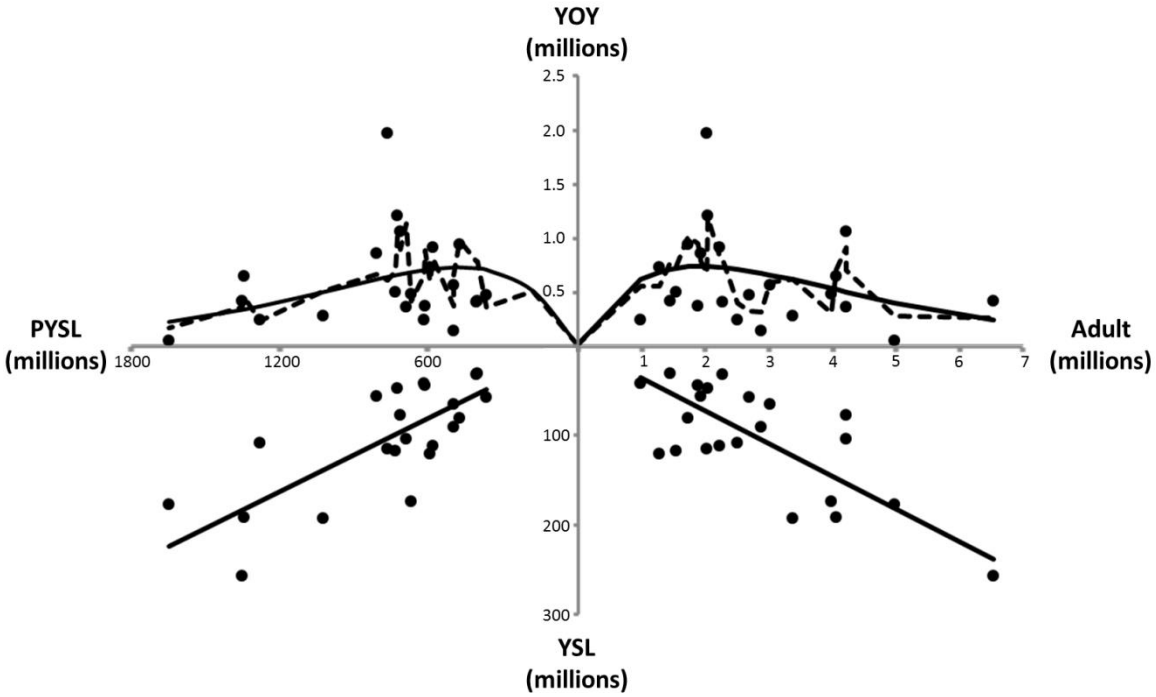

Figure 4. Plots of statistically significant correlations between white perch mean YOY length in October and summer temperature (a), summer flow (b) and PYSL standing stock (c) and between white perch migrant fraction and the brackish shoal proportion (d).

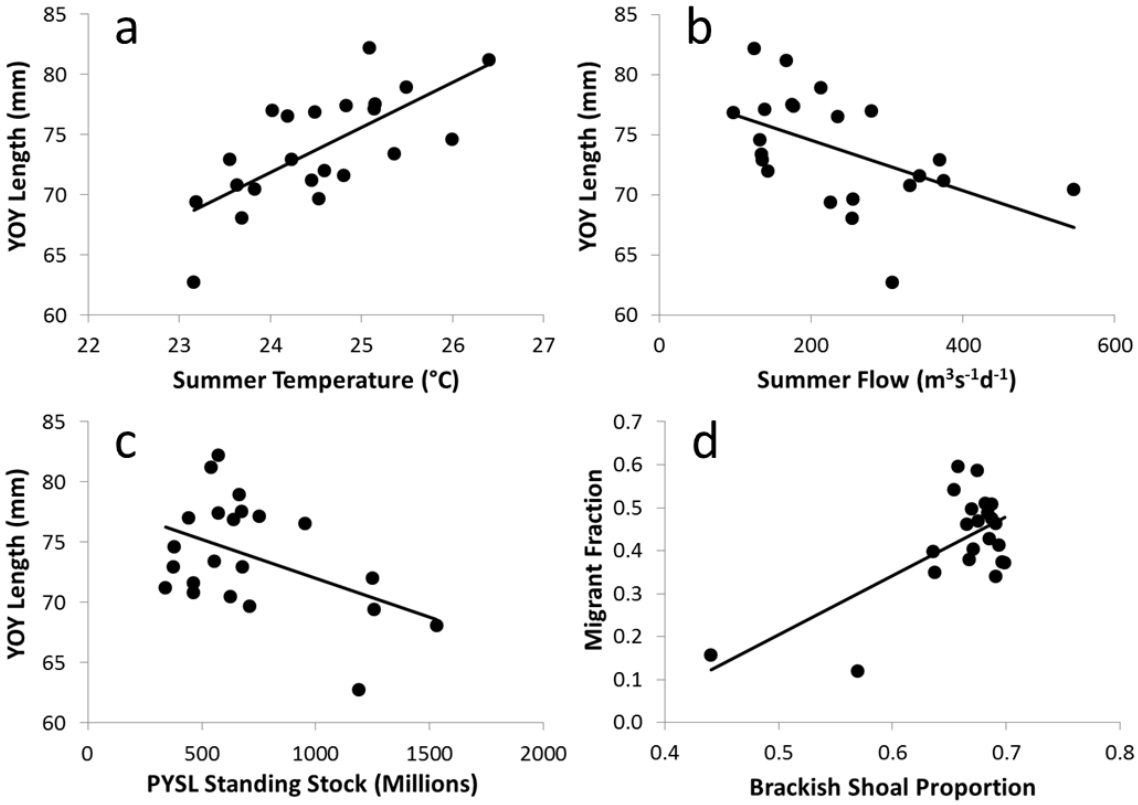

Figure 5. Annual mean standing stocks of resident (blue line) and migratory (red line) YOY white perch contingents from 1992-2013. The fraction of YOY in the migratory contingent each year (black line) is plotted on the secondary y-axis (right side).

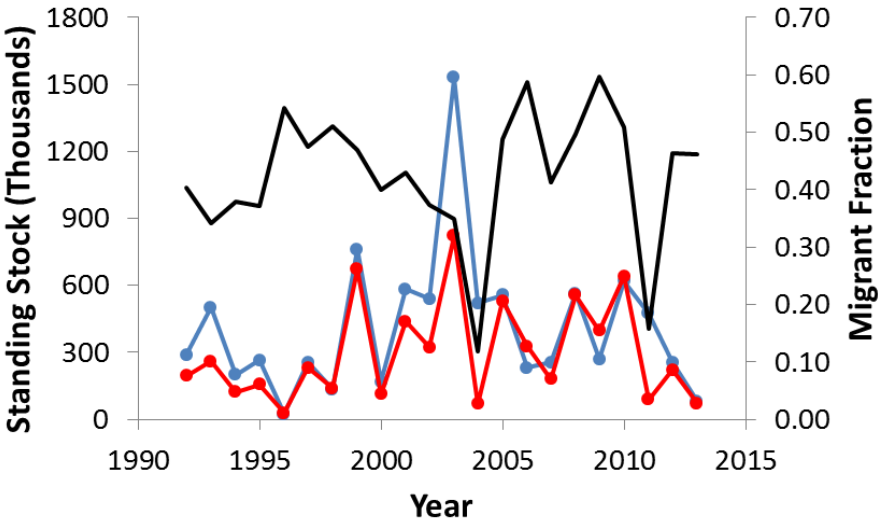

Figure 6. Paulik diagram depicting (clockwise from top right) egg-YOY, egg-YSL, YSL-PYSL and PYSL-YOY life-stage transitions based on indices of abundance during pre-invasion (1974-1991; black points; fitted by solid lines) and post-invasion (1992-2013; white points; fitted by dashed lines) time periods. Note that all four plots within the diagram have a common origin. Ricker models are plotted with freshwater flow during the PYSL period as a covariate (see Methods).

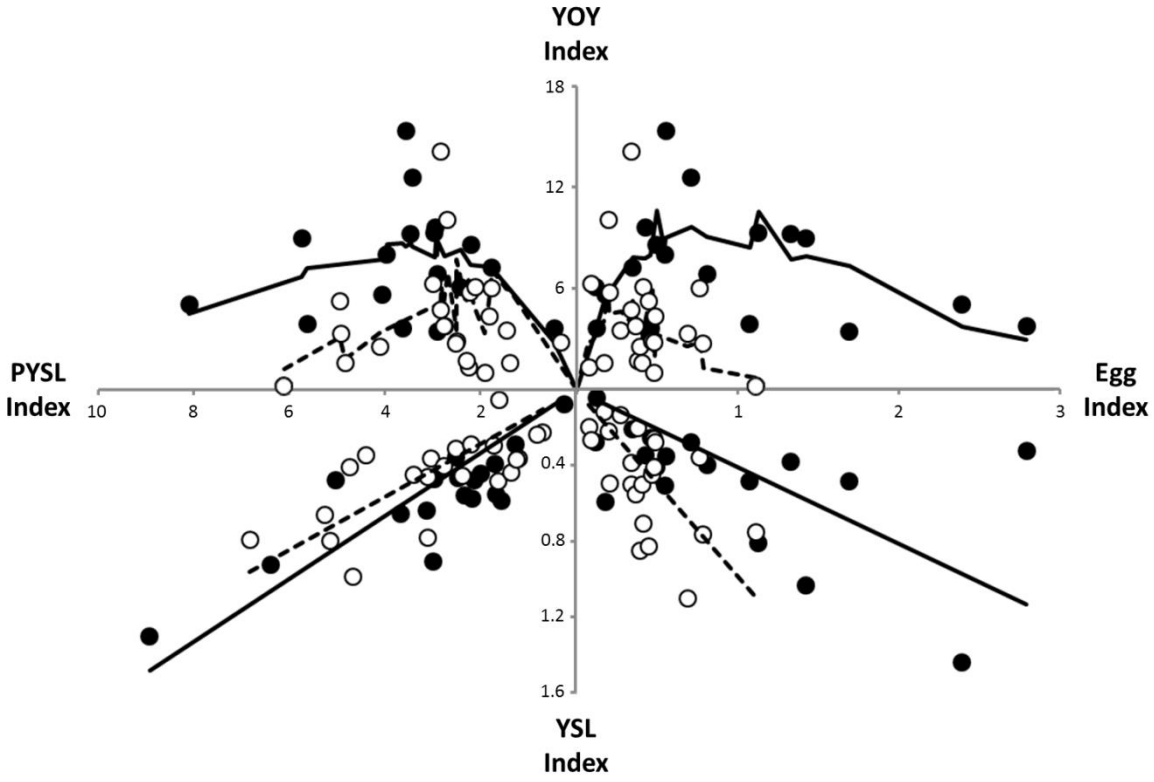

Figure 7. Relationship between white perch yearling abundance and YOY abundance from the previous year based on indices of abundance for each life-stage during pre-invasion (1974-1991; black points; fitted by solid line) and post-invasion (1992-2013; white points; fitted by dashed line) time periods.

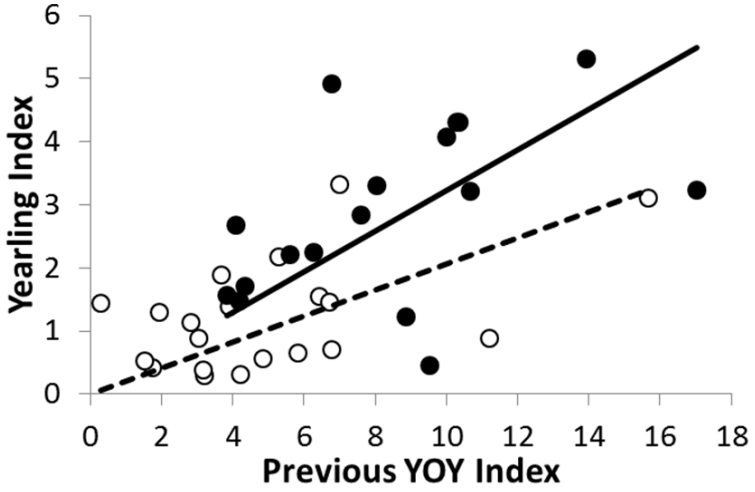

Figure 8. Plot of mean freshwater flow at Green Island in Troy, NY (USGS 2015c) during weeks 19-28, when white perch post yolk-sac larvae (PYSL) are most abundant, from 1992-2013. The regression equation is displayed in the top right corner, and the slope (7.99 year^{-1}) corresponds to an increase of 1.9% year^{-1}.

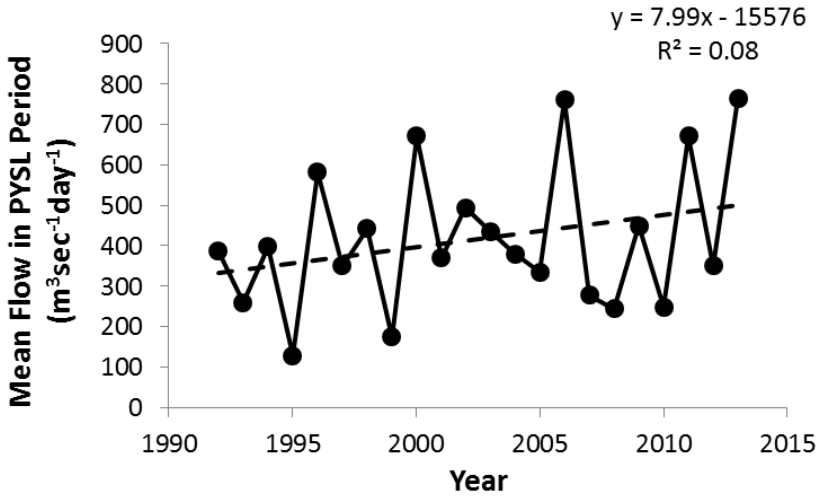

Supplementary Material

Table S.1. Survey, gear and time-span descriptions for each white perch life-stage. Depth strata that were sampled included shore-zone (< 3 m in depth), shoal (< 6 m), channel (water > 3 m above the river bottom in depths > 6 m) and bottom (water < 3 m above the river bottom in depths > 6 m). Note that YSL and eggs were also sampled in the LRS, and thus have the same strata, gear, mesh size and sampling weeks displayed for PYSL.

Life-Stage	Survey	Depth Strata	Gear	Mesh Size	Sampling Weeks	Weeks Averaged
Adult	FJS	Channel, Shoal and Bottom	1 m^2 Tucker Trawl (Channel), 3 m Beam Trawl (Shoal and Bottom)	3 mm (Channel), 1.3 cm (Shoal and Bottom)	27-48	27-41
YOY	UBSS	Shore zone	30.5 m x 2.4 m Seine Net	0.5 cm	24-43	28-40
PYSL	LRS	Channel, Shoal and Bottom	1 m^2 Tucker Trawl (Shoal and Channel), 1 m^2 Epibenthic Sled (Bottom)	505 µm	11-41	19-28
YSL	LRS					18-26
Egg	LRS					17-25

Table S.2. Correlations between response variables related to white perch growth and spatial distribution and a suite of environmental, density-dependent and habitat availability factors reported before the zebra mussel invasion (1971-1988). Statistically significant ($p < 0.05$) correlations are marked with an asterisk (*).

Response	Predictor	Type	Time Period	Years	Correlation	Source
Early Juvenile Growth Rate	Spring Temperature	Environmental	Jun-Jul	1973-1979	0.93*	Klauda et al. 1988
Late Juvenile Growth Rate	Spring Temperature	Environmental	Jun-Jul		0.12	
	Summer Flow	Environmental	Aug-Sep	1975-1979	0.21	
	YOY Catch	Density-dependent	Oct-Dec	1974-1979	0.45	
Weight at 70mm	Summer Flow	Environmental	Aug-Sep	1975-1979	-0.96*	
	YOY Catch	Density-dependent	Oct-Dec		-0.95*	
YOY Length in November	Summer Temperature	Environmental	Jul-Sep	1971-1988	0.64*	LMS 1989

	Summer Flow	Environmental	Jul-Sep		-0.52*	
	Fall YOY CPUE	Density-dependent	Oct-Dec		-0.26	
	PYSL Abundance Index	Density-dependent	May-Jun	1974-1988	0.06	LMS 1989 and ASA 2014
Mean Fall Population Center	Summer Temperature	Environmental	Jul-Sep	1983-1988	0.79	LMS 1989
	Summer Flow	Environmental	Jul-Sep		-0.81*	
	Fall YOY CPUE	Density-dependent	Oct-Dec		0.19	
Weekly Fall Population Center	Weekly Salt Front Position	Habitat availability	Oct-Nov	1985-1988	0.46*	

Simulating the effects of contingent structure and long-term environmental change in white perch within the Hudson River Estuary

Methods:

Age-structured Population Model:

Contingent-specific population dynamics of white perch were modeled based on an existing age-structured model developed by Kerr et al. (2010), with each contingent having different growth and maturity schedules while sharing a common stock-recruitment relationship. A two-stage recruitment process was assumed, starting with recruitment into a common abundance pool at age-0, which was subsequently split into contingent-specific abundances at age-1. This assumption was meant to reflect observations that contingents likely mix on spawning grounds (Klauda et al. 1988) and adopt migration strategies shortly after metamorphosing into fully-formed juveniles (Kraus and Secor 2004, Gallagher et al. in review). The model was parameterized using empirical data from analyses of young-of-the-year (YOY) and adult white perch sampled from the HRE in 2013 and 2014, and long-term monitoring data from 1992-2013, in addition to previously published estimates from the literature (Table 1).

There were 14 age-classes (*a*; ages 0-13) in each model, simulated over 150 annual time-steps (*t*), with two contingents (*c*). Recruitment to a common abundance pool at age *0* and time *t* (N_{0t}) was defined by a Ricker stock-recruitment function with freshwater flow as a covariate, calculated by:

(1) $$N_{0t} = \alpha(SSA_{pop(t-1)})e^{-\beta(SSA_{pop(t-1)})-\gamma(U_t)} \times error$$

where $SSA_{pop(t-1)}$ is the spawning stock abundance of the population at the previous time-step, α is a density-independent parameter indicating the slope at the origin, β is a density-dependent parameter representing the inverse of the spawning stock abundance at which maximum recruitment occurs, while γ can be interpreted as a density-independent effect of freshwater flow at time *t* (U_t), on white perch mortality (North and Houde 2003). U_t is calculated based upon the annual mean freshwater flow from weeks 19-28, when white perch post yolk-sac larvae (PYSL) are most abundant (ASA 2014). The relationship between PYSL and YOY largely determines the shape of the stock-recruitment function in Hudson River white perch, with the expected abundance of YOY being negatively impacted by freshwater flow during the PYSL period (Gallagher and Secor in review). The multiplicative *error* term was modeled as a log-normally distributed deviation with a mean of 1 and SD of σ_R (Table 1).

Contingent structure was imposed at age-1, with the abundance of each contingent (*r* or *d*) expressed as a function of the total abundance at age-0:

(2) Resident: $$N_{1tr} = N_{0t}(1 - D)$$

Dispersive: $N_{1td} = N_{0t}(D)$

where N_{1tr} and N_{1td} denote the abundance of white perch contingents at age *1* at time *t*, and D is the proportion of white perch that are considered to be dispersive. This proportion was varied at five levels (see *Scenarios*). After the initiation of contingent dynamics, abundance at ages 2 through 13 was calculated as:

(3) $$N_{(a+1)(t+1)c} = N_{atc}e^{-Z_c}$$

where N_{atc} is the abundance at age *a* at time *t* in contingent *c*, and Z_c is the instantaneous mortality rate for contingent *c*. Depending on the scenario, the mortality rate was assumed to be either equal to 0.27 for both contingents or 0.27 for residents and 0.41 for migrants (see *Scenarios*).

Spawning stock abundance at time *t* for contingent *c* (SSA_{tc}) was calculated as a function of the abundance-at-age and contingent-specific maturity-at-age, which were subsequently summed to obtain the spawning stock abundance of the population at ($SSA_{pop(t)}$), which served as an input for the stock-recruitment function at the next time-step (*Equation 1*):

(4) $$SSA_{tc} = \sum_{a=1}^{13} N_{atc}p_{ac}$$
$$SSA_{pop(t)} = \sum SSA_{tc}$$

where N_{atc} is the abundance of white perch of age *a* at time *t* in contingent *c* and p_{ac} is the proportion of white perch at age *a* in contingent *c* that were considered sexually mature. Maturity-at-age estimates for each contingent were based on previous estimates of maturity as a function of total length in Hudson River white perch (Klauda et al. 1988; Table 2).

The spawning stock biomass was estimated as:

(5) $$SSB_{tc} = \sum_{a=1}^{13} N_{at}p_{ac}W_{ac}$$
$$SSB_{pop(t)} = \sum SSB_{tc}$$

where W_{ac} is the average weight at age *a* of contingent *c*. This weight-at-age (in kg) for each contingent was, in turn, calculated as a function of total length by the power model:

(6) $$W_{ac} = AL_{ac}{}^{B}$$

where L_{ac} is the average total length at age a for contingent c. Length at age a for contingent c (in mm), estimated from von Bertalanffy growth functions for each contingent:

$$L_{ac} = L_{\infty c}\left[1 - e^{-k_c(a-a_0)}\right] \quad (7)$$

where $L_{\infty c}$ is the asymptotic length for contingent c, k_c is the growth coefficient for contingent c, describing the rate at which the asymptote is approached, and a_0 was assumed to be 0 for both contingents (Table 1). The dispersive contingent of Hudson River white perch displays a faster growth rate and attains a larger maximum size than their resident counterparts, resulting in substantial differences in growth (by both weight and length) and maturity schedules between contingents, with the dispersive contingent reaching full maturity two years before residents on average (Tables 1 and 2).

Freshwater Flow Projections:

Periods of low freshwater flow in the HRE correspond to increases in light penetration and water residence time which result in more favorable conditions for primary production (Howarth et al. 2006). Secondary production of benthic, epibenthic and pelagic invertebrates are also influenced by freshwater flow, as many of these organisms are sensitive to advection and generally acquire energy from phytoplankton or inputs of suspended organic material, which are both controlled by flow (Gladden et al. 1988, Pace et al. 1992). In addition, zebra mussels (*Dreissena polymorpha*) invaded the HRE in 1991 had a substantial negative impact on the abundance of phytoplankton, zooplankton and fish (Caraco et al. 1997, Strayer et al. 2003), and increased the sensitivity of many organisms to freshwater flow (Strayer et al. 2014). Thus, the discovery of a significant negative effect of annual mean freshwater flow during the post yolk-sac larval period (U_t; averaged across weeks 19-28 from 1992-2013) on the white perch stock-recruitment relationship (*Equation 1*; Gallagher and Secor in review) is consistent with the pervasive influence of freshwater flow on biota within the HRE.

Given the importance of freshwater flow to white perch recruitment dynamics, we attempted to explicitly incorporate shifts in freshwater flow that are expected to occur over the next century due to climate change (Howarth et al. 2000). Nearly continuous daily freshwater flow data are available from Green Island Dam at the head of the HRE since 1950 (USGS 2015), which were used to inform flow projections. Mean annual freshwater flow during weeks 19-28 (U_t), when white perch post yolk-sac larvae are most abundant, was characterized by an increase of over 30% from 1950-2014, while the rate of increase was approximately 2.5 times higher from 1980-2014 than it was for the whole time-series (B. Gallagher, unpublished data). Additional analyses of U_t data from 1950-2014 revealed that flow was log-normally distributed and lacked autocorrelation among adjacent years, which prompted the use of a simple linear projection of U_t with an intercept, slope and a multiplicative log-normal error:

(8) $$U_t = (U_0 + m_U(t)) \times error$$

where U_0 is the initial value of flow at the first time-step, m_U is the slope or rate of change in flow over time, t is the time step, and the *error* term is log-normally distributed with a mean of 1 and SD of σ_U (Table 1). The rate of change of flow (m_U) was varied at three levels in order to explore white perch population responses to realistic long-term changes in freshwater flow (see *Scenarios*).

Scenarios:
Stochastic simulations were implemented to estimate and compare the yield, stability and resilience of the HRE white perch population across 60 scenarios representing different combinations of values in D, Z_d, m_U, and σ_U (Table 3). Each simulation was run 500 times over 150 years (t), although only the last 100 years were retained for comparative analyses in order to remove the influence of initial conditions. Here, the 150 years timespan in the model is coarsely aligned with the period 1951-2100, and the last 100 years retained in each simulation corresponds to 2001-2100.

Five different levels of D were centered on estimated values from 1992-2013 (mean=0.42; Gallagher et al. in review) in addition to plausible values as a result of hypothetical littoral habitat restoration efforts in either freshwater (D=0.2) or brackish water (D=0.6). These restoration scenarios are based upon observations that the proportion of YOY white perch that are dispersive is influenced by the amount of available littoral habitat in the brackish portion of the HRE (Gallagher and Secor in review). Endmembers of D (0 and 1) were also included. Z_d values included two scenarios, one assuming a value of 0.27, which is equal to the estimated mortality rate for the whole population, and another assuming a value of 0.41, in which the dispersive contingent experiences much higher mortality. This latter scenario is meant to reflect observations that, while survey data showed that 30-50% of YOY white perch were dispersive from 1992-2013 (mean=42%; ASA 2014), otolith strontium:calcium profiles indicated that less than 10% of adult white sampled during spring and fall of 2014 displayed dispersive behavior in their first year of life. This disparity in contingent representation suggests that the dispersive contingent may be subjected to higher rates of mortality than residents (Gallagher et al. in review).

To reflect plausible changes in freshwater flow throughout the next century, three different slopes (m_U) were used in projections of U_t, with values of 0.965, -0.965, or 0 $m^3sec^{-1}year^{-1}$, which correspond to a 25% increase, 25% decrease, or no change over 100 years. U_t has been steadily increasing since 1950 (USGS 2015), and averages of several statistically down-scaled global climate models indicate that annual mean freshwater flow in the HRE is most likely to increase by 5-25% by 2099 (Najjar et al. 2009).. However, Najjar et al. (2009) emphasized the uncertainty in their flow projections and noted that increased evapotranspiration driven by warming temperatures could conceivably result in long-term decreases in freshwater flow.

Finally, two scenarios were tested in relation to the variance of U_t in our flow projections, one in which the standard deviation in flow (σ_U) was constant, and another in which σ_U was allowed to increase at a rate of 0.0011 $m^3sec^{-1}year^{-1}$, corresponding to a 25% increase over 100 years. This latter scenario is meant to explore the consequences of concurrent change in the mean and variability of U_t (Salinger 2005), which may act in synergy to increase the likelihood of extreme events such as floods and droughts (Katz and Brown 1992).

Similar to Kerr et al. (2010), the response variables used to compare outcomes across scenarios were the yield, stability and resilience of the population. The mean spawning stock biomass of the population (SSB_{pop}) was used as a surrogate for yield. The mean coefficient of variation of SSB_{pop} (CV_{SSB} *= mean/SD x 100*) was calculated as the stability metric. Resilience was measured as the recovery time of the population to the mean SSB_{pop} after imposing low recruitment (10% of the maximum recruitment (*1/β*) from the Ricker stock-recruitment function) for five consecutive years in the simulation. The yield, stability and resilience were calculated within each of the 500 simulations of each scenario, and a grand mean of these metrics was subsequently taken across all simulations, which served as the response of interest for comparisons across scenarios.

Table 1: List of parameters used in age-structured models of white perch, along with their sources and, where applicable, brief descriptions of how they were estimated.

Para-meter	Definition	Joint Value	Resident Value	Dispersive Value	Source
α	Density-independent parameter in the Ricker stock-recruitment function	2.46			Estimated parameters in a linearized Ricker model via multiple regression, using adult abundance, YOY abundance and freshwater flow data from 1992-2013 (R^2 = 0.59; Gallagher and Secor, in review)
β	Density-dependent parameter in the Ricker stock-recruitment function, equal to the inverse of maximum recruitment	5.60×10^{-7}			
γ	Density-independent effect of annual mean freshwater flow during the white perch post yolk-sac larval period (U_t in m^3/sec) in the Ricker stock-recruitment function	2.18×10^{-3}			
σ_R	Log-normal error in the Ricker stock-recruitment	0.75			CV of white perch YOY abundance from 1992-2013 (Gallagher 2016)

	function				
Z	Instantaneous mortality rate after age-0, assumed to be equal between sexes		0.23	0.23 or 0.46	Estimated by catch curve, with higher mortality in the dispersive contingent supported by lower representation of first-year migrants in adult samples from fall and spring 2014 than would be expected under equal mortality (Gallagher 2016)
L_∞	Theoretical maximum length (mm) in von Bertalanffy growth function		194	204	Estimated by maximum likelihood using length-at-age data from adult samples collected during fall 2014. Contingent-specific estimates were based upon location of capture (R^2 = 0.73, Gallagher et al. in review)
k	Growth coeffecient ($year^{-1}$) in von Bertalanffy growth function		0.52	0.69	
a_0	Theoretical age (year) when length is 0 in von Bertalanffy growth function	0			
A	Multiplier for length-weight relationship	4.32×10^{-9}			Estimated by non-linear regression (R^2 = 0.98,

	(kg/mm)				Gallagher 2016)
B	Exponent for length-weight relationship	3.22			
U_0	Initial value (m^3/sec) of U_t at the beginning of the simulation period	385			Grand mean of U_t from 1950-2013 (USGS 2015)
σ_U	Initial value of the log-normal error in U_t at the beginning of the simulation period	0.45			CV of U_t from 1950-2013 (USGS 2015)

Table 2: Length, weight, and maturity schedules for resident and dispersive contingents of white perch within the Hudson River Estuary. Maturity-at-age was determined from a logistic length-maturity function fitted to data from from Klauda et al. (1988).

	Resident			Dispersive		
Age (year)	**Length (mm)**	**Weight (kg)**	**Proportion Mature**	**Length (mm)**	**Weight (kg)**	**Proportion Mature**
0	0	0.00	0.00	0	0.00	0.00
1	78	0.01	0.02	102	0.01	0.09
2	125	0.02	0.38	153	0.05	0.85
3	153	0.05	0.84	179	0.08	0.98
4	169	0.06	0.95	191	0.09	1.00
5	179	0.08	0.98	198	0.10	1.00
6	185	0.08	1.00	201	0.11	1.00
7	189	0.09	1.00	203	0.11	1.00
8	191	0.09	1.00	203	0.11	1.00
9	192	0.09	1.00	204	0.11	1.00
10	193	0.10	1.00	204	0.12	1.00
11	193	0.10	1.00	204	0.12	1.00
12	193	0.10	1.00	204	0.12	1.00
13	193	0.10	1.00	204	0.12	1.00

Table 3: List of 60 scenarios run in the age-structured population model, each with different combinations of dispersive fraction (D), instantaneous mortality rates for the dispersive contingent (Z_d), slopes of U_t used in flow projections (m_u), and slopes of σ_U used in flow projections

Scenario Number	D: Dispersive Fraction	Z_d: Dispersive Mortality	m_U: Slope in U_t ($m^3sec^{-1}year^{-1}$)	Slope in σ_U ($m^3sec^{-1}year^{-1}$)
1	0	0.27	-0.965	0
2	0	0.41	-0.965	0
3	0	0.27	-0.965	0.0011
4	0	0.41	-0.965	0.0011
5	0	0.27	0.965	0
6	0	0.41	0.965	0
7	0	0.27	0.965	0.0011
8	0	0.41	0.965	0.0011
9	0	0.27	0	0
10	0	0.41	0	0
11	0	0.27	0	0.0011
12	0	0.41	0	0.0011
13	0.2	0.27	-0.965	0
14	0.2	0.41	-0.965	0
15	0.2	0.27	-0.965	0.0011
16	0.2	0.41	-0.965	0.0011
17	0.2	0.27	0.965	0
18	0.2	0.41	0.965	0
19	0.2	0.27	0.965	0.0011
20	0.2	0.41	0.965	0.0011
21	0.2	0.27	0	0
22	0.2	0.41	0	0
23	0.2	0.27	0	0.0011
24	0.2	0.41	0	0.0011
25	0.4	0.27	-0.965	0
26	0.4	0.41	-0.965	0
27	0.4	0.27	-0.965	0.0011
28	0.4	0.41	-0.965	0.0011
29	0.4	0.27	0.965	0
30	0.4	0.41	0.965	0
31	0.4	0.27	0.965	0.0011
32	0.4	0.41	0.965	0.0011
33	0.4	0.27	0	0
34	0.4	0.41	0	0
35	0.4	0.27	0	0.0011

36	0.4	0.41	0	0.0011
37	0.6	0.27	-0.965	0
38	0.6	0.41	-0.965	0
39	0.6	0.27	-0.965	0.0011
40	0.6	0.41	-0.965	0.0011
41	0.6	0.27	0.965	0
42	0.6	0.41	0.965	0
43	0.6	0.27	0.965	0.0011
44	0.6	0.41	0.965	0.0011
45	0.6	0.27	0	0
46	0.6	0.41	0	0
47	0.6	0.27	0	0.0011
48	0.6	0.41	0	0.0011
49	1	0.27	-0.965	0
50	1	0.41	-0.965	0
51	1	0.27	-0.965	0.0011
52	1	0.41	-0.965	0.0011
53	1	0.27	0.965	0
54	1	0.41	0.965	0
55	1	0.27	0.965	0.0011
56	1	0.41	0.965	0.0011
57	1	0.27	0	0
58	1	0.41	0	0
59	1	0.27	0	0.0011
60	1	0.41	0	0.0011

References:

ASA (Applied Science Associates, Inc). 2014. 2013 Year class report for the Hudson River Estuary monitoring program and Central Hudson Gas and Electrical Corporation. New Hampton, NY.

Caraco, N.F., J.J. Cole, P.A. Raymond, and D.L. Strayer. 1997. Zebra mussel invasion in a large, turbid river: phytoplankton response to increased grazing. Ecology 78(2): 588-602.

Gladden, J., F. Cantelmo, J. Croom and R. Shapot. 1988. Evaluation of the Hudson River ecosystem in relation to the dynamics of fish populations. *in*: Science, Law and Hudson River Power Plants. American Fisheries Society Monograph 4:69-88.

Howarth, R., D. Swaney, T. Butler, and R. Marino. 2000. Rapid communication: Climatic control on eutrophication of the Hudson River Estuary. Ecosystems 3:210–215.

Howarth, R, R. Marino, D. Swaney and E. Boyer. 2006. Wasterwater and watershed influences on primary productivity and oxygen dynamics in the Lower Hudson River Estuary. *in:* J.S. Levinton and J.R. Waldman (eds). The Hudson River Estuary. Cambridge University Press, New York, NY, 121-136.

Katz, R., and B. Brown. 1992. Extreme events in a changing climate: Variability is more important than averages. Climatic Change 21:289–302.

Kerr, L., D. Secor, and P. Piccoli. 2009. Partial migration of fishes as exemplified by the estuarine-dependent white perch. Fisheries 34(3): 114-123.

Kerr, L., and D. Secor. 2010. Latent effects of early life history on partial migration for an estuarine-dependent fish. Environmental Biology of Fishes 89:479–492.

Kerr, L.A., S.X. Cadrin, and D.H. Secor. 2010. The role of spatial dynamics in the stability, resilience, and productivity of an estuarine fish population. Ecological Applications 20(2): 497-507.

Kerr, L., and D. Secor. 2011. Partial migration across populations of white perch (*Morone americana*): a flexible life history strategy in a variable estuarine environment. Estuaries and Coasts 35(1): 227-236.

Klauda, R.J., J.B. McLaren, R.E. Schmidt and W.P. Dey. 1988. Life history of white perch in the Hudson River Estuary. *in*: Science, Law and Hudson River Power Plants. American Fisheries Society Monograph 4:69-88.

Kraus, R.T., and D.H. Secor. 2004. Dynamics of white perch *Morone americana* population contingents in the Patuxent River estuary, Maryland, USA. Marine Ecology Progress Series. 279: 247-259.

Kraus, R., and D. Secor. 2005. Connectivity in estuarine white perch populations of Chesapeake Bay: evidence from historical fisheries data. Estuarine, Coastal and Shelf Science 64(1): 108-118.

Mansueti, R.J. 1964. Eggs, larvae, and young of the white perch, *Roccus americanus*, with comments on its ecology in the estuary. Chesapeake Science. 5(1-2): 3-45

Najjar, R., L. Patterson, and S. Graham. 2008. Climate simulations of major estuarine watersheds in the Mid-Atlantic region of the US. Climatic Change 95:139–168.

Salinger, M.J. 2005. Climate variability and change: past, present and future- an overview. Climatic Change 70: 9–29.

Secor, D.H., L.A. Kerr, and S.X. Cadrin. 2009. Connectivity effects on productivity, stability, and persistence in a herring metapopulation model. ICES Journal of Marine Science 66(8): 1726-1732.

Seekell, D.A. and Pace, M.L. 2011. Climate change drives warming in the Hudson River Estuary, New York (USA). Journal of Environmental Monitoring 13:2321–2327

Seltzer-Hamilton, E. 1991. White Perch, *Morone americana*. *in*: Funderbunk S.L., Mihursky J.A., Jordan S.J., Riley D. (eds) Habitat requirements for Chesapeake Bay living resources (2nd edition). Chesapeake Research Consortium, Solomons, MD. pp. 12–1–12–20.

Strayer, D., K. Hattala, and A. Kahnle. 2004. Effects of an invasive bivalve (*Dreissena polymorpha*) on fish in the Hudson River estuary. Canadian Journal of Fisheries and Aquatic Sciences 61:924–941.

Strayer, D.L., M.L. Pace, N.F. Caraco, J.J. Cole, and S. Findlay. 2008. Hydrology and grazing jointly control a large-river food web. Ecology. 89(1): 12-18.

Strayer, D., J. Cole, S. Findlay, D. Fischer, J. Gephart, H. Malcom, M. Pace, and E. Rosi-Marshall. 2014a. Decadal-scale change in a large-river ecosystem. BioScience 64:496-510.

USGS (United States Geological Survey). 2015. National Water Information System data available on the World Wide Web (USGS Water Data for the Nation), accessed May 6, 2015. (Available: http://waterdata.usgs.gov/usa/nwis/uv?site_no=01358000)